MEDICAL UNIVERSITY OF VIENNA

MUTANT SELECTIVE SMALL MOLECULE INHIBITORS OF CALRETICULIN FOR THE TREATMENT OF CALR MUTATION POSITIVE MYELOPROLIFERATIVE NEOPLASMS

Doctoral thesis at the Medical University of Vienna
for obtaining the academic degree

Doctor of Philosophy

Submitted by

MSc, Ruochen Jia

Supervisor:
Professor, Robert Kralovics

Department of Laboratory Medicine, Medical University of Vienna
Lazarettgasse 14 BT 25.2 1090 Wien, Österreich

CeMM Research Center for Molecular Medicine of the Austrian Academy of Sciences
Lazarettgasse 14, BT 25.3, 1090 Vienna, Austria

Vienna, date of submission (format: 08/2019)

Declaration

All the work from the author was conducted in the research group of Robert Kralovics. The majority of the work was carried out in CeMM Research Center for Molecular Medicine of the Austrian Academy of Sciences before the lab moved to the department of Laboratory Medicine on 1 June 2019. The work since then was done in the current department.

All the experimental work was conducted by the author of the thesis except the ones mentioned below. For result 2.1, the computational docking study and chemical synthesis were conducted in collaboration with Roman Lesyk's group in Danylo Halytsky Lviv National Medical University Ukraine. The NanoBRET assay (Figure 2.1.4a) was carried out by Thomas Balligand from Stefan Constantinescu's group in Ludwig Cancer Research/de Duve Institute, Brussels, Belgium. For result 2.2, the chemical screening in CALR mutated cell lines was conducted in collaboration with Platform Austria for Chemical Biology (PLACEBO) led by Stefan Kubicek. The platform supplied and prepared the drug library and conducted the CellTiter-Glo reading as well as the preliminary data analysis. Leon Kutzner, the former master student from Kralovics group, conducted his master project relating to result 2.2 under the supervision of the author. He performed experiments relating to Figure 2.2.2, 2.2.3 and 2.2.4a as well as Supplementary figure 2.2.1 and Supplementary figure 2.2.2. The relevant results were recorded in his master thesis. Figure 2.2.1 was generated by the author but was permitted to be included in Leon Kutzner's master thesis due to scientific logistics of it. Jakob Weinzierl provided hands-on help to create CALR KO cell line models that were used in some assays. MyeloPro Diagnostics and Research GmbH, Vienna, Austria provided mutant calreticulin specific antibodies which were used in western blot. The patient samples was provided by Professor Heinz Gisslinger. My supervisor Robert Kralovics initiated the ideas of the two projects included in the thesis and provided supervision throughout the projects. He also advised on the thesis writing.

All the illustration figures from the introduction section were drawn by the author. In the case of published concept or summarized information adapted into the illustration, the related publications were referenced.

Part of the result 2.1 was used for a patent application of which the author designated as one of the inventors. The notification from the European Patent Office was included in the Appendix section.

Table of contents

Acknowledgements

I would like to thank CeMM providing me an opportunity to conduct PhD study. CeMM has always been a dynamic and interactive place where I have made many friends during the years. It has been my pleasure to be part of this institute as a PhD student.

I would like to thank my supervisor Robert Kralovics for his guidance in the project management and the training to be a qualified scientist. It has been a great experience working in an environment where I feel very trusted by my supervisor and have always been given freedom to express my ideas and explore the science. Robert also affects me by his passion in science and his optimism when we encounter difficulties.

I would like to thank the whole Kralovics group for creating a helpful and friendly environment during my PhD. Many members have left the group but they have been an important part of my PhD life. Particularly, I appreciate Harini Nivarthi for her guidance during my first year of PhD to help me adapt to the group. Leon Kutzner was a wonderful master student who I worked with for one year and he has made a great contribution to one of the projects included in the thesis. Roland Jaeger helped me with the German translation of the thesis abstract. I would also like to thank members from Myelopro for their support in the projects.

Another very important group of people are the PhD students of my year. They have been my most reliable friends in Vienna. They are the people that I would like to share my work and my life stories with. We also had some wonderful trips together.

I appreciate the constructive scientific input from my PhD committee members Stefan Kubicek and Veronika Sexl. Stefan made some crucial suggestions to the project with his expertise in chemical biology and provided valuable collaboration in both projects.

I also appreciate our collaborators from Group of Roman Lesyk and Stefan Constantinescu for their data and intelligence input in the projects.

Abstract

Myeloproliferative neoplasms (MPNs) are driven by clonal expansion of mutated clones among hematopoietic stem and progenitors. Searching for pharmaceuticals that can selectively kill mutated clones has great implications in MPN therapy. In this thesis, two independent research projects were described, both aiming to find small molecule inhibitors for CALR mutated MPN patients. We first applied direct targeting approach by computationally screen for chemicals that bind to the glycan binding domain of calreticulin. A mutagenesis study was conducted to show the essentiality of this domain to the oncogenicity of the mutant protein. A comprehensive virtual screening approach was applied to generate the candidate drug library that was used for cytotoxicity screen in our cell line models. Hematoxylin was selected as our top hit, as it preferentially depleted the CALR mutated cells, confirmed by both the CellTiter-Glo assay and the competition assay. Significant induction of apoptosis was observed in mutant cells upon drug treatment. The cytotoxic effect was specific to the mutant C-terminus of CALR, since neither knock out nor C-terminus truncation of CALR did not show hypersensitivity. A reduced CALR-MPL interaction was observed following hematoxylin treatment in a dose-dependent manner, as measured by the NanoBRET assay. The cellular thermal shift assay (CETSA) suggested binding of the chemical to both mutant and wild type calreticulin. The drug also reduced the cellular abundance of mutant calreticulin by increasing the secretion of the protein and downregulating JAK2-STAT5 signaling. Lastly, the number of colony forming units (CFUs) from CD34+ cells derived from CALR mutant patients was significantly reduced by hematoxylin treatment. We thus proposed hematoxylin as a candidate drug lead and the glycan binding domain of CALR as a promising drug target for MPN treatment.

In the second project, we applied an unbiased high-throughput screening approach to search for CALR mutant specific drugs based on their selective cytotoxicity in CALR mutated cell lines. We endeavoured to reveal drug targets that were synthetic lethal with mutant CALR. The screen revealed theATR-CHK1 pathway as our top candidate. Several CHK1 inhibitors were subsequently used in validation assays that confirmed the selective cytotoxicity of those drugs in CALR mutant clones. We also conducted experiments in CALR knockout and JAK2V617F mutated cell lines to show drug specificity. The CFU assay was performed with CD34+ cells isolated from CALR patients and healthy control individuals to confirm drug selectivity. We hypothesized that mutant cells showed increased vulnerability to ATR-CHK1 inhibition due to increased replication stress. A significantly higher level of H2AX and RPA phosphorylation was induced by the drug treatment in mutant cells compared with wild type control. An elevation of pan-nuclear staining of γH2AX was observed in mutant cells by the immunofluorescence assay.

The mutant cells also underwent an intra-S cell cycle arrest. Based on those findings we propose the use of CHK1 inhibitors in the treatment of mutated CALR driven MPN treatment.

Zusammenfassung

Myeloproliferative Neoplasien (MPNs) werden durch klonale Expansion mutierter Klone hämatopoetischer Stamm- und Vorläuferzellen ausgelöst. Die Suche nach Arzneimittel, welche mutierte Klone selektiv abtöten können, hat große Auswirkungen auf die MPN-Therapie. In dieser Arbeit sind zwei unabhängige Forschungsprojekte beschrieben, die beide darauf abzielen, niedermolekulare Inhibitoren für CALR-mutierte MPN-Patienten zu finden. Wir haben zuerst einen direkten Targeting-Ansatz angewendet, indem wir computerunterstützt nach Chemikalien gesucht haben, die an die Glycan-Bindungsdomäne von Calreticulin binden. Eine Mutagenese-Studie wurde durchgeführt, um die Wesentlichkeit dieser Domäne für die Onkogenität des mutierten Proteins aufzuzeigen. Des Weiteren wurde ein umfassender virtueller Screening-Ansatz angewendet, um eine Wirkstoffkandidatensammlung zu generieren, aus welcher die Wirkstoffe für ein Zytotoxizitätsscreening in Zelllinienmodellen verwendet wurden. Hämatoxylin wurde als Top-Hit identifiziert, da es bevorzugt die CALR-mutierten Zellen dezimiert hat, was sowohl durch einen CellTiter-Glo-Assay als auch durch einen Kompetitions-Assay bestätigt wurde. Eine signifikante Induktion von Apoptose wurde in mutierten Zellen unter Zugabe von Hämatoxylin beobachtet. Die zytotoxische Wirkung war spezifisch für den mutierten C-Terminus von CALR, da sowohl ein Knockout als auch die Verkürzung des CALR C-Terminus keine Überempfindlichkeit induzierten. Nach einer dosisabhängigen Hämatoxylin-Behandlung wurde eine verringerte CALR-MPL-Wechselwirkung beobachtet, gemessen mit einem NanoBRET-Assay. Die Ergebnisse eines Cellular Thermal Shift Assay (CETSA) legen die Bindung der Chemikalie sowohl an mutiertes als auch an Wildtyp-Calreticulin-Proteine nahe. Der Wirkstoff reduzierte auch mutiertes Calreticulin, indem es die Sekretion des Proteins erhöhte und den JAK2-STAT5-Signalweg herunterregulierte. Schließlich wurde die Anzahl der koloniebildenden Einheiten (CFUs) von CD34+ Zellen isoliert aus Patienten mit mutiertem CALR durch Hämatoxylin-Behandlung signifikant verringert. Anhand dieser Resultate identifizierten wir Hämatoxylin als Lead-Wirkstoffkandidat, und die Glycan-Bindungsdomäne von CALR als vielversprechendes Wirkstoffziel für die MPN-Behandlung.

Im zweiten Projekt haben wir einen unvoreingenommenen Hochdurchsatz-Screening-Ansatz angewendet, um nach CALR-mutationsspezifischen Wirkstoffen zu suchen, basierend auf ihrer selektiven Zytotoxizität in CALR-mutierten Zelllinien. Wir haben versucht, Drug Targets zu finden, welche synthetisch lethal zu mutiertem Calreticulin sind. Das Screening identifizierte den ATR-CHK1-Pathway als unser top Target. Darauf aufbauend wurden mehrere CHK1-Inhibitoren für anschließende Validierungstests verwendet, welche die selektive Zytotoxizität dieser Arzneimittel in CALR-mutierten Klonen bestätigten. Des Weiteren führten wir

Experimente in CALR-knockout und JAK2V617F-mutierten Zelllinien durch, um die Spezifität der Wirkstoffe zu zeigen. CFU-Assays wurden mit aus CALR-Patienten und gesunden Kontroll-Individuen isolierten CD34+ Zellen durchgeführt, um die Selektivität zu bestätigen. Wir stellten die Hypothese auf, dass mutierte Zellen aufgrund von erhöhtem Replikationsstress anfälliger für die Hemmung des ATR-CHK1-Pathways sind. Unter Zugabe der Wirkstoffe wurde ein signifikant höherer Phosphorylierungsgrad von H2AX und RPA in mutierten Zellen im Vergleich zu Wildtyp-Kontrollen induziert. Anhand von Immunfluoreszenz-Assays konnten wir eine Erhöhung der pan-nukleären Färbung von γH2AX in mutierten Zellen zeigen. Des Weiteren wurde ein Stillstand der mutierten Zellen in der S-Phase des Zellzyklus beobachtet. Unsere Erkenntnisse weisen auf eine potentielle Wirksamkeit von CHK1-Inhibitoren in der Behandlung von CALR-mutierten MPN-Patienten hin.

List of Figures

List of tables

Abbreviation

ABL1	Abelson murine leukemia viral oncogene homolog 1
ASXL1	Additional sex comb like 1
ATM	Ataxia Telangiectasia mutated
ATR	Ataxia Telangiectasia And Rad3-Related Protein
BCR	Breakpoint cluster region
CD	Cluster of differentiation
CDK	Cyclin dependent kinase
CEL	Chronic eosinophilic leukemia
CETSA	Cellular thermal shift assay
CFU	Colony forming unit
CHIP	Clonal hematopoiesis of indeterminate potential
CHK1	Checkpoint Kinase 1
CLP	Common lymphoid progenitor
CML	Chronic myelogenous leukemia
CMP	Common myeloid progenitor
CNL	Chronic neutrophilic leukemia
CSF	Colony stimulating factor
CUX1	Cut Like Homeobox 1
DNA-PK	DNA-dependent protein kinase
DNMT3A	DNA Methyltransferase 3 Alpha
EPO	Erythropoietin
ERAD	Endoplasmic-reticulum-associated protein degradation
ET	Essential thrombocythemia
EZH2	Enhancer of zeste homolog 2
FERM	4.1 protein ezrin radixin moesin
Flt-3	Fms-like tyrosine kinase 3
GMP	Granulocyte-monocyte progenitor
H2AX	Histone Family Member X
HSC	Hematopoietic stem cell
HU	Hydroxyurea
IDH	Isocitrate Dehydrogenase (NADP(+))
IL	Interleukin
InsP3R	Inositol 1,4,5- trisphosphate receptor
JAK	Janus kinase

JH	Janus kinase homology
Lin	Lineage
MEP	Megakaryocyte-erythroid progenitor
MHC	Major histocompatibility complex
MPL	Myeloproliferative leukemia protein
MPN	Myeloproliferative neoplasms
MPP	Multipotent progenitor cell
mTOR	Mammalian target of rapamycin
MYC	V-myc avian myelocytomatosis viral oncogene homolog
NMR	nuclear magnetic resonance
NOS	Not otherwise specified
PCR	Polymerase chain reaction
PI	Propidium iodide
PI3K	Phosphotidylinositol 3-kinase
PMF	Primary myelofibrosis
PRC	Polycomb repressive complex
PV	Polycethemia vera
ROS	Reactive oxygen species
RPA	Replication protein A
RUNX1	Runt-related transcription factor 1
Sca1	Stem cells antigen-1
SCF	Stem cell factor
SCT	Stem cell transplantation
SERCA	Sarcoplasmic/endoplasmic reticulum Ca2+-ATPase
SF3B1	Splicing factor 3B subunit 1
SH2	Src-homology-2
SOCS	Suppressor of cytokine signaling
SRSF2	Serine And Arginine Rich Splicing Factor 2
STAT	Signal transducer and activators of transcription
TET2	Tet Methylcytosine Dioxygenase 2
TP53	Tumor protein p53
TPO	Thrombopoietin
WSXWS	Tryptophan-Serine-X-Trptophan-Serine
β2M	β2-microglobulin

1 INTRODUCTION

1.1 Hematopoiesis

Human hematopoiesis describes the process of the generation and maintenance of human hematopoietic system. Starting from a hematopoietic stem cell (HSC) and ending with terminally differentiated blood cells of multiple lineages, a cellular hierarchy is formed. HSCs possess the capacity of self-renewal as well as differentiation into multipotent progenitor cells (MPPs). Further differentiation generates progenitor cells for both myeloid and lymphoid lineages. This process is well regulated both temporally and spatially. Hematopoiesis occurs as early as in the embryonic yolk sac and goes through major development in fetal liver(1,2). It also lasts throughout the adult life for the replenishment of human blood system constantly. HSCs are homing to adult bone marrow that serves as a major site of hematopoiesis. The bone marrow niche consists of not only HSCs, but also osteoblast, endothelial cells and stroma cells. Cytokines and chemokines secreted from these cells support HSCs migration and their self-renewal(3,4). Multiple organs such as spleen, thymus and lymph node are also involved in subsequent hematopoiesis or differentiation and maturation of certain hematopoietic lineages(2,5–8).

Cytokine regulation is another key factor in hematopoietic cell differentiation. Hematopoietic cells from different lineages or differentiation status selectively express cytokine receptors on their surface and therefore activate different cytokine signaling. Cytokines such as colony-stimulating factor (CSF), erythropoietin (EPO), thrombopoietin (TPO), interleukins (ILs) play important roles in stem cell maintenance as well as committed differentiation to certain lineages (Figure 1.1)(8–12). The cytokine receptors undergo homo- or heterodimerization and conformational change upon receiving their ligands and engage components of the downstream signaling pathways. A cascade of phosphorylation events catalyzed by kinases occur and subsequently activate or repress transcription factors that are involved in hematopoietic cell differentiation and proliferation. The Box1/2 motif of the cytokine receptors mediate the interaction with Janus kinases (JAK) that plays a central role in the signaling cascade regulation(13,14). The cytokine receptors are categorized into type I and type II that are distinguished by the presence of WSXWS motif(15).

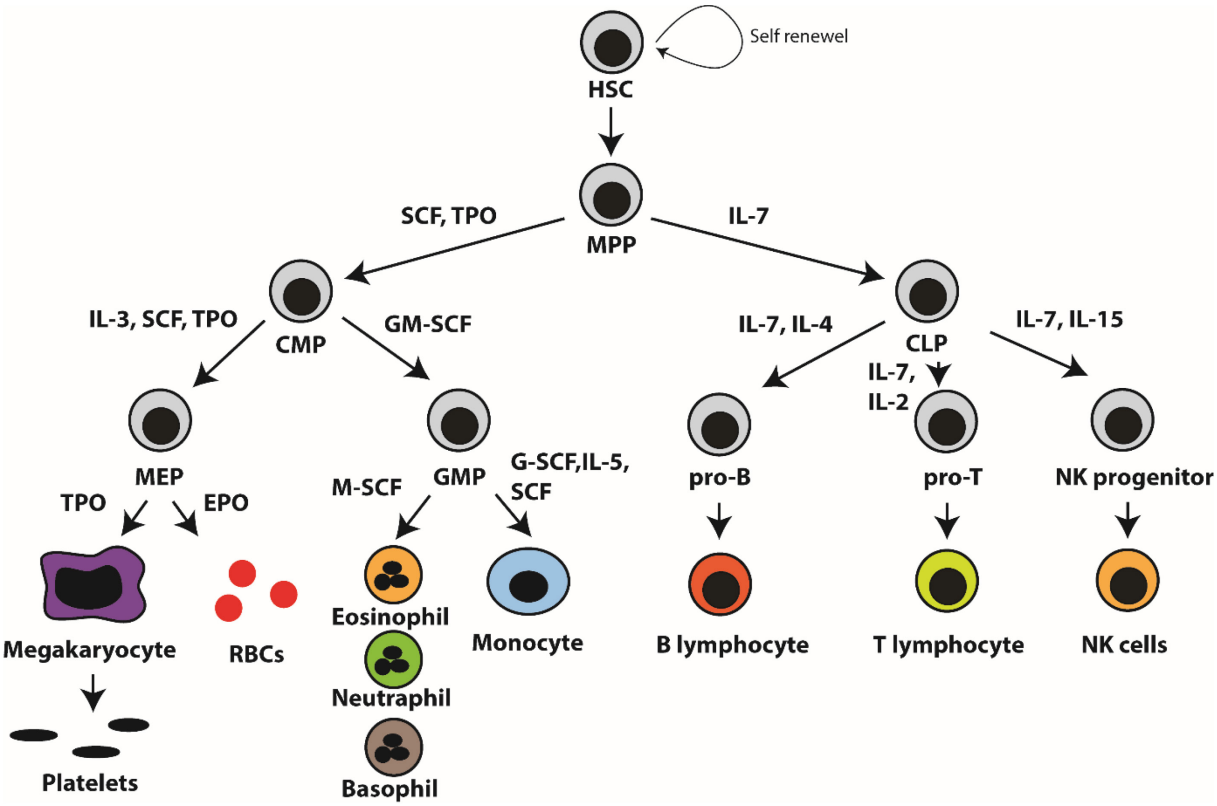

Figure 1. 1 Simplified schematic diagram of hematopoiesis and hematopoietic cytokine regulation

Human HSCs have the capacity to repopulate themselves as well as construct the whole hematopoietic system. Cytokines play an indispensable role in hematopoietic differentiation. Divergent differentiation paths are taken by MPPs, leading to progenitors committed to myeloid and lymphoid lineage. Stem cell factor (SCF) and thrombopoietin (TPO) tend to induce the production of common myeloid progenitors (CMPs). Interleukin-7 (IL-7) is believed to induce the differentiation into common lymphoid progenitors (CLPs). In myeloid lineages, CMPs are further differentiated into megakaryocyte-erythroid progenitors (MEPs) or granulocyte-monocyte progenitors (GMPs). Granulocyte-macrophage colony-stimulating factor (GM-CSF) is particularly important for the formation of GMPs. TPO and erythropoietin (EPO) are essential for megakaryocytic and erythroid lineage differentiation respectively. In lymphoid lineages, CLPs further differentiate into precursors for B,T and NK cells. Several interleukins (IL)-2, 4, 15 are important for this procedure. It is worth to mention that many cytokines such as CSF, GM-SCF, IL-2, IL-3, IL-7 and Fms-like tyrosine kinase 3 ligand (Flt-3) (not in the figure) broadly activate multiple processes of hematopoiesis rather than exclusively specific lineage differentiation(5,7–9).

The discovery of lineage specific cell surface markers has contributed tremendously to the isolation and classification of hematopoietic stem and progenitor cells. For instance, CD34, a cell surface glycoprotein, is the first marker identified to enrich human HSCs(16). Similarly, Lin-Scal+cKit+ (LSK) is experimentally used to isolate and enrich mouse HSCs(17). Combined with *in vitro* colony assay and *in vivo* transplantation assay in mice models, this allows experimental study of the function of hematopoietic stem and progenitor cells. Although advanced transcriptomic technologies have recently challenged the conventional use of cell surface marker to identify different hematopoietic lineages and differentiation status(18,19), these markers are still widely used in laboratory due to its long-standing credibility and practicability. Here we have listed common surface markers used in both human and mouse (Table 1) (7,20,21).

Table 1 Cell surface markers for human and murine hematopoietic progenitor cells

Cell type	Surface markers in human	Surface markers in mice
HSC	CD34+CD38-CD45RA-CD90+CD49f+	Long-term: Lin-Sca1+cKit+CD34-CD150+CD48-CD41-Flt3- Short-term: Lin-Sca1+cKit+CD34-CD150+CD41-Flt3+
MPP	CD34+CD38-CD45RA-CD90-CD49f-	Lin-Sca1+cKit+CD34+CD150-Flt3+
CMP	CD34+CD38+CD45RA-CD135+CD10-CD7-	Lin- Sca1-cKit+CD34+CD16/32(low)
CLP	CD34+CD38-CD45RA+CD10+CD7-	Lin-Sca1(low)cKit(low)Flt3+CD127+
GMP	CD34+CD38+CD45RA+CD135+CD10-CD7-	Lin-cKit+Sca1-CD16/32(high)CD34(high)
MEP	CD34+CD38+CD45RA-CD135-CD10-CD7-	Lin-cKit+Sca1-CD16/32(low)CD34(low)

Considering the importance of early stem and progenitor cells in the generation of the whole hematopoietic system, genetic or epigenetic dysregulation in these compartments often lead to various blood diseases. In the case of the acquisition of oncogenes or loss of tumor suppressor genes, stem and progenitor cells often cause clonal expansion of malignant cells. This results in hyperplasia in certain lineages depending on the biological context.

1.2 Overview of myeloproliferative neoplasms

Myeloproliferative neoplasms (MPN) is one of the major disease categories of chronic hematological malignancies. Like other hematological disorders, MPN is characterized by somatic mutations that occur in HSCs, which lead to clonal expansion and excessive production of mature blood cells. As a myeloid disease, hyperplasia of differentiated blood cells in MPN is mainly restricted in myeloid lineages including erythrocytes, megakaryocytes and granulocytes(22,23). Among sub-categories of MPN, chronic myelogenous leukemia (CML) distinguishes itself from others by a predominant translocation mutation called *BCR-ABL* or Philadelphia chromosome. *BCR-ABL* is the driver mutation in the majority of CML cases and the presence of this mutation shapes the diagnosis and treatment of the disease(24–26). *BCR-ABL* negative MPN consists of polycythemia vera (PV), essential thrombocythemia (ET), primary myelofibrosis (PMF), chronic eosinophilic leukemia (CEL), chronic neutrophilic leukemia (CNL), not otherwise specified (NOS) and unclassifiable MPNs. PV, ET and PMF together are also classified as classical MPN. PV is characterized by excessive production of progenitors and mature cells in erythroid lineage. ET is featured with hyperplasia in megakaryocytic lineage. PMF is a more aggressive disease than PV and ET with bone marrow fibrosis and megakaryocytic lineage expansion as main features(23).

1.2.1 Overview of genetic pathogenesis of MPN

The genetic basis of classical MPNs has been extensively studied. A single amino acid mutation of Janus Kinase 2 (JAK2), named *JAK2V617F* mutation, is present in more than 95% of PV patients and over 50% of ET and PMF patients(27–30). *JAK2V617F* is the main causative mutation of the disease and its discovery has changed the genetic landscape of MPN. *CALR* mutation is the second most frequent mutation following *JAK2V617F* and is present in 25-35% of ET and PMF patients(31,32). Mutation of thrombopoietin receptor (*MPL*) is the other main driver that contribute to 3-5% of ET and PMF(33,34). The three mutations occur in an almost mutually exclusive way, although few cases of co-occurrence have been reported(35–38). Patients who carry none of these three mutations are reported to be polyclonal and classified as “Triple negative” patients(39).

Apart from *JAK2, CALR* and *MPL* mutations, many other mutations also contribute to MPN phenotype and the disease heterogeneity. Although most of them are not MPN-specific, these mutations are believed to play roles in different stages of MPN development including the initiation of clonal hematopoiesis, disease progression to secondary myelofibrosis and leukemic transformation(40–42). Multiple epigenetic regulators have been identified to carry somatic mutations in MPN patients such as *TET2, DNMT3A, IDH1/2, PRC1/2, ASXL1* and *EZH2*(40–43). These genes are involved in the regulation of DNA methylation and histone

modification(41). Several of these mutations, for instance *TET2* and *DNMT3A*, are believed to cause clonal hematopoiesis which is the prior step to establish MPN and other hematological malignancies. The term CHIP (clonal hematopoiesis of indeterminate potential) is used to describe this process(44–46). Both *DNMT3a* and *EZH2* mutations have been shown to induce myelofibrosis phenotype in mice in the presence of *JAK2V617F* mutation(47–49). Mutations of transcription factors such as *TP53, CUX1, RUNX1* are also among the frequent recurrent mutations of the disease. *TP53* mutation has been associated with leukemic transformation in MPN and poor prognosis of the disease(50,51). Mutations of splicing factors, particularly *SF3B1* and *SRSF2*, also occur in cohort of MPN patients(52).

1.2.2 Overview of MPN therapy

In comparison to the advanced progress in the knowledge of the disease genetic pathogenesis, the therapeutic need for MPN patients in clinic is still unmet. MPN patients suffer from various disease symptoms such as fatigue, inactivity and weight loss, a higher risk of thrombotic and hemorrhagic events, disease progression to secondary myelofibrosis and leukemia. Patients, in particular those with MF and high-risk PV, also have reduced life expectancy(53–56).

For low-risk PV and ET patients, since the disease might not affect overall survival, the treatment has been focused on symptomatic management, notably thrombosis and hemorrhage. Low-dose aspirin, phlebotomy and cytoreductive drugs have been used for this purpose for decades in the clinic. Among the cytoreductive drugs, hydroxyurea (HU) shows its superiority over pipobroman and busulfan, as the latter two drugs have proven to induce the risk of leukemic transformation(57–59).

In contrast to PV and ET, MF is a more aggressive disease with severe symptoms such as splenomegaly and anemia. Both life quality and expectancy are compromised in MF patients, which raised the need for more effective treatment. Allogeneic stem cell transplantation (allo-SCT) is the only curative treatment for MF, but carries a risk of graft-related complications and even mortality(60).

The discovery of *JAK2* mutation and the subsequent development of JAK1/2 inhibitor, in particular ruxolitinib, have improved the medical condition of the patients. Ruxolitinib has shown its efficacy in reducing splenomegaly and weight loss as well as the alleviation of systemic inflammation(61,62). Long-term treatment with ruxolitinib has also achieved reduction of mutant allele burden in some patients and improved overall survival. Ruxolitinib is the first approved targeted therapy in MPN, first in MF and later in PV (61–72). Despite its success in clinics, one should keep in mind that the drug is designed to target the kinase domain of both JAK1 and JAK2 kinase with no evidence of superior affinity against *JAK2V617F* mutant(73,74). Patients treated with ruxolitinib also rarely achieve complete molecular remission(64,66–68).

Therefore, the development of more effective JAK2 inhibitors including allosteric inhibitors are always ongoing and some of them are being tested in clinical trials(75–78).

Although restricted by its severe toxicity, interferon-α (IFNα) has emerged as a promising treatment in MPN. Pegylated IFNα has effectively reduced its toxicity and has been tested in clinical trial. Of a particular note is the high response rate of molecular remission in *JAK2* patients treated with IFNα, suggesting the treatment somehow selectively targets *JAK2* mutant clones with mechanism still elusive(79–81). Investigation of the efficacy and mechanism of IFNα is still particularly interesting for MPN researchers and clinicians.

1.2.3 JAK/STAT pathway and its central role in MPN pathogenesis

Janus kinase (JAK)/signal transducer and activators of transcription (STAT) pathway plays a central role in hematopoiesis and MPN pathogenesis. The pathway is the link between surface receptors that receive cytokine signals and the transcriptional regulation of responsive genes (15,82,83). JAK kinase family consists of 4 members including JAK1, JAK2, JAK3 and tyrosine kinase 2 (TYK2). Among them, *JAK1* and *JAK2* are essential genes. The deletion of *JAK1* leads to embryonic lethality in mice due to the lack of cytokine response(84). *JAK2* knockout mice are also embryonic lethal due to defect in hematopoiesis(85,86). Conditional knockout of the gene in adult mice causes impairment in erythropoiesis and thrombopoiesis as well as compromised development of monocytic and granulocytic lineages, suggesting its indispensable role in myeloid hematopoiesis(87). JAK3 regulates lymphopoiesis and deletion of *JAK3* gene in mice impairs lymphoid development(88,89). Patients carrying *JAK3* mutation reportedly develop immunodeficiency (90,91). TYK2 is particularly important for interferon response and IL-12/18 signaling(92,93).

Taken JAK2 as an example, the kinase mediates the downstream signaling of a number of type 1/2 cytokine receptors like erythropoietin receptor (EPOR), thrombopoietin receptor (TPOR), granulocyte-macrophage colony-stimulating factor (GM-CSF) receptor as well as members of interleukin (IL) receptors, which are essential to myeloid lineage development and differentiation(15,94,95). Once receptors bind to cytokines, they form homodimers and subsequently activate JAK2 to phosphorylate itself and cytosolic domain of the receptors. STAT molecules, mainly STAT3 and STAT5a/b are then engaged and are phosphorylated by JAK2. STAT form homo/hetero-dimers or even tetramers and translocate into nucleus for transcription regulation(96) (Figure 1.2). JAK2 kinase is constitutively associated with cytokine receptors but is activated only upon cytokine induction in healthy state. The structure of the kinase has been partially resolved and the important function domains are shown (Figure 1.3) (97,98).

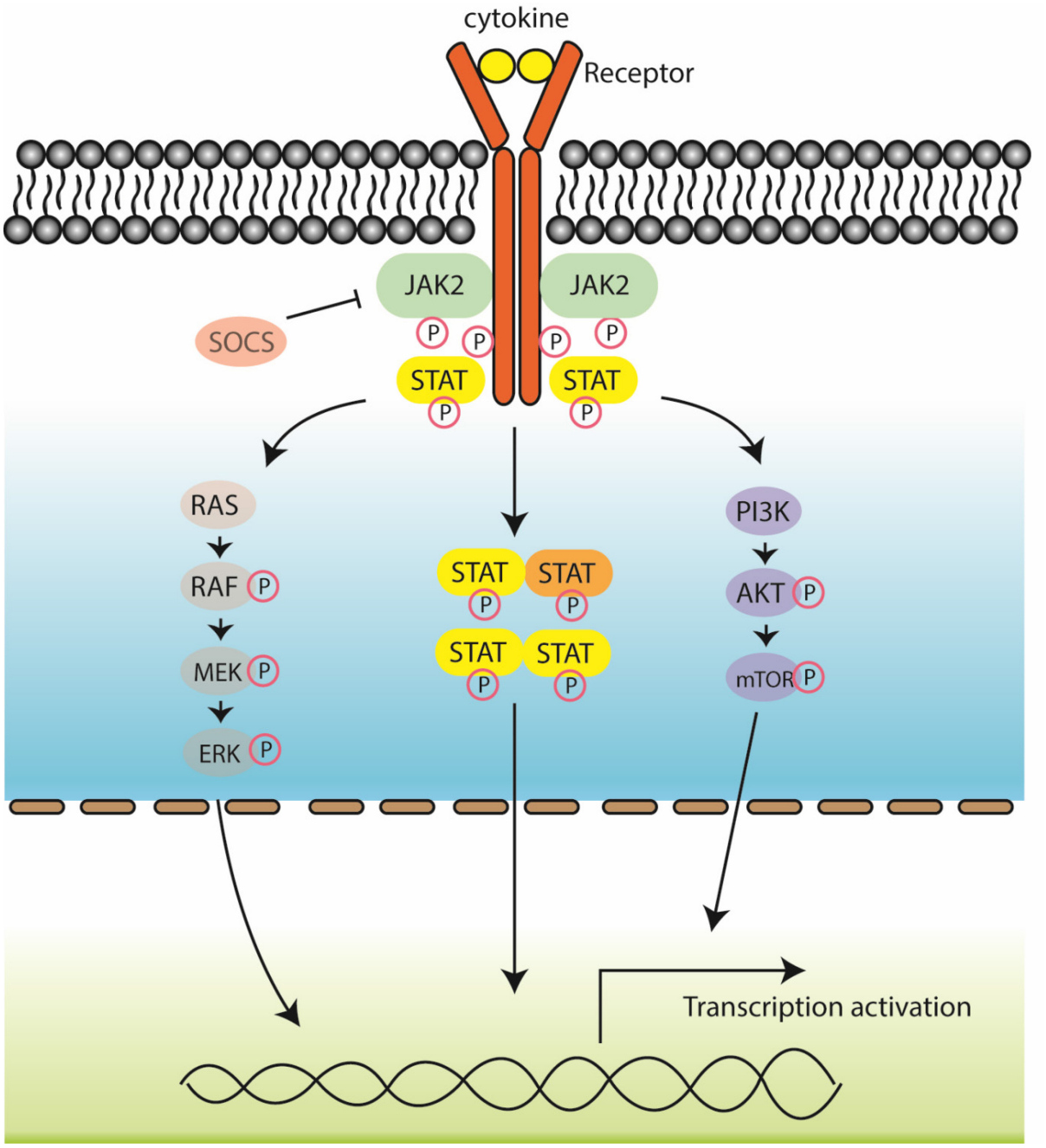

Figure 1. 2 Cytokine induced JAK-STAT pathway

Upon induction by cytokines such as EPO, TPO, GM-SCF, IL-3/5, cytokine receptors dimerize and activate JAK2 that phosphorylate and activate STAT3/5 as well as phosphotidylinositol 3-kinase (PI3K)/AKT/mTOR and mitogen activated protein kinase (MAPK) pathways. The downstream signaling pathways eventually activate transcription of pro-survival and proliferation genes. Negative regulators of the pathway such as SOCS and LNK were also mutated in small cohort of MPN patients(94,95,99,100).

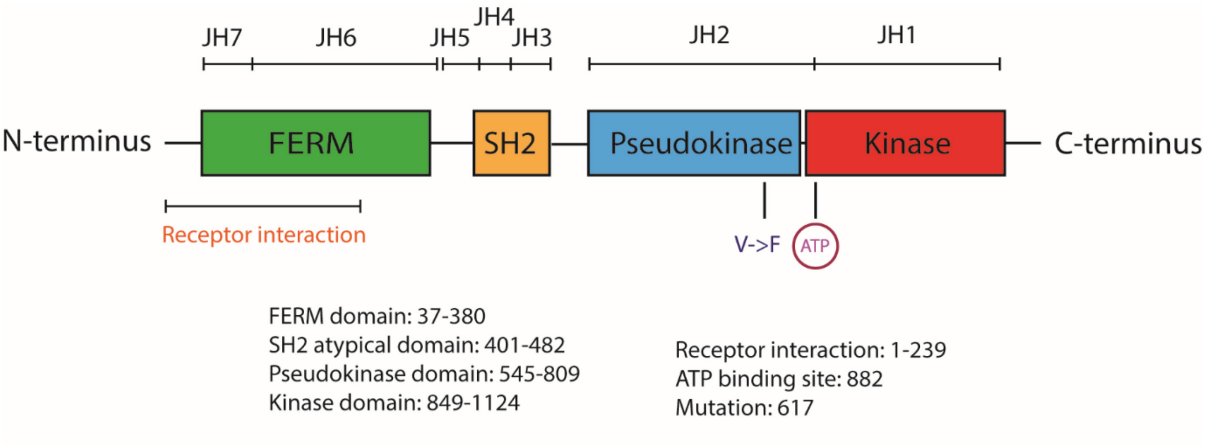

Figure 1. 3 Schematic structure of JAK2 kinase

JAK2 kinase is a tyrosine kinase with a length of 1132 amino acids. It consists of 4 functional domains including a FERM domain to mediate the binding with receptors, a Src-homology-2(SH2)-like domain for binding of phosphorylated tyrosine peptides, a pseudokinase domain for regulatory function of kinase activity and a ATP binding kinase domain(101). It also contains 7 Janus kinase homology (JH) domains (JH1-7) shared with other kinases in the family. The binding site of cytokine and interferon receptors is located at N-terminus. Pseudokinase domain plays a negative regulatory role in kinase activity. Structure information was collected from UniProt database(102,103).

STAT family consists of 7 members including STAT1, STAT2, STAT3, STAT4, STAT5a, STAT5b and STAT6 (104). Upon activation, oligomerization is formed through the N-terminal domain. Their transcription factor activity is mediated through the DNA-binding domain and the transactivation domain at C-terminus (Figure 1.4)(96). STAT1 is mainly activated by interferon receptors. *STAT1* knockout mice has impaired interferon signaling and immunodeficiency in response to viral infection(105,106). STAT2 is also involved in interferon signaling regulation by forming heterodimer with STAT1(107,108). STAT1 and STAT2 are linked with potential mechanism of interferon-α treatment in MPN patients(109–111). STAT4 and STAT6 are both regulators of T cell development by mediating IL-3 and IL-12 signaling(112–116). STAT5a deleted mice have impaired mammary gland development and a defect in lactogenesis(117,118). Sexual dimorphism is lost in STAT5b knockout mice(119). STAT3 is essential for early embryonic development(120). STAT3 and STAT5 are extensively associated with MPN disease, as they are constitutively activated in the presence of either *JAK2, CALR or MPL* mutations(121,122). STAT5a and STAT5b play an essential role in the establishment and development of *JAKV617F* driven PV, as the disease phenotype are abolished upon STAT deletion(123,124). Interestingly, although activated by JAK2 mutation,

STAT3 ablation exacerbate the disease in JAK2V617F mice by increasing thrombocytosis and reducing survival(122).

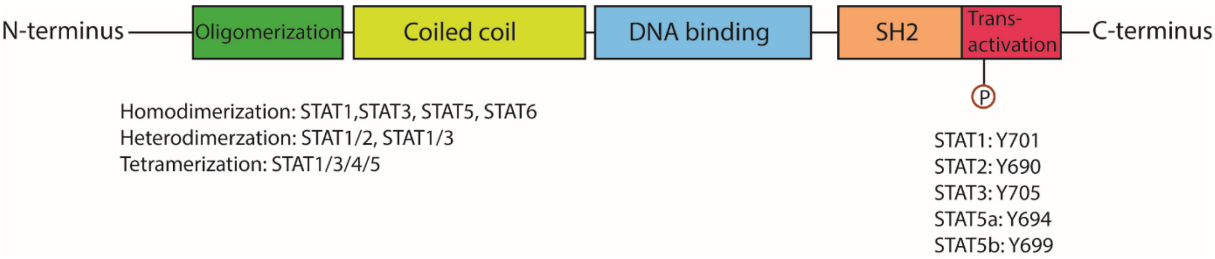

Figure 1. 4 Schematic structure of STAT protein

Human STAT family consists of 5 domains as showed. Tyrosine phosphorylation by JAK or other tyrosine kinases occurs at transactivation domain(102,103). Coiled coil domain is formed by 4 strands of helix and seems to mediate the nuclear exportation of STAT. All STAT family members could function as homodimers except STAT2 which requires dimerization with STAT1 in response to interferon stimulation(96,104).

1.3 Main driver mutations in MPN

1.3.1 *JAK2* mutation

As the most predominant somatic mutation present in BCR-ABL negative MPN, *JAK2V617F* occurs as a point mutation from G to T at the exon 14 of *JAK2* gene. The mutation substitutes a valine with phenylalanine in the pseudokinase domain of JAK2 kinase, blocking its inhibitory effect and therefore constitutively activates JAK2 kinase(27–30). The discovery of acquired uniparental disomy of chromosomal 9p (9pUPD) explains the frequent occurrence of homozygosity of the mutation(125). Other than V617F mutation, *JAK2* exon 12 mutations have also been identified in MPN. They occur at residues between 537 and 543 located at the linker between SH2 and pseudokinase domain(126). These mutations also lead to constitutive activation of JAK-STAT pathway but possibly act in a different mechanism compared with V617F mutation, as the former ones only present in PV but not ET and PMF patients(127).

Interestingly, *JAK2V617F* mutation could lead to both PV and ET and the mechanism of disease subtype selectivity is still elusive. *JAK2V617F* allele burden seems to be highly relevant to MPN disease phenotype, as ET patients tend to have low burden (around 25% or lower) and PV patients tend to have higher burden (around 50% or higher). Secondary PV and ET patients are often to be fully clonal(128–130). This correlation is also revealed in transgenic mice model, as mice with high copy number of *JAK2V617F* tend to show PV phenotype(131,132).

1.3.2 *MPL* mutation

Liver is the primary organ for TPO production. TPO is crucial in megakaryopoiesis and thrombopoiesis by inducing CMP and MEP cells differentiating into megakaryocytic lineage. It also plays an important role in stem cell maintenance. Instead of transcriptional level of modulation, the regulation of TPO relies on a negative feedback that platelets internalize TPO to reduce its circulated abundance. Therefore, high circulating TPO is observed in both thrombocytopenia patients and *MPL* knockout mice model(133,134).

As the receptor of TPO, MPL is expressed mainly in HSCs and megakaryocytic lineage (Figure 1.5). It seems that *MPL* is not essential for the development of other hematological lineages as *MPL* knockout mice have normal blood count except megakaryocytes and platelets(133).

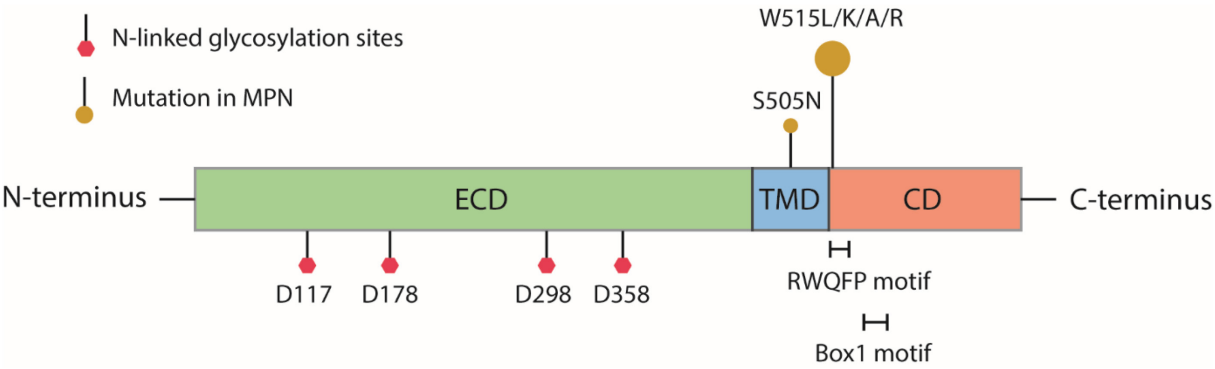

Figure 1. 5 Schematic structure of thrombopoietin receptor

The receptor has 635 amino acids, consisting of an extracellular domain (ECD), a transmembrane domain (TMD) and a cytosolic domain (CD). A signal peptide is located at the first 25 amino acids at N-terminus(134). 4 N-linked glycosylation sites are identified at ECD of the protein which mediate the trafficking of the receptor(135). Although crystal structure of the receptor is not resolved, predication of the structure could be obtained through the sequences in homology with other type-1 cytokine receptors. TMD and the adjacent amphipathic helical RWQFP motif block the activation of the receptor without the cytokine(136). Box1 motif at the CD is required for the docking and activation of JAK2(137,138). The activation of the receptor requires homodimerization like the other type-1 cytokine receptors such as EPOR and GM-SCF receptor(139).

Tryptophan 515 located at the boundary of TMD and CD is the mutation hotspot in ET and PMF patients. The most common mutation is W515L followed by W515R(34,140). Other missense mutations at the same position also occur in small cohort of patients. Serine 505 is another site where mutations are identified in MPN, although the frequency is much lower(141). All these mutations are located at the RWQFP motif or TMD, leading to cytokine-independent

activation of the receptor and the downstream JAK-STAT pathway. Unlike *JAK2V617F* and *CALR* mutations, no knock-in mouse model for *MPL* mutations have been described. Instead, retroviral-transduced transplantation model suggest an ET to MF phenotype which also significantly reduce the life expectancy of the animals(41).

1.3.3 *CALR* mutation

The discovery of *CALR* mutation in MPN was a surprise finding, as calreticulin had not been connected to the disease pathogenesis before(31,32). Wild type calreticulin is a 46kDa protein located primarily in endoplasmic reticulum (ER) lumen (Figure 6). The main functions of the protein are the maintenance of calcium (Ca2+) homeostasis in ER and as molecular chaperone for quality control of protein folding(142–144). Apart from that, surface localization of calreticulin on apoptotic cells has been found as a signal to macrophages for being cleared up(145). The structure of calreticulin has been partially resolved, as the X-ray crystal structure of globular domain has been published and nuclear magnetic resonance (NMR) of P-domain is also available (Figure 1.6)(146–148).

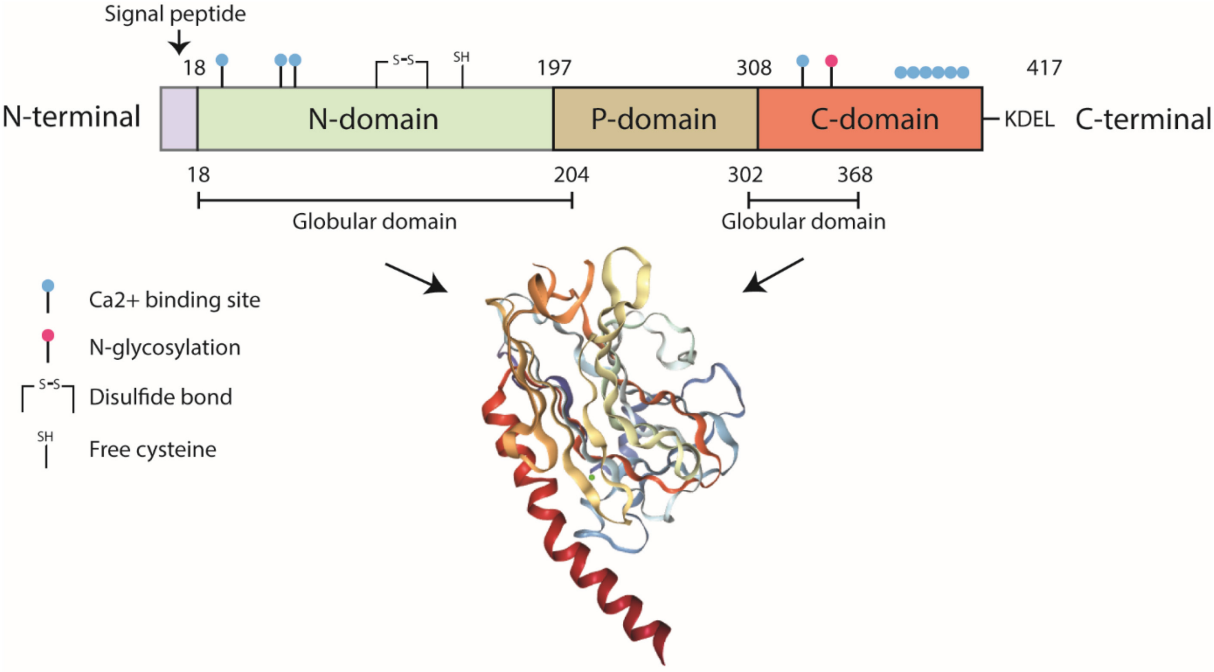

Figure 1. 6 Schematic structure of human wild type calreticulin

Human calreticulin consists of 417 amino acids, containing an N-terminal ER signal peptide, an N-domain, P-domain, C-domain and an ER-retention signal (KDEL) at C-terminus. The globular lectin domain has a jelly-roll structure with two anti-parallel β-sheets formed by N-domain and part of C-domain. An extended α-helix structure is formed by a stretch of C-domain. The surface patches of lectin domain bind to glycosylated or non-glycosylated protein for the protein chaperone function(146,148).

4 amino acids at N-domain form interaction with a Ca2+ ion, which is important for maintaining the secondary structure of the protein. An intra-molecular disulfide bond is formed between C105 and C137, leaving a free cysteine (C163) which might be involved in inter-molecular interaction. The majority of P-domain and the C-terminal part of C-domain was deleted in the crystallography study due to its flexible structure. P-domain is proline-rich and has an extended arm-like structure, revealed by NMR study(147). It is where the oxidoreductase ERp57 binds and is crucial for the molecular chaperone function. The C-terminus of calreticulin contains several stretches of negative charged amino acids that bind to Ca2+ with high capacity, serving as the structure basis of the Ca2+ buffering function of the protein. The last 4 amino acids KDEL make a ER retention signal which is responsible for the ER localization of the protein.

Calreticulin is the main protein in the ER that have high capacity Ca2+ binding sites(149,150). They are the key regulators of Ca2+ storage in the ER lumen and hence mediate the cytosolic Ca2+ concentration(144). As the fluctuation of Ca2+ concentration could trigger a variety of signaling and its homeostasis is essential for the function of many intracellular proteins, ER storage of Ca2+ is tightly regulated by the ER membrane transporters and Ca2+ buffering proteins. In the case of calreticulin deficiency or overexpression, Ca2+ storage capacity is heavily affected and therefore the regular release/influx of Ca2+ into cytosol cannot be maintained (Figure 1.7)(151–153).

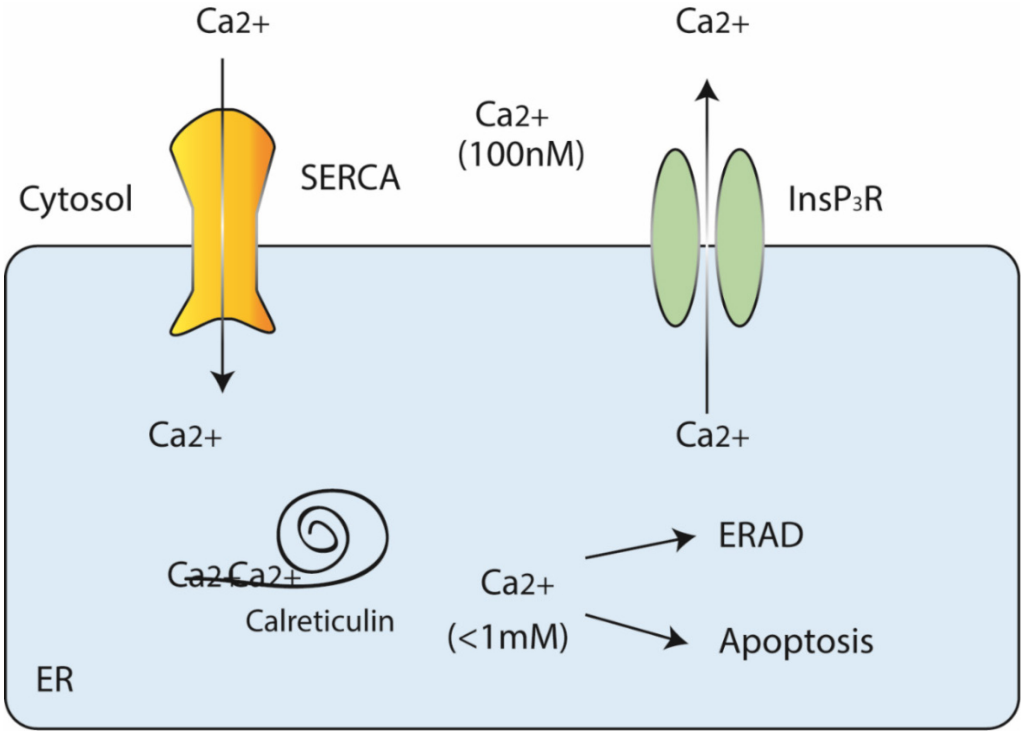

Figure 1. 7 Calcium buffering function of calreticulin

The acidic region at C-terminus of calreticulin has high capacity (25mol/molecule) and low affinity binding to free Ca2+. This allows calreticulin to be the main Ca2+ buffering protein in the ER, responsible for more than 50% of the Ca2+ storage. Ca2+ homeostasis is important for both the signaling cascades inside ER such as ERAD or apoptotic pathway and the release of the stored Ca2+ to cytosol where Ca2+ concentration is approximately 100 times lower than that in the ER(144). Sarcoplasmic/endoplasmic reticulum Ca2+-ATPase (SERCA) and inositol 1,4,5-trisphosphate receptor (InsP3R) are the transporters for Ca2+ exchange between ER and cytosol(154,155).

The molecular chaperone function of calreticulin relies on its glycan binding domain and its vicinity to interact with glycosylated or non-glycosylated proteins(156). The concave β-sheet of the protein contains a cavity binding to tetrasaccharide of the glycosylated protein(Figure 1.8)(157). Calreticulin and its ER membrane-bound homologs calnexin create calreticulin/calnexin cycle for the quality control of N-linked glycosylated proteins (Figure 1.9)(143,158,159). The chaperone functions of calreticulin and calnexin are partially redundant with some shared substrates identified(160–162). Cells carrying loss-of function mutations of calreticulin still retain chaperone activity compensated by calnexin(143). Independent from its glycan binding activity, calreticulin also mediates folding of non-glycosylated proteins. The most extensively studied example is the binding of calreticulin to β2-microglobulin (β2M) in the process of folding and loading of major histocompatibility complex (MHC)-class I complex(163–165).

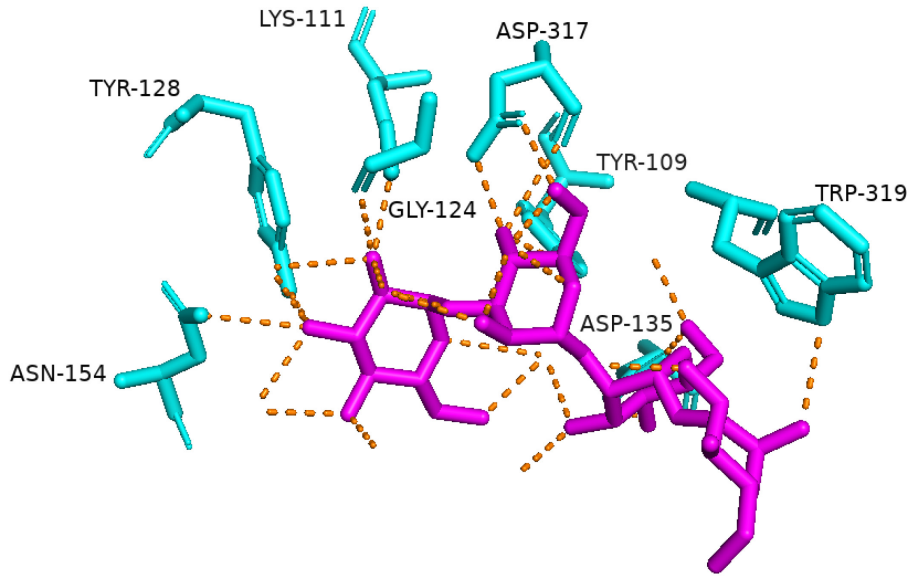

Figure 1. 8 Zoom in structure of calreticulin lectin domain interacting with carbohydrate

The glycan binding domain of calreticulin is located in the cavity of the lectin domain. One glucose and three mannoses (labeled magentas) from the carbohydrate chain of the mono-glucosylated protein interact with a couple of amino acid residues (labeled cyans) through hydrogen bonds (labeled orange dashes). Mutations of these residues could lead to defects of calreticulin chaperone activity on N-linked glycosylated proteins(148,166,167).

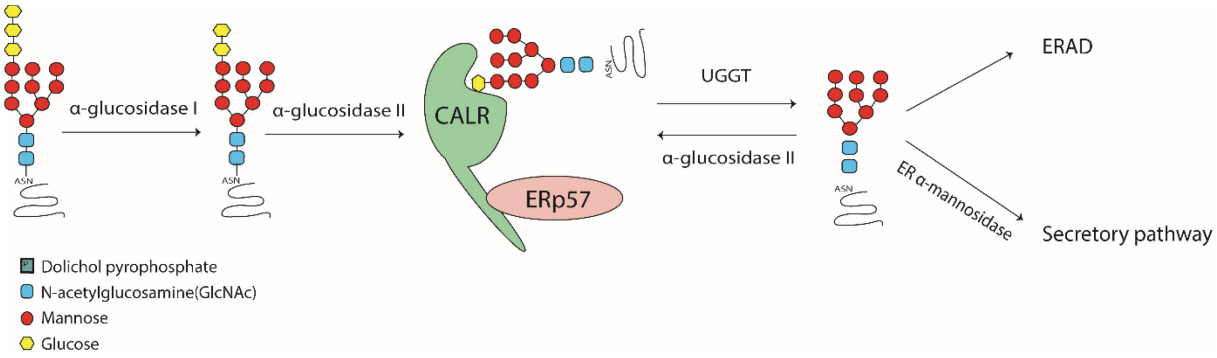

Figure 1. 9 Calreticulin/Calnexin cycle for N-linked glycosylated protein in ER

Calreticulin and its homologous lectin protein calnexin function as molecular chaperone for N-linked glycosylated protein. In ER lumen, after being catalyzed by α-glucosidase I and II to remove 2 glucoses on the oligosaccharide chain of the newly synthesized protein, the mono-glucosylated protein enter calreticulin/calnexin cycle by interacting with their lectin domain. Together with ERp57, calreticulin/calnexin facilitate the proper folding of the protein. As a quality control step, UGGT and α-glucosidase II decide whether to exit the cycle by removing or adding back the last glucose on the sugar chain of the protein. Until the protein is properly folded, the last glucose will be removed and the protein move on to the next step of the process of being catalyzed by ER α-mannosidase I/II before being secreted out of ER. Alternatively, improperly folded protein will be degraded through endoplasmic-reticulum-associated protein degradation (ERAD) pathway(158,159,161).

The study in transgenic mouse model has shown that calreticulin is essential for early cardiac development, as knockout of *CALR* causes defects in cardiomyeogenesis and leads to embryonic lethality(151). This is due to that calcium homeostasis cannot be maintained in the absence of calreticulin, supported by that ectopic expression of calcineurin in heart could rescue the embryos(168). Calreticulin might also be crucial to the central nervous system (CNS) development at embryonic stage, as a defect in neural tube closure has been observed in *in*

vitro culture of *CALR* -/- embryonic stem cells(151,153). Calreticulin expression in cardiac tissue, brain and liver is high in early embryonic stage but is later downregulated during development. In fact, many *CALR* -/- cell lines are viable and the embryonic development of organs other than heart and CNS does not dependent on calreticulin, indicating that whether CALR is essential in adult mice still needs to be clarified. Moreover, the essentiality of the gene in early tissue development is mostly associated with its function in calcium homeostasis rather than its chaperone function(143).

CALR mutations are a group of insertion and deletions located at the exon 9 of *CALR* gene, all leading to +1 frameshift and a novel C-terminal peptide sequence (Figure 1.10). Deletion of 52bp (del52), named type-I mutation, and insertion of 5bp (Ins5), named type-II mutation, are the most frequent mutation types identified in approximately 85% of *CALR* patients. The rest of *CALR* mutations can be categorized into type I-like or type II-like mutations. The mutations substitute the C-terminal acidic residues of calreticulin with an arginine/lysine-rich basic peptide and remove the KDEL ER retention sequence(31,32). Heterozygous mutation is the predominant form in clinical cases and very few patients carrying homozygous *CALR* mutation have been identified. Interestingly, the majority of homozygous mutations are type-II and the reason for this is unclear. Type-I mutation has higher penetrance of PMF, but the patients have better prognosis than those with *JAK2* or type-II *CALR* mutations(169–171). *CALR* patients also tend to have higher allele burden than *JAK2* patients, suggesting the *CALR* mutation might be a stronger clonal driver than *JAK2* mutation.

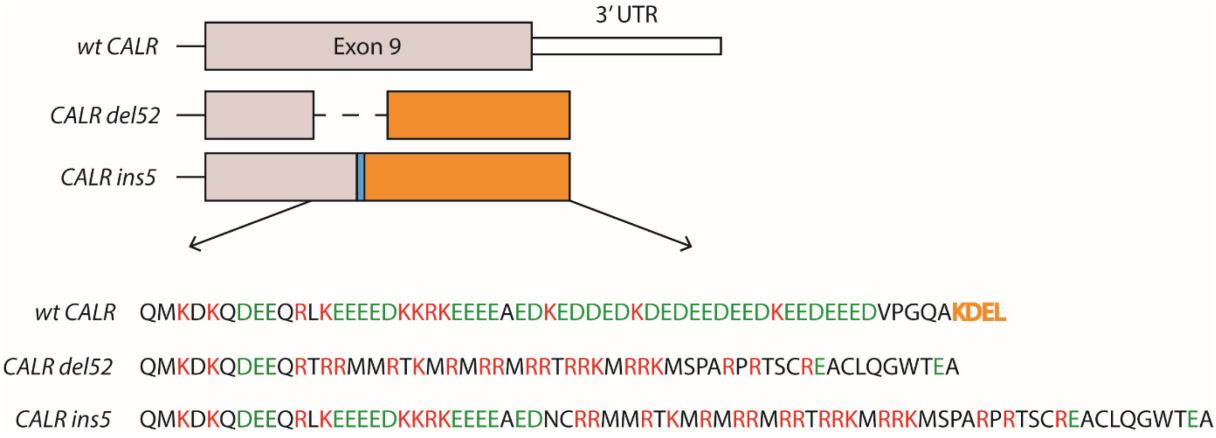

Figure 1. 10 Sequence alignment of type-I/II CALR mutations and WT CALR

CALR mutations are generated at the last exon of *CALR* gene. Both mutations replace the original acidic peptide at C-terminus with basic peptide sequence (colored orange). *CALR del52* mutation starts at Leucine 367 of the original protein sequence. *CALR ins5* starts at lysine 385 position and retains two more stretches of acidic sequence than *CALR del52*(172). Both mutations remove the KDEL ER retention sequence. Amino

acid sequence coloring: green indicates acidic/negatively charged amino acids; red indicates basic/positively charged amino acids.

1.4 Molecular pathogenesis of CALR mutation

Like *JAK2* and *MPL* mutations, *CALR* mutations also drive MPN disease by activating JAK-STAT pathway. STAT5 luciferase reporter assay in *JAK2* deficient γ2A cells and cytokine-independent growth of BaF3 cell lines have been used as the most common models to study this. It has been revealed that mutant calreticulin depends on MPL for its activity, as both STAT5 activation and cytokine-independent growth of Ba/F3 cells requires the presence of MPL (Figure 1.11)(173–178). This also explains why *CALR* mutations are only present in ET and PMF patients but not in PV patients, considering MPL is mainly expressed in megakaryocytic lineage. Interestingly, when mutated, calreticulin has been found to form a stable complex with MPL and activate it constitutively regardless of cytokine presence(178,179). The mechanism of how this interaction is formed still requires further investigation, but a couple of discoveries have helped to elucidate this. Firstly, the binding and activation of MPL by mutant calreticulin requires its N-glycan binding domain, as glycan-deficient *CALR del52* is unable to activate JAK-STAT pathway(173). Several studies also show that this protein-protein interaction could not be maintained when certain amino acid residues at this domain is mutated(179,180). Secondly, since N-glycan binding domain is located at the common part of wild type and mutated calreticulin, it is reasonable to hypothesize that the mutant peptide at C-terminus plays a role in the binding mechanism. Araki and his colleagues has proposed a P-domain interference model. In this model, N-domain of calreticulin is able to bind to MPL but the binding is inhibited by its P-domain. The mutant C-terminus blocks the inhibitory effect of P-domain and enables the interaction to occur(178). They have also showed that unlike wild type form of the protein, mutant calreticulin tend to form homomultimerization due to its novel C-terminus. They also bind to MPL as multimers(181). Moreover, Elf and the colleagues have shown that the positive charge rather than the actual amino acid sequence of the mutated C-terminal tail is the key for the oncogenic activation, as substitution of lysine and arginine residues with glycine abrogates its activity whereas changing the neutral residues do not show such effect(177).

The localization of mutant calreticulin is also intriguing. Since the ER retention signal is lost, mutant form of the protein is expected to leave ER. Indeed, mutant calreticulin is primarily located in Golgi apparatus, supported by both immunofluorescence and subcellular fractionation experiments(173,180). Cell surface localization of MPL-CALR complex has also been detected and is believed to be essential for the oncogenic activity by a recent study from Pecquet and the colleagues. They show that whether mutant CALR is able to activate a few traffic deficient MPL mutants depending on whether MPL could travel to the cell surface. Also,

the ER signal peptide is required for the oncogenic function of mutant calreticulin, suggesting that the MPL-CALR interaction starts from ER(180). Another important finding, firstly made by Han and the colleagues, is mutant calreticulin is secreted out of cells and brefeldin A increases the intracellular abundance of the protein(182). This could explain the observation that mutant form of the protein seems to be much less abundant compared with the wild type form whereas no proteasome or lysosome inhibitors could rescue it.

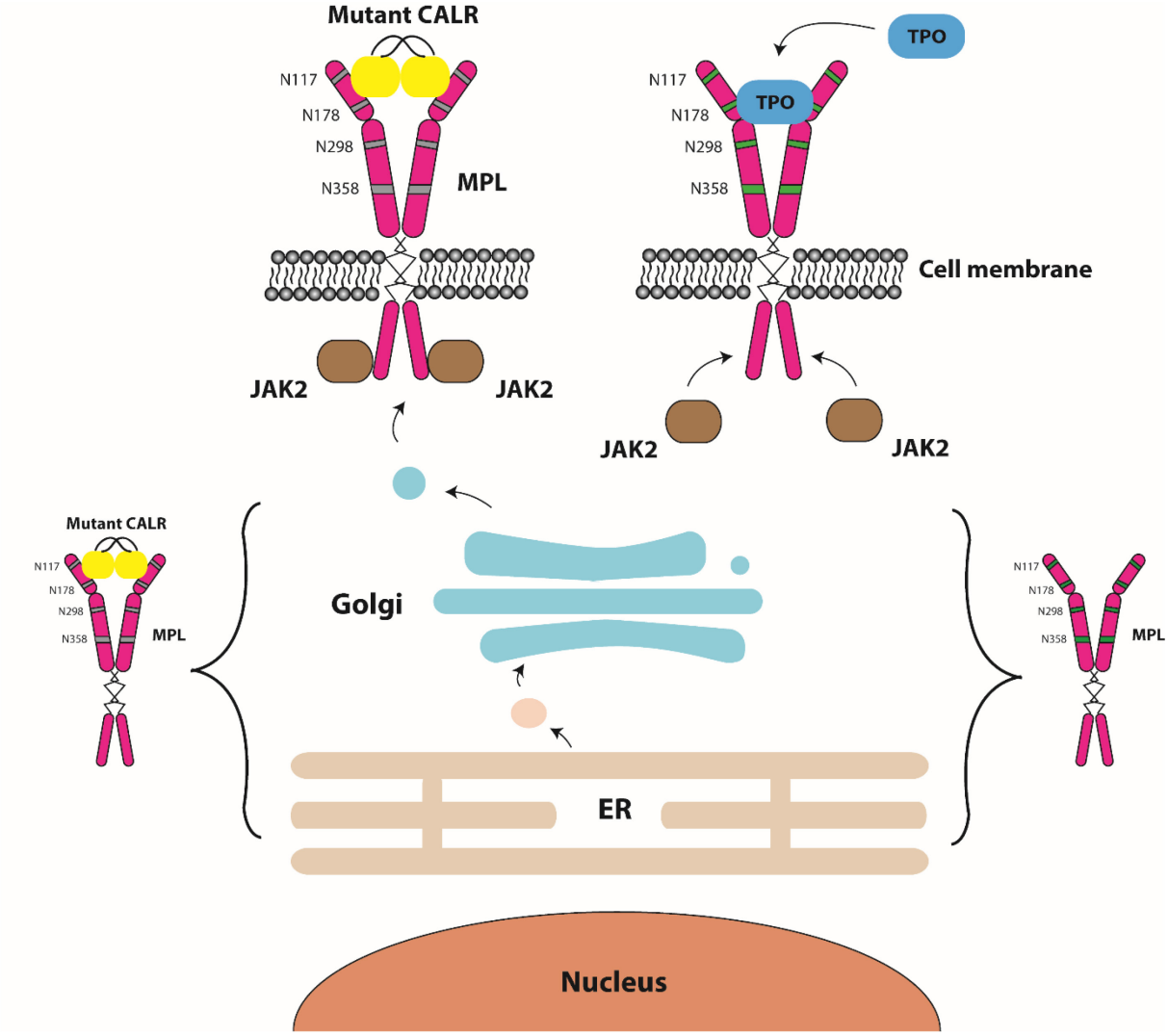

Figure 1. 11 Mechanism of mutant calreticulin in MPN

In normal physiological condition, MPL goes through N-glycosylation process and traffic to cell surface where it is activated only in the presence of TPO. Wild type calreticulin is primarily located in the ER and might have a temporary interaction with MPN during the glycosylation process. In *CALR* mutated ET and PMF patients, mutant calreticulin binds to the extracellular domain of MPL in the ER and the complex then traffics to Golgi apparatus through secreted vesicles before making its way to the cell surface membrane. The surface located CALR-MPL complex constitutively activate

JAK-STAT pathway independent from TPO binding. The N-glycosylation sites of MPL, particularly N117, are crucial to its activation by mutant calreticulin. Immature glycosylated form of MPL has been found in mutated *CALR* cells(173).

Additionally, a couple of *in vivo* studies of mutated *CALR* in mice model have been published. Marty and her colleagues first generated a retrovirally transduced-transplantation model using both type I and type II mutant *CALR*. The primary transplanted mice develop an ET-like phenotype with thrombocytosis as the main disease feature. Secondary transplanted mice develop myelofibrosis and splenomegaly. Mice carrying type I mutation have stronger phenotype than type II mutation(174). Shida and colleagues generated a transgenic model by ectopically express cDNA encoding *CALR del52* under H2K promoter. The mice develop thrombocytosis but not myelofibrosis or leukocytosis(183). Li and co-workers generated conditional knock-in *CALR del52* model and investigated the phenotype under Mx1-Cre and Vav-Cre. Although both heterozygous and homozygous model show ET phenotype, the latter one has a much stronger phenotype with higher platelets count and transformation into myelofibrosis featuring bone marrow fibrosis, splenomegaly and reduced hematocrit(184). Unexpectedly, neither Shida nor Li's mice model shows competitive advantage of mutant cells over wild type cells in the transplantation assay(183,184). However, a concrete conclusion requires further *in vivo* studies.

1.5 DNA replication stress

DNA replication stress occurs when the progression of DNA replication faces obstacles during S-phase. Although referring to the term of replication stress (RS), it is not a single defined biological phenomenon due to its complexity, as the actual physical structure and the molecular response vary in different conditions. In general, RS is often associated with stalled replication forks, exposure of stretches of single-strand DNA (ssDNA) and the involvement of ataxia telangiectasia and Rad3-related protein (ATR)-checkpoint kinase 1 (CHK1) pathway in response to the stress. The source of the stress inducers could be exogenous, such as DNA damaging agents, antimetabolite and UV lights, causing DNA lesions that serve as physical obstacles to DNA replication. Alternatively, endogenous source of stress inducers can also cause RS. Uncoordinated replication and transcription, DNA secondary structure caused by certain nucleotide sequences and incorporation of ribonucleotides during replication are sources of RS.

Once DNA replication stress is induced, ATR-CHK1 pathway plays a central role in the response pathway (Figure 12). As the first step, replication protein A (RPA) complex binds to ssDNA as a heterotrimer consisting of a 70kDa-subunit RPA1, a 32kDa-subunit RPA2 and a 14kDa-subunit RPA3(185–187). RPA trimer has 4 oligonucleotide/oligosaccharide-binding

(OB) domains for ssDNA binding(188). RPA2 subunit contains a couple of serine and threonine residues that are phosphorylated by cyclin-dependent kinases (CDKs) in G1/S phase transition or by the family members of phosphatidylinositol-3-kinase-like kinase family (PIKKs) in response to replication stress(189–192). RPA hyperphosphorylation coordinate DNA replication and DNA repair and is important for the cells to recover from RS(189,192,193). Apart from stabilizing ssDNA, RPA functions as the recruiter of other proteins which are needed for RS response. ATR-interacting protein (ATRIP) co-localizes with RPA-coated ssDNA and enables the engagement of ATR(194). ATR is a serine/threonine kinase which belongs to PIKK family. It autophosphorylates at T1989 site in the presence of RS or DNA damage and activates many downstream protein regulators(195). One of the important substrates is Histone H2AX which is phosphorylated at serine 139, referring to as γH2AX(196). γH2AX is the most commonly used DNA damage marker and is responsible for the engagement and activation of the DNA repair machinery(197). ATR also phosphorylate and activate the serine/threonine kinase CHK1(198,199). The kinase modulates cell cycle checkpoints control the phosphorylation of CDC25A/B/C, phosphatases that inhibit cyclin-dependent kinase activity(200). CHK1 also controls origin firing, as the inhibition of ATR or CHK1 causes an uncontrolled global origin firing and an exhaustion of RPA(201). The kinase is required for multiple DNA repair pathways such as homologous recombination and Fanconi anemia(202,203).

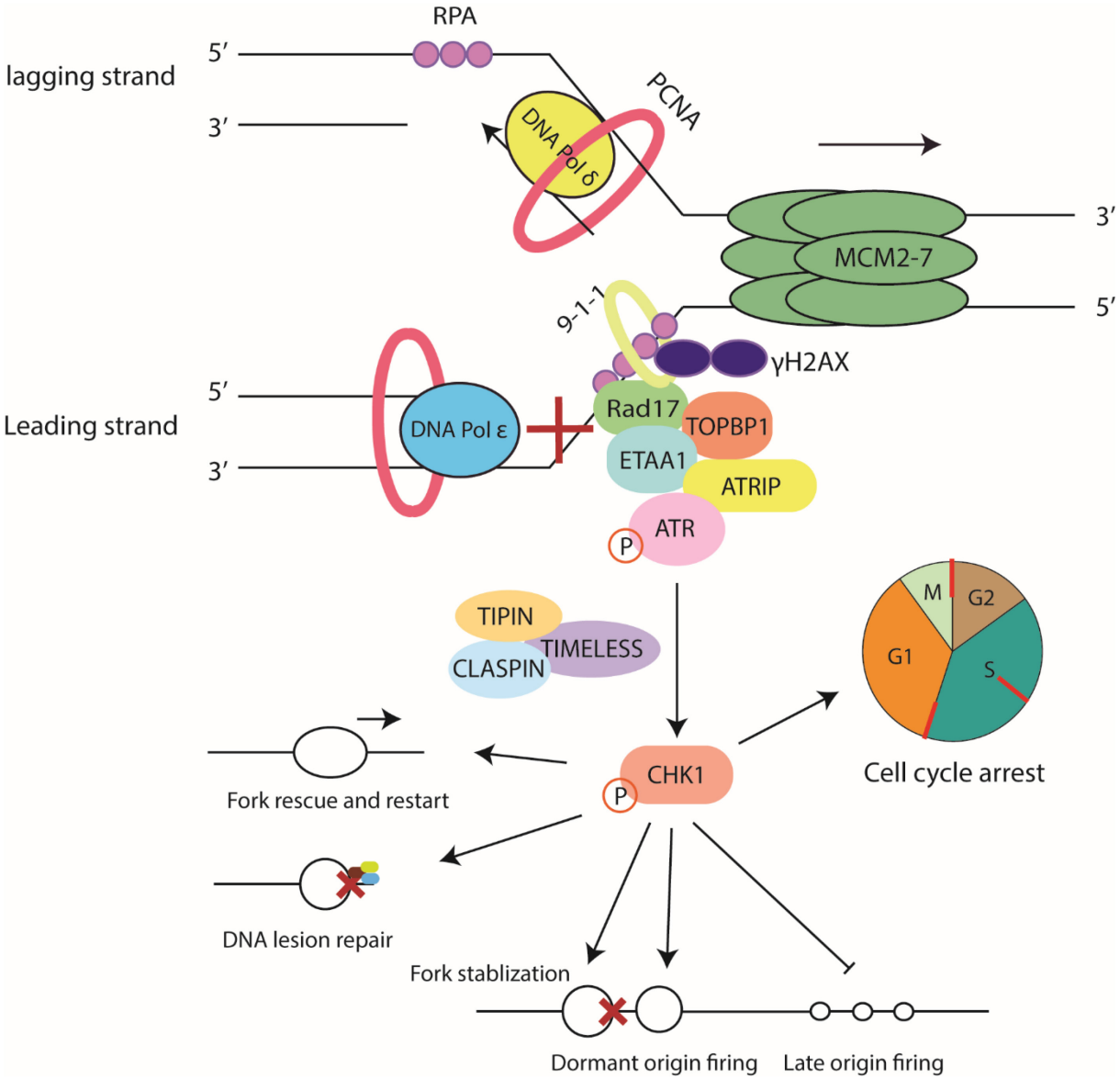

Figure 1. 12 DNA replication stress and the central regulation role of CHK1

In S-phase, once a replication fork is stalled, RPA is recruited to bind to the exposed ssDNA to stabilize it. ATR kinase is recruited to the locus through ATRIP and is activated by a protein complex consisting of Rad17, TOPBP1, 9-1-1 (RAD9-RAD17-HUS1) and ETAA1. ATR phosphorylates histone H2AX and CHK1 kinase through TIMELESS/TIPIN/CLASPIN complex. CHK1 subsequently regulate multiple biological processes responding to the stalled replication fork that include cell cycle arrest at G1/S, intra-S, G2/M phases, fork stabilization, inducing dormant origin firing, inhibiting late origin firing, fork rescue and restart and initiating DNA repair(204,205).

1.5.1 Oncogene-induced replication stress

Additionally, multiple oncogenes have been shown to induce RS and consequently genomic instability as a hallmark of cancer. For instance, it has been revealed that MYC co-localizes

with pre-replication complex and regulates replication origin activity. The overexpression of *c-MYC* generates RS and DNA damage(206). Overexpression of *H-RAS* induces RS by increasing the global transcription activity and causing the accumulation of RNA-DNA hybrids (R-loops)(207). Ectopic activation of cyclin E and CDC25A inhibits the progression of replication forks and induces DNA damage response(208). AKT activation causes replicative senescence or apoptosis through the induction of reactive oxygen species (ROS)(209). The mechanisms of the oncogene-induced RS are still not fully understood, but increasing number of oncogenes have been linked to RS.

1.5.2 Targeting ATR-CHK1 pathway

The dependence of ATR-CHK1 pathway in coping with oncogene-induced RS could give cancer cells vulnerability to inhibitors targeting this pathway. For this rationale, a number of inhibitors have been developed to target ATR, CHK1 as well as another pathway component Wee1, the tyrosine kinase phosphorylating CDK1 at Y15. The majority of the inhibitors target the ATP binding site of those kinases and inhibit the kinase activity on its downstream target (Figure 13). A number of the inhibitors have been tested in clinical trials for the use in various cancer types, but often in combination with radio- or chemotherapy that can induce DNA damage or replication efficiency(210–215). The inhibitors are shown to enhance the efficacy of the DNA replication targeting agents, inducing DNA damage and impairing cell cycle checkpoint. Interestingly, it has been found that combinatorial targeting of CHK1 and Wee1 shows synergistic effect with the mechanism of releasing the unrepaired DNA lesions into mitotic stage(216,217). Moreover, synthetic lethal effect has been identified for ATR and CHK1 inhibitors when another key component of DNA damage response pathway is defective, for instance ATM and p53(218).

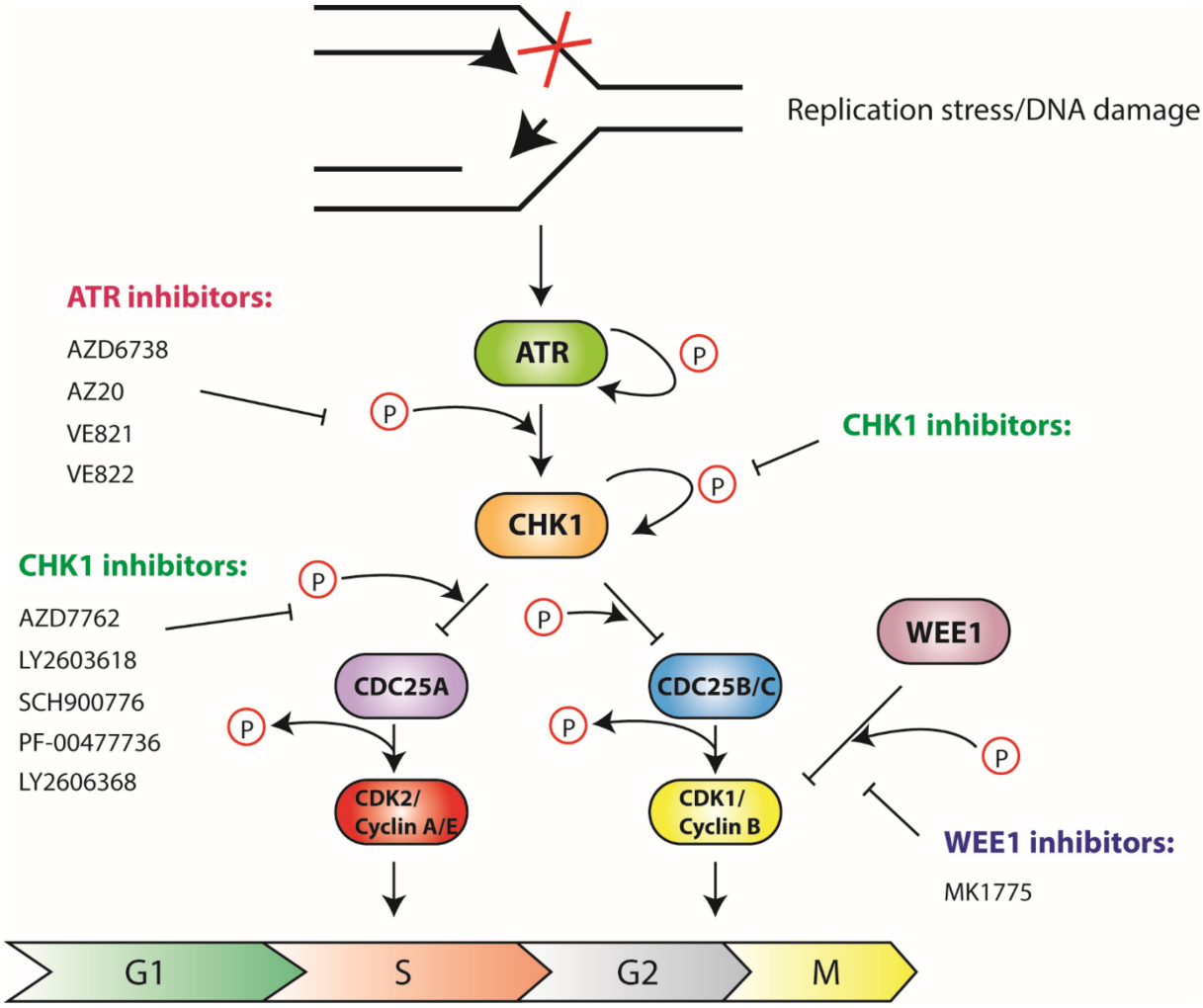

Figure 1. 13 Targeting ATR-CHK1 pathway by small molecule inhibitors

In response to DNA damage or replication stress, multiple kinases and phosphatases are involved in the central regulation of ATR-CHK1 pathway. Most of the available small molecular inhibitors are ATP competitors for kinases including ATR, CHK1 and WEE1. ATR inhibitors reduce the phosphorylation of CHK1 at S345 and therefore inhibit CHK1 kinase activity. CHK1 inhibitors stabilize phosphatases like CDC25A, CDC25B and CDC25C by suppressing their phosphorylation by CHK1 kinase. Some of them show inhibitory effect on the autophosphorylation at S296 of CHK1 kinase, but induce phosphorylation at S345. WEE1 has been identified as another kinase target in the pathway, as the inhibitor MK1775 shows synergistic effect when combined with CHK1 inhibitors(219,220).

1.6 Aims

The aim of the scientific projects in the thesis was to identify novel drug or target in the treatment of CALR mutated MPN including:

a) Explore the therapeutic potential of glycan binding domain of calreticulin by small molecule inhibitors
b) Establish CALR mutated cell line models for in vitro test of drug candidates
c) Ex vivo test of drug candidates using primary patient samples
d) Mechanistic study of drug candidates to explore vulnerability of CALR mutated cells
e) Establish high-throughput drug screening method to identify synthetic lethal partner of mutant calreticulin

2 RESULTS

2.1 Mutant selective small molecule inhibitors of calreticuliln for the treatment of CALR mutation positive myeloproliferative neoplasms

Prologue

Somatic mutations of CALR gene have been discovered as disease driver mutations of primary myelofibrosis and essential thrombocythemia, diseases that belong to the classical myeloproliferative neoplasms (MPN). The requirement of thrombopoietin receptor in the activation of the oncogenic function of mutant CALR has been described previously and the N-glycan binding domain of mutant CALR is found to be crucial to its downstream pathway activation. Here, we show that through an in silico molecular docking study, a chemical library targeting calreticulin is identified and further validated. Hematoxylin, together with its chemical analogues are found to be lead compounds targeting CALR N-glycan binding domain. CALR mutated cell lines show hypersensitivity to the treatment of hematoxylin. Knockout of calreticulin or truncation of its C-terminus can rescue this selective cytotoxicity. We demonstrate a direct binding of the compound to both mutant and wild type CALR as well as a disruption of the interaction between mutant CALR and MPL upon the compound treatment. Hematoxylin also reduces the intracellular abundance of mutant calreticulin by inducing the secretion of the protein. Altogether, we here propose the N-glycan binding domain of CALR to be an attractive drug target for small molecule inhibitors.

2.1.1 Molecular docking study identifies a chemical library as potential compounds targeting calreticulin

Based on the published crystal structure of the globular domain of wild type calreticulin (146,147,156,157), the lectin domain of the protein consists of an N-glycan binding site, an ATP binding site and a calcium binding site (Figure 2.1.1a). The N-glycan binding site is of particular interest based on the previous findings suggesting the importance of this domain in mutant CALR function. To validate the therapeutic potential of this domain in our models, we mutated human CALR del52 sequence at residue lysine-111 and aspartate acid-317 respectively (Figure 2.1.1b). These are two amino acid residues which are shown to be essential for the N-glycan binding capacity of calreticulin(157,167,221,222). We transduced Ba/F3-MPL cells with retroviral vectors carrying CALR WT and CALR del52 as well as the glycan domain mutated CALR del52 respectively. Both K111G and D317G mutations abolished the transforming properties of CALR del52 in Ba/F3-MPL cell line in the absence IL-3 or TPO, which confirmed the essentiality of N-glycan binding domain of mutant calreticulin in its oncogenic function (Figure 2.1.1c).

Since the pathological mutations of calreticulin in MPN only changes the sequence at the c-terminus of the protein, we expect the globular domain of the mutant protein to be conserved and the structure information based on the wild type protein can be used in the study. We therefore generated a 3D structural model based on crystallized structures of both human and mouse calreticulin and performed a molecular docking study to identify potential chemical candidates targeting this domain (Figure 2.1.1d). To get an insight on the specificity and selectivity of each ligand interacting with calreticulin, we selected two other proteins as negative controls including calnexin which is structurally and functionally similar to calreticulin, and ER Mannosidase I, an enzyme involved in ER-associated degradation of glycoproteins in mammalian cells but structurally different compared to calreticulin(223,224). Among 140000 structures, a list of compounds which have the highest binding energy and specificity to calreticulin was generated. By searching for the available compounds either commercially or from the DTP Databases of NCI, we managed to build up a docking compound library for experimental validation.

2.1.2 Hematoxylin selectively reduce the viability of CALR mutant cells compared to wild type cells

To exclude the compounds with low biological activity, we performed a cytotoxicity screen at 10uM concentration in Ba/F3-MPL and UT7-TPO cell lines carrying heterozygous CALR mutations. The chemicals which show cytotoxic effect in both cell lines (inhibitory effect >10%) and have more than 50% inhibitory effect in at least one of the cell lines were taken as hits for

the subsequent multiple-dose response test (Figure 2.1.2a). The hits were tested in both CALR wild type and mutant cell lines to acquire data of their cytotoxic selectivity. We identified hematoxylin, the compound predicted to form hydrogen bonds with 4 amino acids at CALR glycan domain through its hydroxyl groups, to be our top hit, as both heterozygous and homozygous mutant CALR Ba/F3-MPL cell lines showed hypersensitivity to the compound treatment compared with the wild type control (Figure 2.1.2b,c). In UT7-TPO cell lines, the hypersensitivity of mutant cell line to the compound also occurred despite a smaller effective magnitude and a higher drug concentration used (Figure 2.1.2d).

In order to further confirm the selective cytotoxicity of hematoxylin, we set up a two-color competition assay by co-culture of CALR wild type and mutant cells in the presence of the compound treatment (Figure 2.1.2e). In Ba/F3-MPL cells, the CALR mutant cells were rapidly depleted during the 7 days treatment while mutant cells gradually dominated the population by outgrowing the wild type cells in the DMSO control group. We used reverse-color setup to avoid potential artefact brought by mCherry expression and could reproduce the data (Figure 2.1.2f, S2.1.1). The differential killing effect of hematoxylin can also be observed in UT7-TPO cell lines. While the depletion effect was not achieved, hematoxylin inhibited the outgrowth of the mutant cells from the cell population (Figure S2.1.2). This result is consistent to the result in the short-term dose response assay. As the CALR mutant cells in this assay were cultured in the presence of TPO, it also suggests that the drug hypersensitivity cannot be rescued by the addition of cytokines.

To elucidate the mechanism of cell death caused by the drug treatment, an apoptosis assay by Annexin V/PI staining was conducted. We observed significantly elevated apoptosis induced by hematoxylin in CALR mutated cell line but not in wild type control. The addition of TPO did not have a significant impact on apoptosis (Figure 2.1.3a).

To validate target specificity, we first knocked out CALR in Ba/F3-MPL cell line and checked the dose response of hematoxylin. The removal of the expected target of the drug abolished the hypersensitivity we observed in the mutant cell lines (Figure 2.1.3b). To clarify if the efficacy is specifically caused by the mutant calreticulin, we used CRISPR-Cas9 technology to generate Ba/F3-MPL cell lines that carry the alternative frameshift mutations at the exon 9 of CALR gene, leading to the reading frame that encounters a stop codon shortly after the mutation and a truncation at CALR C-terminus (Figure 2.1.3c top panel). In the cytotoxicity assay, the cell lines carrying the truncated mutations did not show hypersensitivity to the drug treatment, suggesting the efficacy of hematoxylin is caused specifically by the mutant c-terminus (Figure 2.1.3c bottom panel). Furthermore, we tested the drug effect in cells carrying JAK2V617F mutation and did not observe any vulnerability (Figure S2.1.3), indicating specific drug effect on CALR mutations but not JAK2 mutations or activated JAK-STAT pathway.

2.1.3 Hematoxylin binds to calreticulin and disrupt MPL interaction with mutant CALR

As the glycan binding domain might mediate the interaction of MPL and mutant CALR, we hypothesized that the binding of a docking compound could disrupt this interaction. Therefore, we used NanoBRET assay to measure CALR del52-MPL interaction. EPOR was used as a background control, as the receptor has large in homology sequence with MPL and no interaction was supposed to form with CALR del52. As expected, the addition of hematoxylin reduced CALR-MPL interaction in a dose-dependent manner, indicating that the occupancy of glycan binding pocket by the drug blocked MPL binding to mutant CALR (Figure 2.1.4a). To further prove the direct binding of the compound to calreticulin, we performed cellular thermal shift assay (CESTA)(225,226). Calreticulin ins5, wild type and MPL were transfected into HEK293T cells and hematoxylin was added into the cell lysates. The melting temperatures of both mutant and wild type calreticulin were increased compared with DMSO control, suggesting the expected target engagement of the drug. This is not surprising to us that the drug binds to both mutant and wild type proteins, since the target region is a common domain. We also used MPL as a control protein in the assay to test the specificity of the drug. The drug-treated sample showed no significant change in MPL protein level in response to heat compared with the DMSO control (Figure 2.1.4b).

2.1.4 Hematoxylin reduces mutant calreticulin and inhibits STAT5 activation

To investigate how hematoxylin affects mutant calreticulin as well as JAK-STAT signaling, we treated Ba/F3-MPL CALR WT and mutant cell lines with the drug for 24h and collected both RNA and protein samples. The real-time PCR result suggested a less than 1.5-fold up-regulation of both wild type and mutant CALR expression caused by the drug treatment, possibly due to a stress response (Figure 2.1.5a). Interestingly, western blot analysis showed a striking down-regulation of both mutant calreticulin and MPL in both heterozygous and homozygous mutant cell lines, whereas the wild type calreticulin was not affected in CALR WT cell line. There was an up-regulation of wild type calreticulin in CALR heterozygous mutant cell line, which was likely due to a stress response effect caused by the drug (Figure 2.1.5b). A time-course experiment showed a decrease of mutant calreticulin and MPL starting from 4 hours post treatment and more drastic reduction at 8-hour time point, which was accompanied by a decrease of STAT5 phosphorylation and upregulation of PARP cleavage which was used as an apoptotic marker (Figure 2.1.5c). The result suggests that hematoxylin may induce cell death of mutant CALR cell lines by inhibiting mutant calreticulin-MPL complex at protein level as well as its downstream JAK-STAT pathway. Combined with the real-time PCR result, we hypothesized that this downregulation of mutant CALR was due to post-translational modification or protein secretion. We used MG132 as proteasome inhibitor and chloroquine as

lysosome inhibitor. Neither the two inhibitors managed to rescue the reduction of mutant CALR. In contrast, brefeldin A (BFA), the drug that inhibits protein secretion, drastically upregulates mutant CALR level and could regain the loss of the protein induced by hematoxylin (Figure 2.1.5d). This result indicated that the reduction of mutant CALR by hematoxylin might be a consequence of increasing secretion of the protein out of the cells. We also generated hematoxylin resistant cell lines by incubating CALR mutant cells with high dose hematoxylin continuously. All the selected clones showed an upregulation of mutant calreticulin and resistance to the drug-induced reduction, revealing a universal hematoxylin resistant mechanism (Figure S2.1.4).

2.1.5 Potency and selectivity of chemical analogs of hematoxylin

Compared with the synthetic tetrasaccharide G1M3, hematoxylin also contains several hydroxyl groups that are predicted to form hydrogen bonds with amino acid residues in the glycan binding pocket of CALR. To explore the chemical space of our docking study, we tested a few chemical analogs based on hematoxylin structure. We could identify a couple of chemicals that also preferentially killed CALR mutant cells. Brazilin, the closely related natural compound of hematoxylin, showed the lowest IC50 among all the compounds tested. Methylation of the hydroxyl groups of hematoxylin seemed to reduce the potency of the drug and the change of the poly-heterocyclic ring structure largely compromised the selectivity (Figure 2.1.6, S2.1.5).

2.1.6 Hematoxylin showed selective cytotoxicity in patient CD34+ cells

To further validate our result in primary patient samples, we isolated CD34+ cells from healthy individuals and CALR patients and performed the colony formation assay. The compound showed significant inhibitory effect on colony forming units from CALR patients, which suggested the efficacy of the drug can be translated into patient samples (Figure 2.1.7a).

Figure 2.1. 1 Molecular docking of calreticulin glycan binding domain

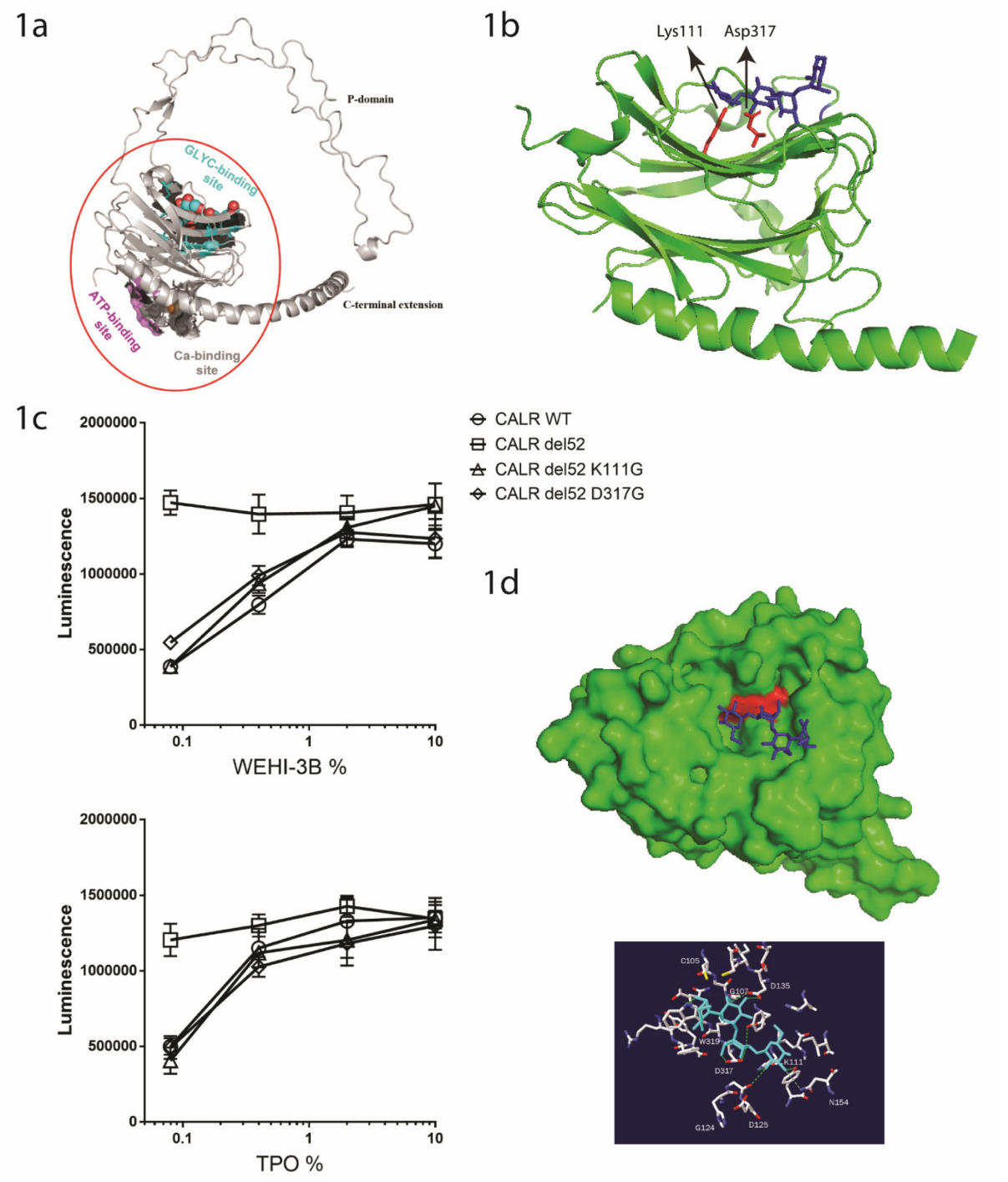

Figure 2.1. 2 Cytotoxic selectivity of hematoxylin in CALR mutated cell lines

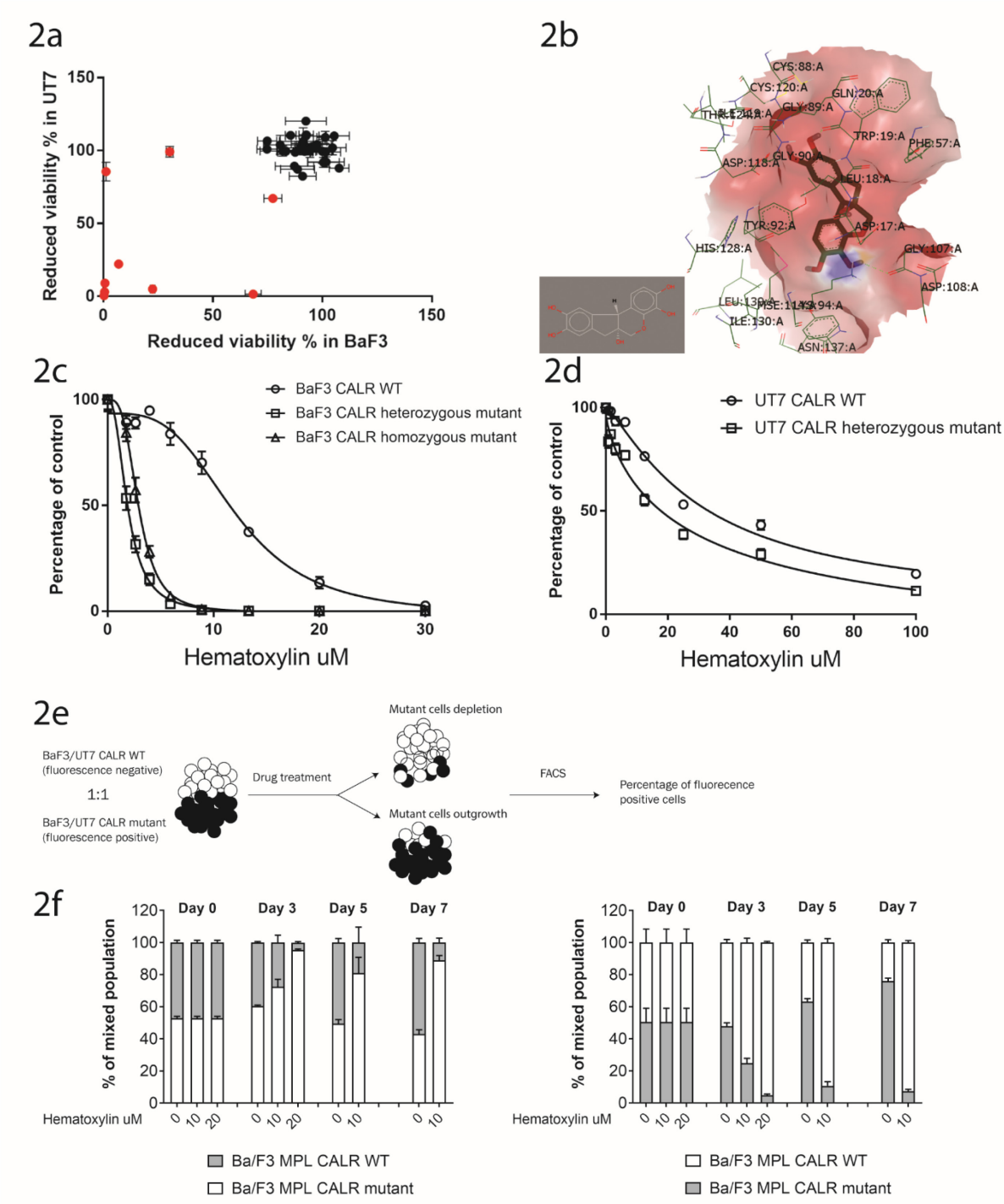

Figure 2.1. 3 C-terminal truncation and knockout CALR rescue apoptosis induced by hematoxylin in CALR mutated cells

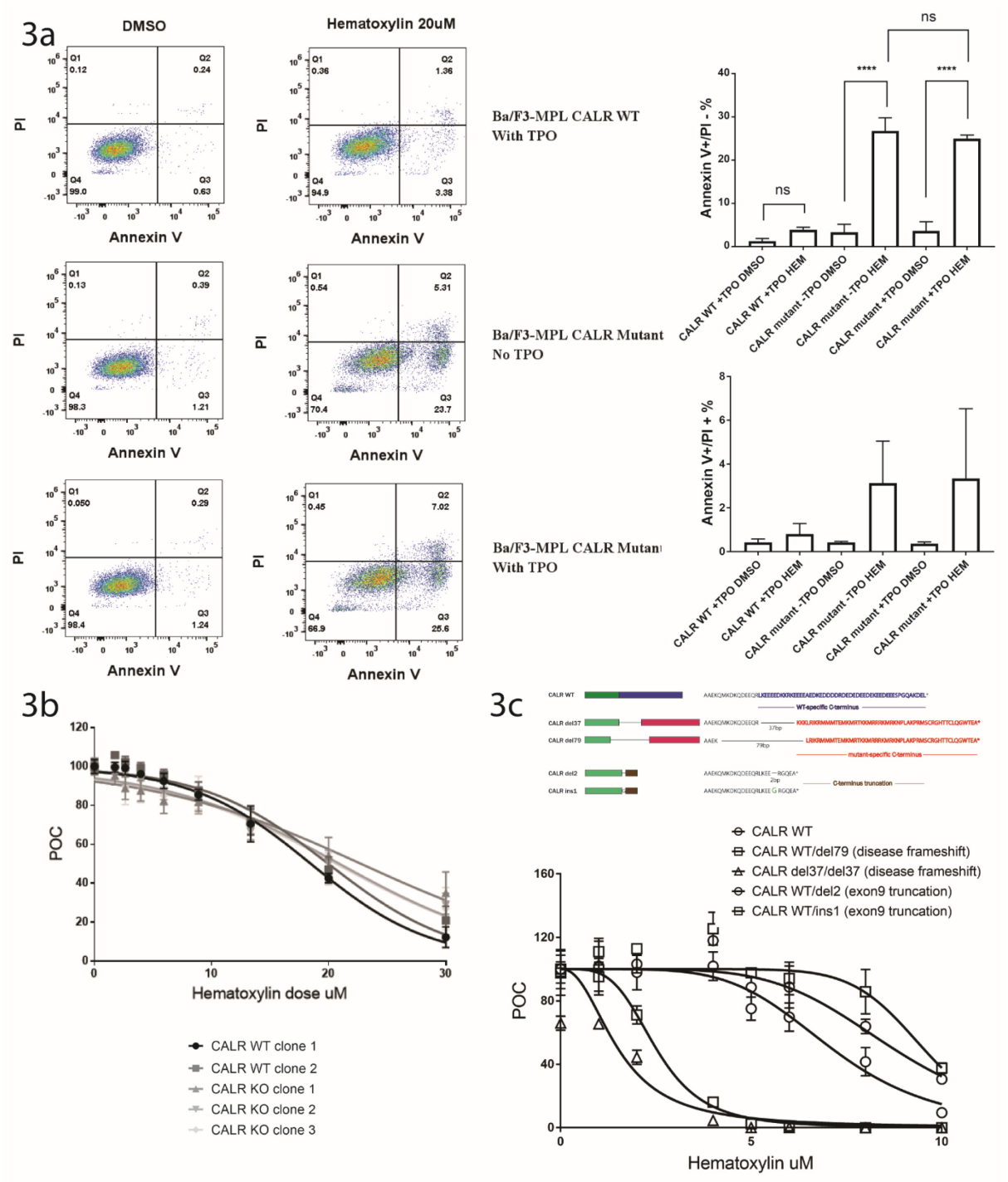

Figure 2.1. 4 Effect of hematoxylin on CALR-MPL interaction

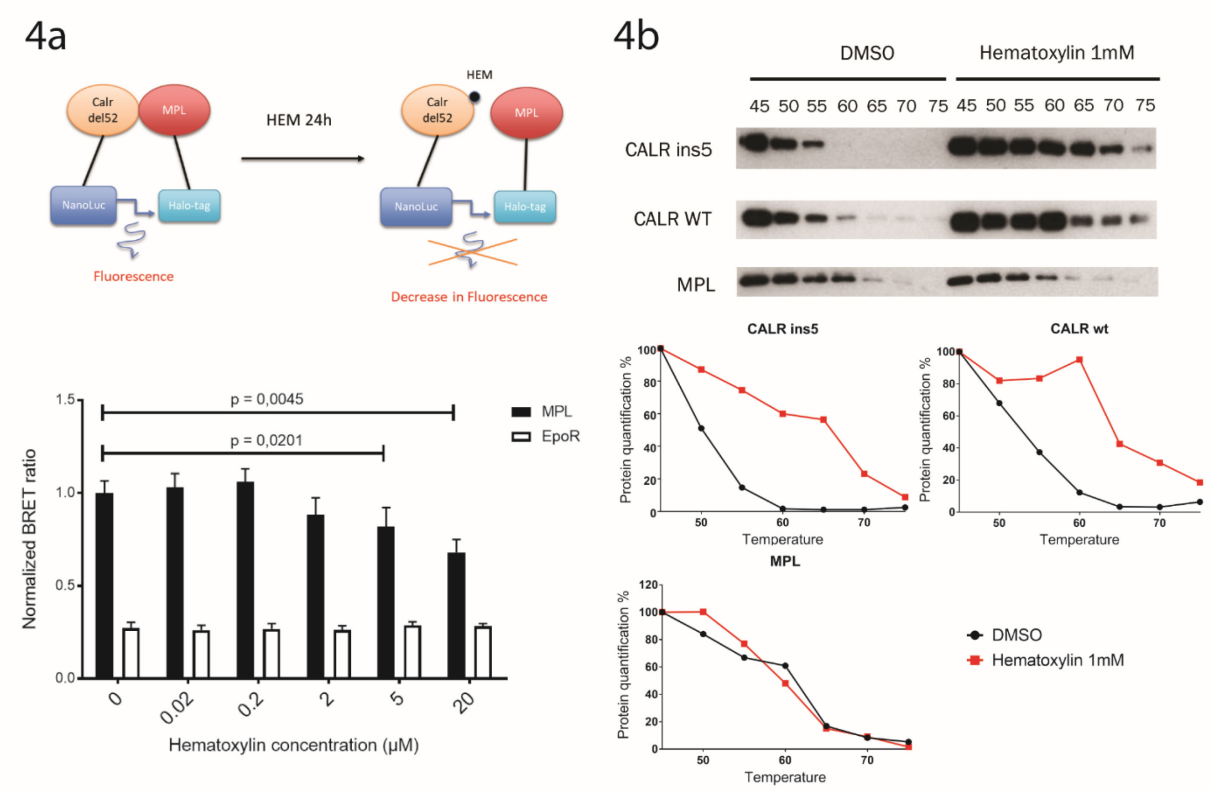

Figure 2.1. 5 Effect of hematoxylin on mutant CALR and JAK-STAT signaling

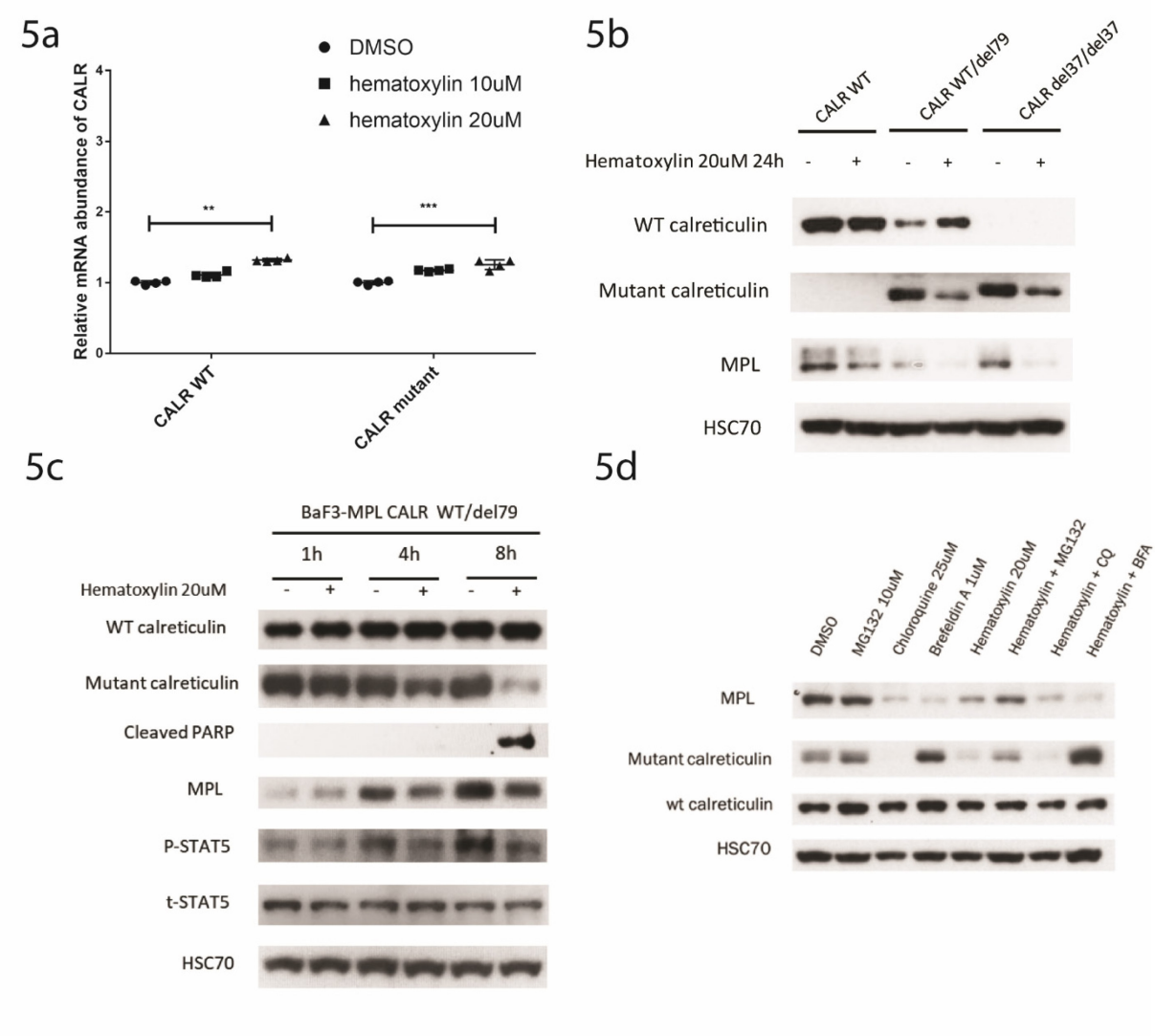

Figure 2.1. 6 Test of chemical analogs of hematoxylin in CALR WT/Mutant cell lines

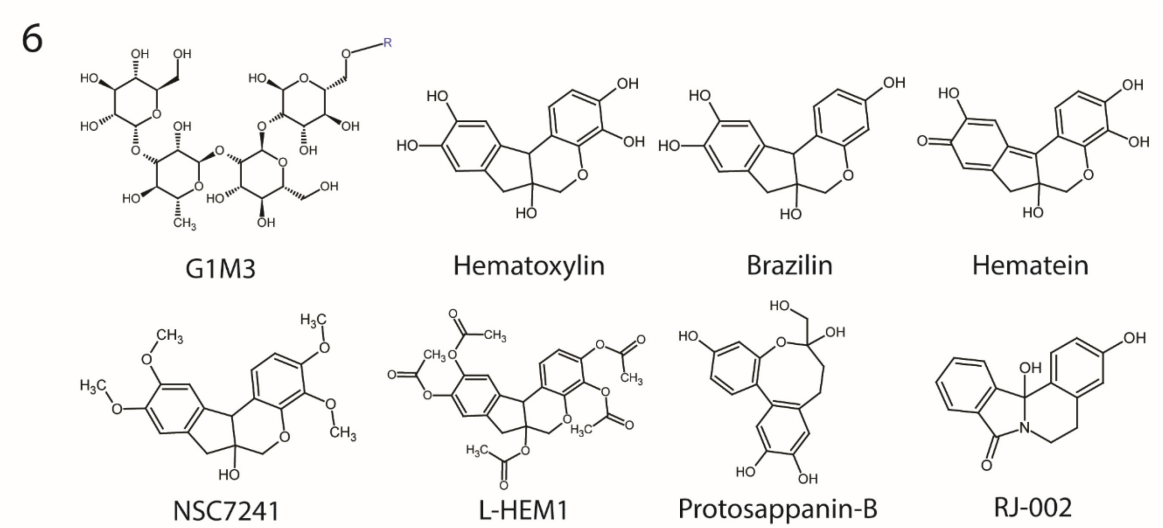

Chemical	IC50 in CALR WT cell line /uM	IC50 in CALR mutant cell line/uM
Hematoxylin	11.18	2.39
Brazilin	6.21	1.86
Hematein	≈38.27	7.64
NSC7241	≈128.5	22.52
L-HEM1	≈13.61	2.78
Protosappanin-B	NA	13.685
RJ-002	5.989	4.19
Ruxolitinib	0.40	0.20
Hydroxyurea	17.99	15.58

Figure 2.1. 7 Effect of hematoxylin on colony forming unit of CD34+ cells

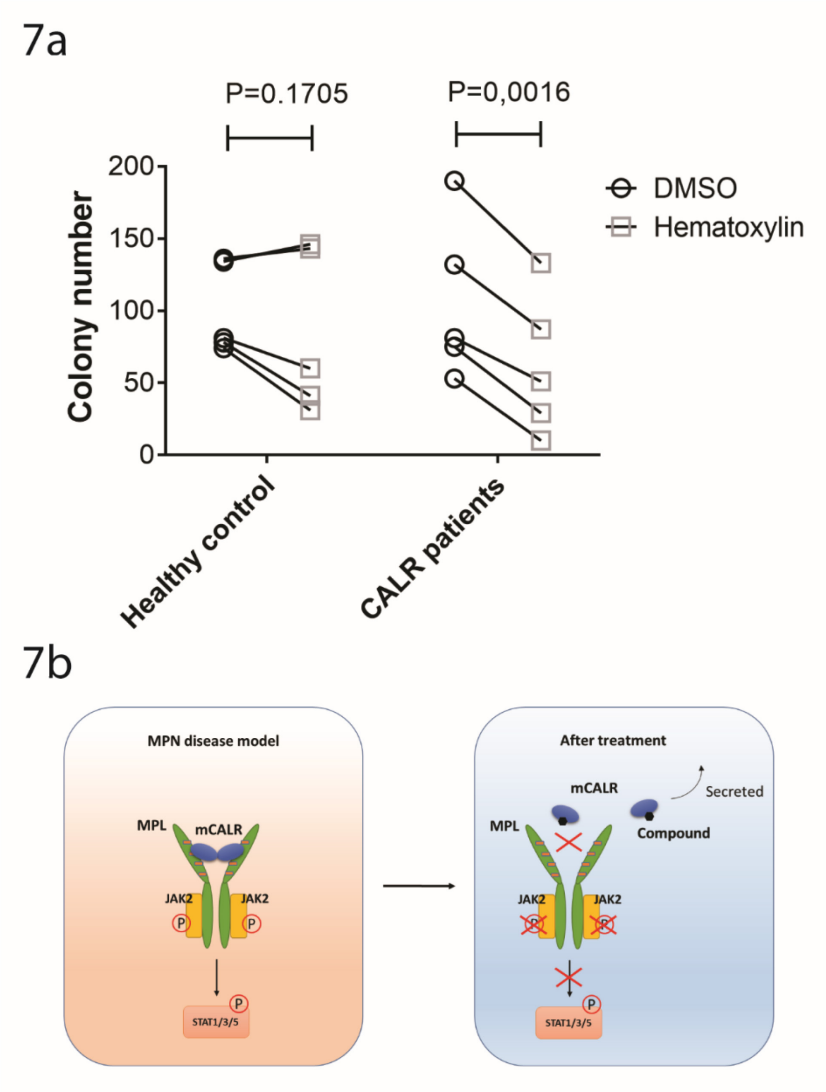

Figure 2.1.1 Molecular docking of calreticulin glycan binding domain

a. Structural model of human calreticulin. Colored surface representations indicate experimentally identified interaction sites: glycan binding site (cyan); ATP-binding site (magenta); main Ca2+ binding site (grey).
b. PDB (ID: 3O0X) Structure of mouse calreticulin lectin domain interacting with tetrasaccharide Glc-Man-Man-Man (blue) with lysine 111 and aspartate acid 317 labeled (red).
c. Cytokine dose response of glycan domain mutated Ba/F3-MPL cells. Ba/F3-MPL cells were transduced with pMSCV-gw-puro constructs carrying CALR WT, CALR del52 as well as Lys111 and Asp317 mutated CALR del52. The CellTiter-Glo luminescent Cell Viability Assay was used to detect cell viability 72h after the addition of cytokine. WEHI-3B conditioned media and TPO conditioned media were used as murine IL-3 and human TPO supplement.
d. Top panel: PDB (ID: 3O0X) Surface structure of mouse calreticulin lectin domain interacting with tetrasaccharide Glc-Man-Man-Man (blue) with lysine 111 and aspartate acid 317 labeled (red). Bottom panel: Zoom in structure of hydrogen-bond network formed at glycan binding domain.

Figure 2.1.2 Cytotoxic selectivity of hematoxylin in CALR mutated cell lines

a. Single dose cytotoxic screen of the docking library in Ba/F3-MPL and UT7-TPO cell lines. CRISPR-Cas9 generated Ba/F3-MPL CALR del79/WT and UT7-TPO CALR del61/WT were treated by each compound at 10uM for 72h. All luminescent signals were normalized to DMSO control to calculate percentage of reduced viability. N=3. Positive hits are shown in red.
b. Molecular docking model of hematoxylin with calreticulin glycan binding domain.
c. Dose response test of hematoxylin in Ba/F3-MPL cell lines. 1 heterozygous and 1 homozygous CALR mutated cell line were used in comparison to wild type control. Wild type cells were grown with 1% TPO conditioned media and mutant cell lines were grown without cytokine. All drug treatment groups contain equal amount of DMSO. N=6.
d. Dose response test of hematoxylin in UT7-TPO cell lines. CALR heterozygous mutant cell line was used in comparison to wild type control. Wild type cells were grown with 1% TPO conditioned media and mutant cell lines were grown without cytokine. All drug treatment groups contain equal amount of DMSO. N=6.
e. Schematic diagram of the experimental process of the competition assay
f. Cytotoxicity test of hematoxylin in Ba/F3-MPL by the two-color competition assay. Left panel: Ba/F3-MPL CALR WT (mCherry positive) and Ba/F3-MPL CALR del79/WT (mCherry negative) cells were treated with indicated concentration of hematoxylin for 7 days. 1% TPO conditioned media and the drug were refreshed every 2-3 days. Right panel: reverse color setting was used. Ba/F3-MPL CALR WT (mCherry negative) and Ba/F3-MPL CALR del79/WT (mCherry positive) cells were used. N=3.

Figure 2.1.3 C-terminal truncation and knockout CALR rescue apoptosis induced by hematoxylin in CALR mutated cells

a. Annexin V/PI staining of Ba/F3-MPL cells following hematoxylin treatment of 24h. Left panel: representative FACS plots of Annexin V/PI staining in both CALR WT and mutant cell lines. Mutant cell lines were tested in +/- 1%TPO condition. Right panel: quantification of early apoptotic cells (Annexin V+/PI-) and late apoptosis cells (Annexin V+/PI+). N=3. Statistical test was conducted by one-way ANOVA followed by Bonferroni's multiple comparison tests. **** P<0.0001.

b. Dose response of Ba/F3-MPL CALR WT and CALR knockout (CALR KO) cell lines. CALR KO cell lines were generated by CRISPR-Cas9 targeting exon 3 of CALR gene from Ba/F3-MPL cell lines. 3 individual KO clones and 2 WT clones which went through the same CRISPR-Cas9 workflow were used in the experiment. N=5.

c. Top panel: sequence alignment of c-terminal sequences of wild type CALR, disease frameshift mutant CALR (CALR del79 and CALR del37 as two examples), c-terminal truncated CALR (CALR del2 and CALR ins1 as two examples) from Ba/F3 cells. * stands for stop codon.

   Bottom panel: dose response of Ba/F3-MPL cell lines carrying wild type CALR, disease frameshift mutant CALR and c-terminal truncated CALR. N=3.

Figure 2.1.4 Effect of hematoxylin on CALR-MPL interaction

a. Interaction of mutant CALR and MPL detected by the NanoBRET assay. EBNA cells were transfected with CALR del52-HaloTag and NanoLuciferase-MPL/EPOR constructs. Cells were treated with hematoxylin for 24h at respective concentrations. EPOR-CALRdel52 was used as negative control for background signal.

b. Compound engagement with mutant and wild type calreticulin tested by the cellular thermal shift assay. HEK293T cells were transfected with pcDNA3.1 CALR ins5/CALR WT/MPL constructs. Hematoxylin or DMSO was added to cell lysates before heating at respective temperatures for 6min. Top panel: western blot for the detection of the soluble fraction of the protein lysates. Bottom: the densitometry of bands was quantified by Fiji and normalized to the band density of the lowest temperature tested.

Figure 2.1.5 Effect of hematoxylin on mutant CALR and JAK-STAT signaling

a. Real-time PCR analysis of 24h treatment of hematoxylin in Ba/F3-MPL cell lines. CRISPR-Cas9 generated Ba/F3-MPL CALR WT, CALR homozygous mutant del37/del37 cell line were treated with 20uM hematoxylin or equivalent amount of DMSO as control for 24h before cell collection and RNA extraction. N=4. Statistical test was conducted by two-tailed paired t-test. ** P<0.01, *** P<0.001.

b. Western blot analysis of 24h treatment of hematoxylin in Ba/F3-MPL cell lines. CRISPR-Cas9 generated Ba/F3-MPL CALR WT, CALR WT/del79 and CALR del37/del37 cell lines were treated with 20uM hematoxylin or equivalent amount of DMSO as control for 24h before cell extraction and lysis.

c. Effect of time course treatment of hematoxylin on Ba/F3-MPL CALR WT/del79 cell line. Hematoxylin was added at 20uM for the indicated time before collection and cell lysis.

d. Effect of multiple inhibitors on calreticulin protein level. All the indicated inhibitors were added for 8h in Ba/F3-MPL CALR del79/WT cell line.

Figure 2.1.6 Test of chemical analogs of hematoxylin in CALR WT/Mutant cell lines

Top panel: chemical structure of the tetrasaccharide as the substrate of calreticulin and structures of other tested hematoxylin analogs. Bottom panel: table of IC50 of tested compounds in Ba/F3-MPL CALR WT and mutant cell lines.

Figure 2.1.7 Effect of hematoxylin on colony forming unit of CD34+ cells

a. The colony formation assay of healthy individuals and CALR patients following hematoxylin treatment. CD34+ cells from 5 healthy control and 5 CALR patients were isolated and plated for 7 days with DMSO or 40uM of hematoxylin treatment before colony counting. Two-way ANOVA followed by Sidak's multiple comparisons test was used for p value calculation.

b. Diagram of mechanism of action of hematoxylin. In MPN disease model, mutant calreticulin physically interact with MPL and constitutively activate JAK-STAT pathway. Our drug binds to mutant calreticulin and disrupt the interaction. Mutant calreticulin therefore lose their membrane-bound interacting partner and are secreted out of cells.

Supplementary figure S2.1. 1 Representative FACS plot of the competition assay in Ba/F3 cells.

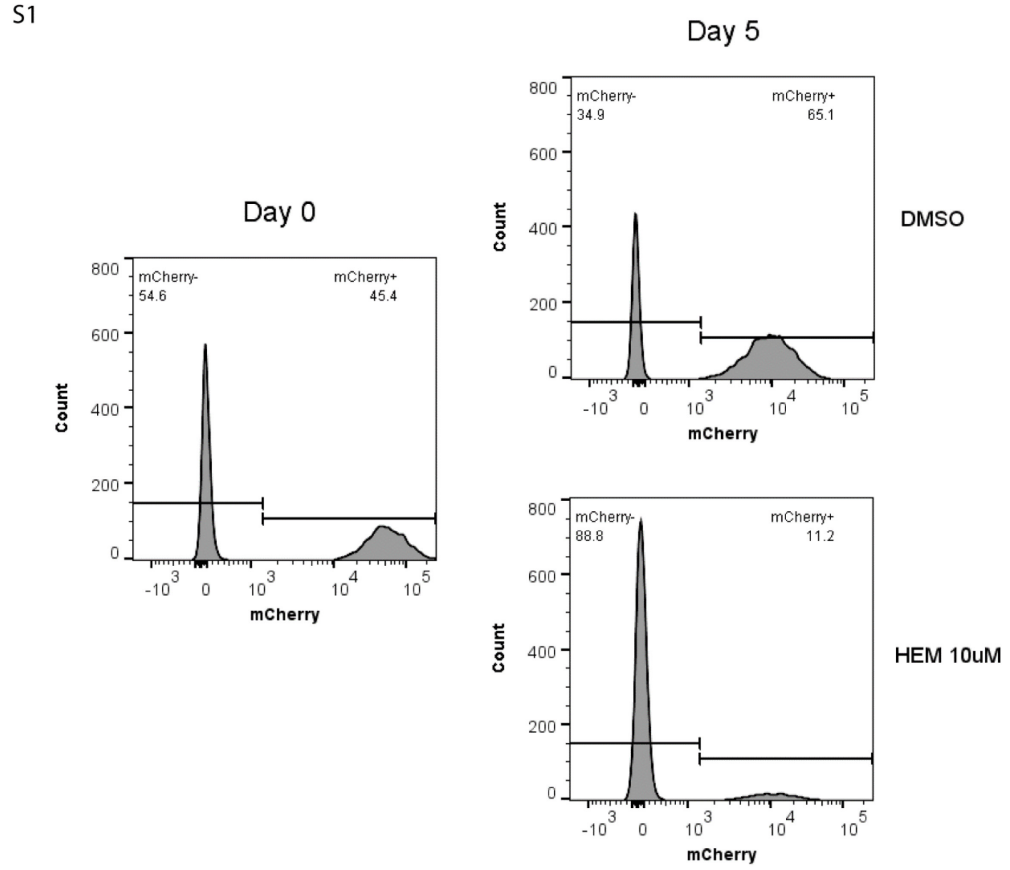

Supplementary figure S2.1. 2 Competition assay with hematoxylin treatment in UT7-TPO cell lines.

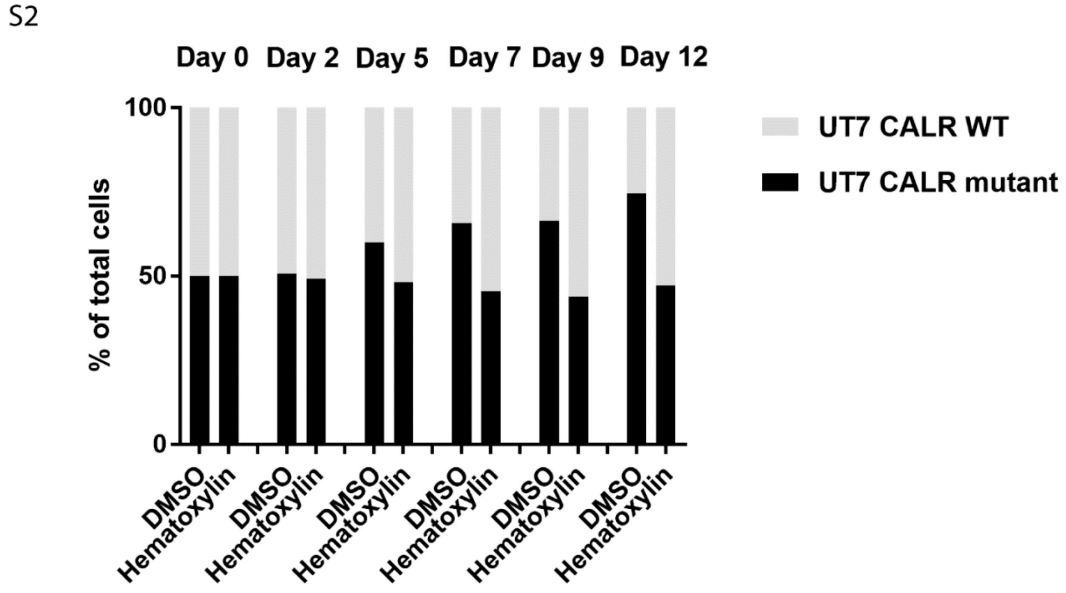

Supplementary figure S2.1. 3 Dose response test of hematoxylin in JAK2 mutant cell line

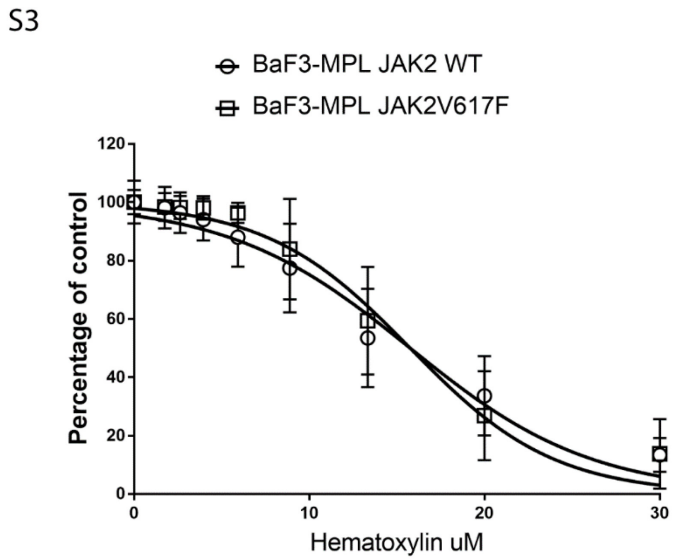

Supplementary figure S2.1. 4 Effect of hematoxylin in Ba/F3-MPL resistant cell lines.

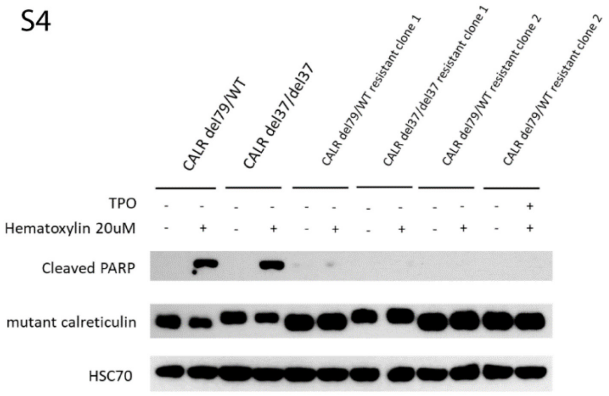

Supplementary figure S2.1. 5 Dose response of chemical analogs of hematoxylin in Ba/F3-MPL cell lines.

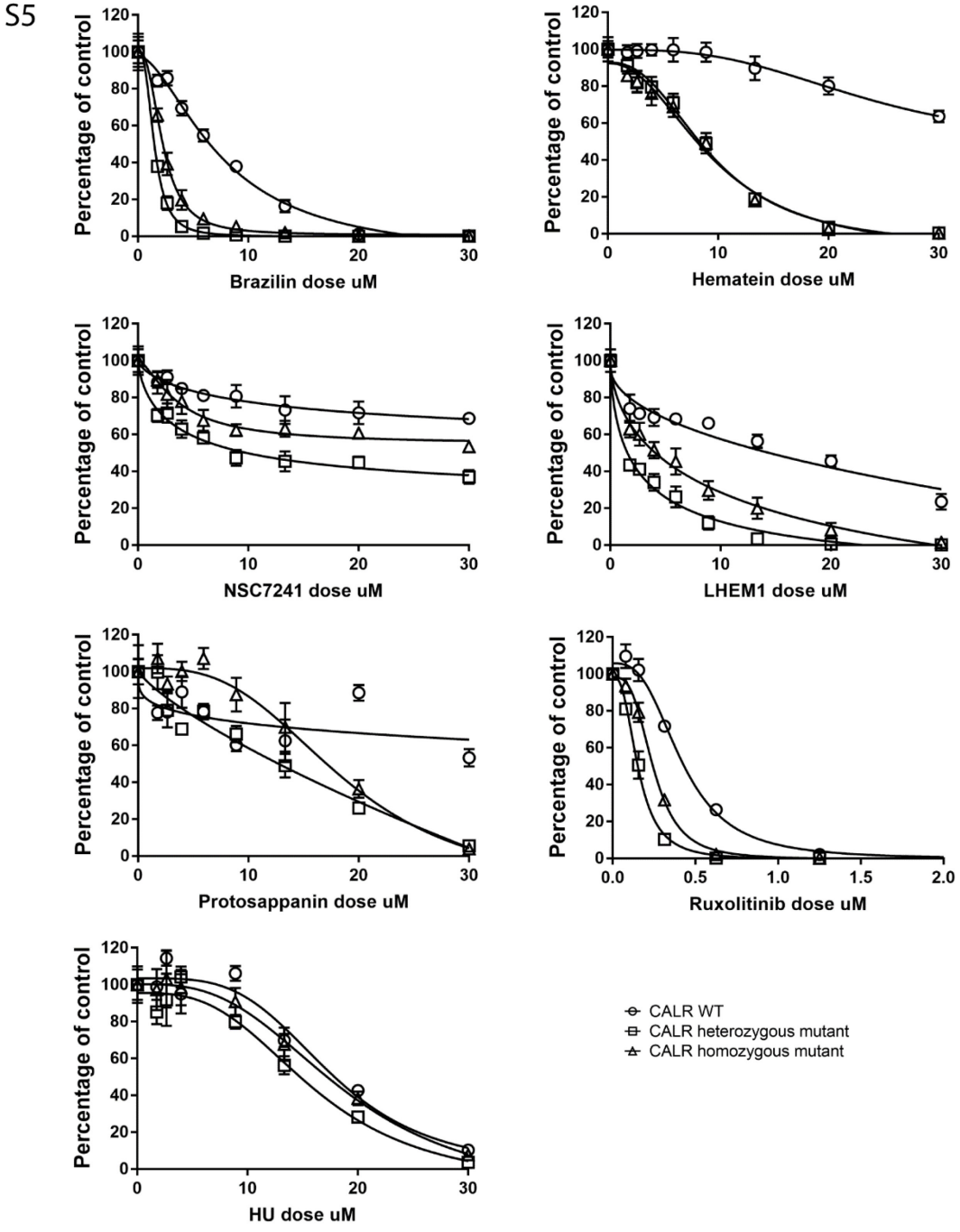

Figure S2.1.1 Representative FACS plot of the competition assay in Ba/F3 cells.

CALR WT (mCherry negative) and CALR mutant cells (mCherry positive) treated with 10uM hematoxylin or equivalent amount of DMSO. Day 0 and day 5 time points were used for representation.

Figure S2.1.2 Competition assay with hematoxylin treatment in UT7-TPO cell lines.

UT7-TPO CALR WT (mCherry negative) and UT7-TPO CALR del58/WT (mCherry positive) were treated with 40uM hematoxylin or DMSO for 12 days in the presence of 1%TPO.

Figure S2.1.3 Dose response test of hematoxylin in JAK2 mutant cell line.

Ba/F3-MPL cells transduced with JAK2WT or JAK2V617F were treated with hematoxylin for 72h. Wild type cells were grown with 1% TPO conditioned media and mutant cell lines were grown without cytokine. All drug treatment groups contain equal amount of DMSO. N=4.

Figure S2.1.4 Effect of hematoxylin in Ba/F3-MPL resistant cell lines.

Ba/F3-MPL CALR del79/WT and Ba/F3-MPL CALR del37/del37 were cultured with hematoxylin at 20uM for 4 weeks. CALR del79/WT resistant clone 1 and CALR del37/del37 resistant clone were cultured without cytokine. CALR del79/WT resistant clone 2 were cultured with 5%TPO.

Figure S2.1.5 Dose response of chemical analogs of hematoxylin in Ba/F3-MPL cell lines.

CALR WT, heterozygous mutant and homozygous mutant cell lines were treated with indicated drugs for 72h. Mutant cells were cultured with no cytokine.

2.2 Targeting ATR-CHK1 pathway in CALR mutated MPN

Prologue

In this project, we aimed to identify small molecule drugs that could preferentially inhibit the growth or be cytotoxic to CALR mutated cells in comparison to CALR wild type cells by performing high-throughput drug screening approach. Through mutant CALR selective drugs, we also hope to identify vulnerabilities of CALR mutated cells and exploit its synthetic lethal targets for further drug development.

Through our drug screen in UT7-TPO cell line, we identified several inhibitors all targeting ATR-CHK1 pathway as promising hits for follow-up studies. In a mixed population with wild type cells, CALR mutated cells were depleted over time by the treatment of ATR and CHK1 inhibitors. We confirmed these results also in Ba/F3 cell line model and excluded the possibility that the cytotoxic selectivity was due to different proliferation rates. Downstream pathway analysis showed that replication stress was induced by CHK1 inhibitors treatment in mutated CALR cells using elevated pan-nuclear staining of γH2Ax and phosphorylation of RPA as markers. The drug treatment also promoted S-phase cell cycle arrest in mutant cells and prohibited them from completing replication. Following CHK1 inhibitor treatment, there was a statistically significant reduction in colony forming potential of CD34+ cells from CALR mutation positive patients, but no such effect was detected in samples from healthy individuals. CALR knockout cells did not show hypersensitivity to the drug treatment, suggesting the vulnerability of CALR mutated cells to ATR-CHK1 inhibition is caused by the oncogenic activation of mutant calreticulin.

2.2.1 High-throughput chemical screening identified ATR and CHK1 inhibitors as hits targeting CALR mutated cells

To discover novel drug candidates for CALR mutated MPN, we performed a high-throughput drug cytotoxicity screen with a library of 89172 compounds in UT7-TPO cell line model. To exclude the compounds with low cytotoxicity, compounds were tested at in a single dose with relatively high concentration (10uM or higher) in CALR mutated cell line in the first round of screen. Compounds which showed more than 75% reduction on cell viability compared with DMSO control, and those that exhibited 50% to 75% inhibition but with annotated targets were taken as toxic compound hits. In the follow-up screen, the selected hits were then tested in both UT7-TPO CALR wild type and mutant cell lines to generate 4-dose response curves. Selectivity of each compound was assessed by comparing its cytotoxicity in CALR wild type and mutant cell lines (Figure 1a).

We performed two independent analysis with the screen result. Firstly, we compared the effect on viability from every tested dose of individual drugs between control and mutant cell lines (Figure 1b). The hits were called when any dose of the drug showed 25% larger inhibitory effect on mutant cells compared to wild type cells with a p value lower than 0.05 (Figure 1c). Alternatively, we calculated Area Under the Curve (AUC) value as a cumulative measure of compound potency (Figure 1d). The hits were called when AUC of the mutant cell line were at least 50% lower than the wild type cell line with at least one standard deviation difference between the two means (Figure 1e).

Interestingly, we observed ATR inhibitor AZD6738 and CHK1 inhibitor LY2603618 as hits in both analysis and another ATR inhibitor AZ20 as a hit in the first analysis (Figure 1c,e). As multiple compounds targeting ATR-CHK1 pathway were called in this unbiased screen, we hypothesized that there might be vulnerability of CALR mutated cell line in this DNA damage response pathway.

2.2.2 Cytotoxic selectivity of CHK1 inhibitors in CALR mutated cells

We then manually validated the hits in a 72-hour 8-dose response assay. All the 3 ATR-CHK1 inhibitors showed only minor selectivity in killing CALR mutant cells (Figure S1). However, ATR-CHK1 is a DNA-damage response pathway and our inhibitors were not tested in combination with any DNA damaging agents. We argued that 72h might not be enough time for UT7 cells to accumulate DNA damage considering that the doubling time of the cell line is between 48-60 hours. Therefore, a long-term cytotoxicity assay needed to be established for a proper test of drug selectivity. Since CALR mutations are somatic and to imitate the clonal expansion model of CALR mutated cells in patients, we then set up a two-color competition assay by co-culturing CALR wild type and mutant cells in the presence of CHK1 inhibitors. By

transducing either CALR mutant or control cell line a construct carrying mCherry, we could distinguish the two populations and detect cytotoxic selectivity of the drug over time (Figure 2a). As the results showed, in the presence of TPO as cytokine, CALR mutated cells outgrew wild type cells in the DMSO control group. Whereas, when treated with CHK1 inhibitors LY2603618 or SCH900776, the clonal expansion of mutant population was reversed and mutant cells were selectively diminished over time (Figure 2b,c). To avoid artefacts brought by mCherry transduction, we performed reverse-color setting for both experiments and the result could be reproduced.

To explore whether this selectivity was due to the inhibitory effect of DNA damage response inhibitors on fast-proliferating cells, we used another UT7 CALR mutant clone that did not show clear growth advantage over wild type cells. The selective effect could still be observed in the presence of CHK1 inhibitors (Figure S2). Moreover, for a further validation of the efficacy, we used murine BaF3-MPL cell line model to test the drug in the same setting. As BaF3 cells have doubling time of less than 24 hours, a shorter length of treatment is expected to show the drug effect. Indeed, over 90% of mutant cells was depleted after 6 days of treatment (Figure 3a).

2.2.3 CHK1 inhibitors did not show selective effect on CALR KO cells

To evaluate the target specificity as well as the possibility of CALR loss-of-function effect on the drug selectivity, we generated CALR knockout cell lines in BaF3-MPL and set up the competition assay co-cultured with wild type control. CHK1 inhibitor SCH900776 did not show selective effect until day 8, suggesting the selectivity was due to mutant CALR (Figure 3b). We also tested the drug in cells carrying JAK2V617F mutation and did not observe selective cytotoxicity, suggesting the drug effect was specific to CALR mutation rather than general effect on the activated JAK-STAT pathway (Figure S3).

2.2.4 CHK1 inhibitor reduced viability of hematopoietic stem cell from CALR patients

To further confirm the drug efficacy in a clinical relevant model, we performed the colony formation assay using CD34+ cells from CALR patients and healthy controls. As the result suggested, SCH900776 showed cytotoxic effect at nanomolar concentration range. 0.25uM of the drug significantly reduced colony forming units of CALR patients' cells but showed almost no effect on healthy individuals (Figure 3c).

2.2.5 Replication stress was induced by CHK1 and Wee1 inhibitors in CALR mutant cells

To explore the underlying mechanism that results in the selective inhibition of CALR mutant cells, we used western blot to detect the DNA damage response markers of drug treated UT7-

TPO cells. CHK1 inhibitors LY2603618 and SCH900776 were used both as single agents and in combination with Wee1 inhibitor MK1775, for the reason that CHK1 and Wee1 inhibitors were reported to work synergistically(216,217). We thus used 6-fold lower concentration of CHK1 inhibitors in the combination treatment. We could observe elevated γ-H2AX in mutant cells compared to wild type cells in any of these treatment groups, indicating more DNA damage or replication stress in mutant cells upon treatment (Figure 4a top panel). A slight basal level induction of γ-H2AX could also be detected, indicating a potential vulnerability of DNA replication or damage response regulation in mutant cells. RPA, as a principal component at replication fork which binds and stabilizes single-strand DNA, showed higher phosphorylation at both S33 and S4/S8 sites upon treatment in mutant cells. We used phosphorylation at S345 of CHK1 as a marker of drug effect. Consistent to previous report, it was induced upon CHK1 inhibitors treatment (227,228). We also detected slight decrease in mutant CALR by LY2603618 and a reduction of MPL in combination treatments. We speculated this to be a secondary effect of cell stress.

Furthermore, we expanded CD34+ cells from a CALR ins5 patient and a healthy individual and treated the cells with SCH900776. Patient cells showed higher induction of γ-H2AX as we observed in UT7 cells (Figure 4a bottom panel).

γ-H2AX was then stained in the immunofluorescence assay in UT7 cells responding to CHK1 inhibitor treatment. Pan-nuclear staining of γ-H2AX was observed, indicating DNA replication stress rather than DNA strand breaks was induced by the drug treatment (Figure 4b top panel). Significant higher percentage of γ-H2AX positive cells was detected in drug treated CALR mutant cells compared to control (Figure 4b bottom panel). This was consistent with our result from western blot.

We then asked the question how the drug affected cell cycle of mutant and wild type cells. After 24 hours treatment of CHK1 inhibitor, S-phase cell cycle arrest was induced in mutant cells. Co-staining of γ-H2AX and DAPI showed the majority of S-phase cells were γ-H2AX positive (Figure 5a). Continuation of the treatment to 72 hours caused most of the mutant cells trapped in S-phase and unable to progress to G2/M phase (Figure 5b). This result suggested a therapeutic window of CHK1 inhibition that might induce origin firing and cause replication stress and eventually cell death in CALR mutant cells. It is still elusive why CALR mutant cells are vulnerable to this inhibition.

Figure 2.2. 1 Drug screen identified ATR-CHK1 pathway as treatment target in mutated CALR cell line.

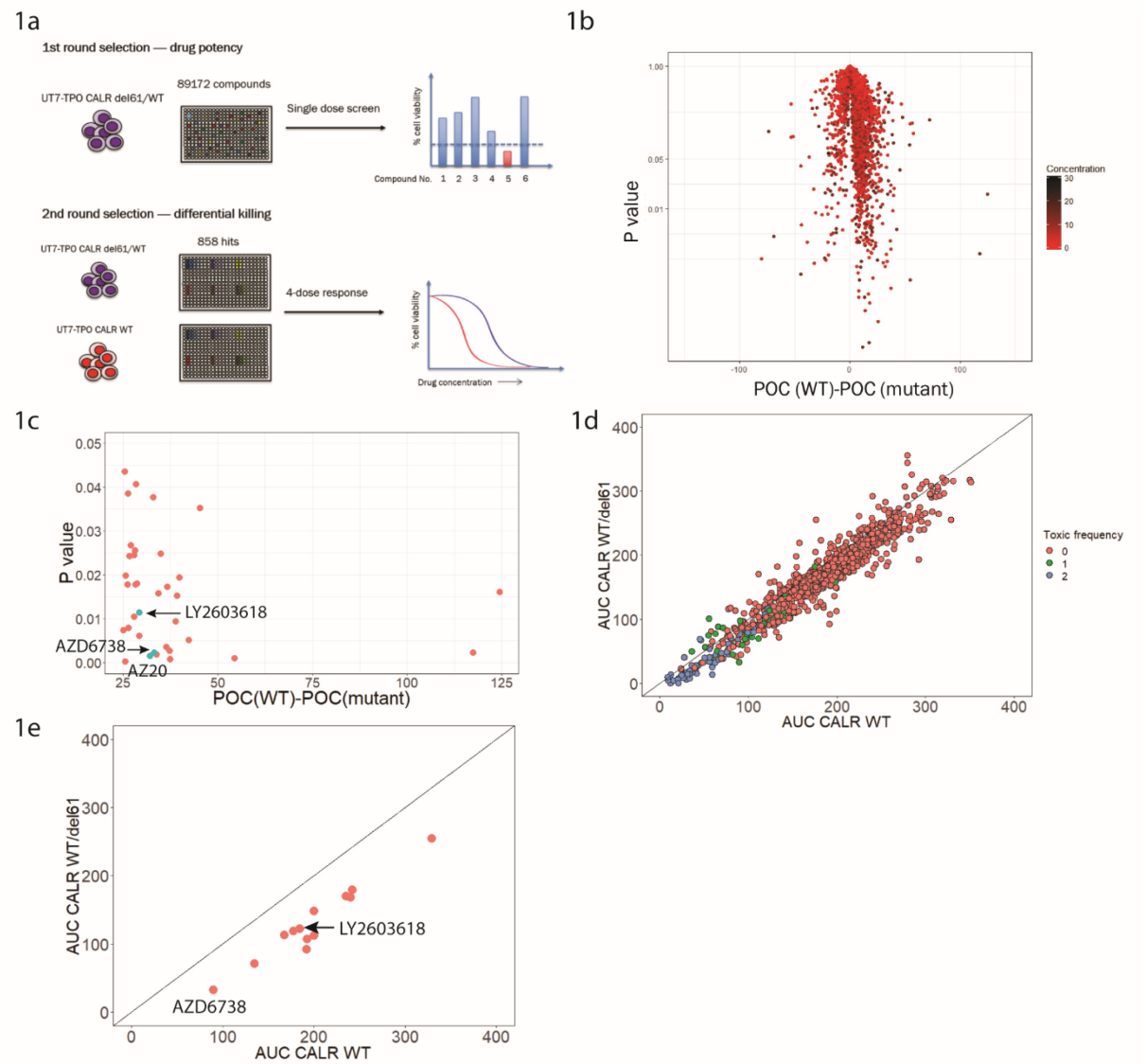

Figure 2.2. 2 Selective cytotoxicity of CHK1 inhibitors in CALR mutated cell lines

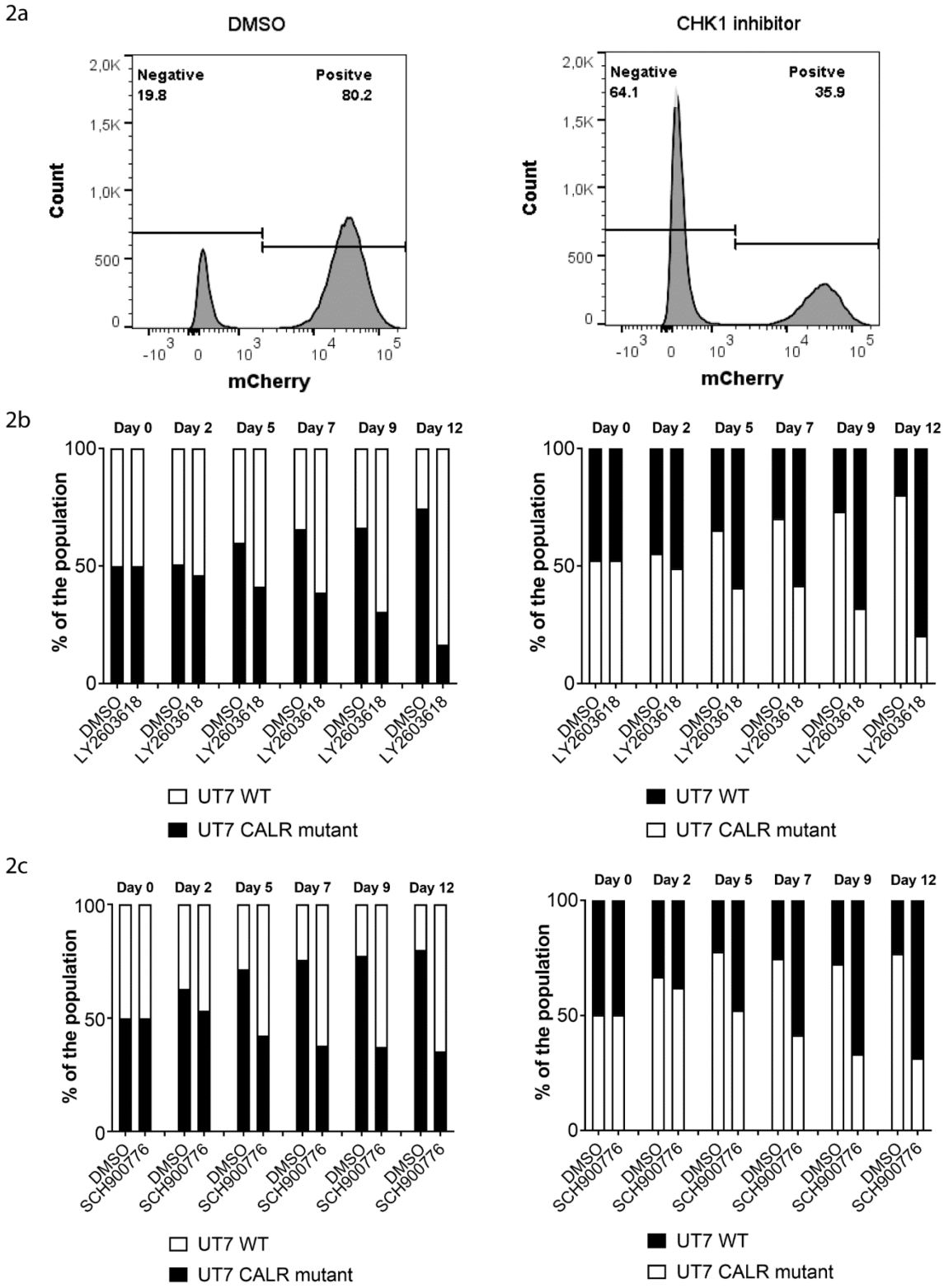

Figure 2.2. 3 Selective cytotoxicity of CHK1 inhibitors in Ba/F3 and primary patient cells

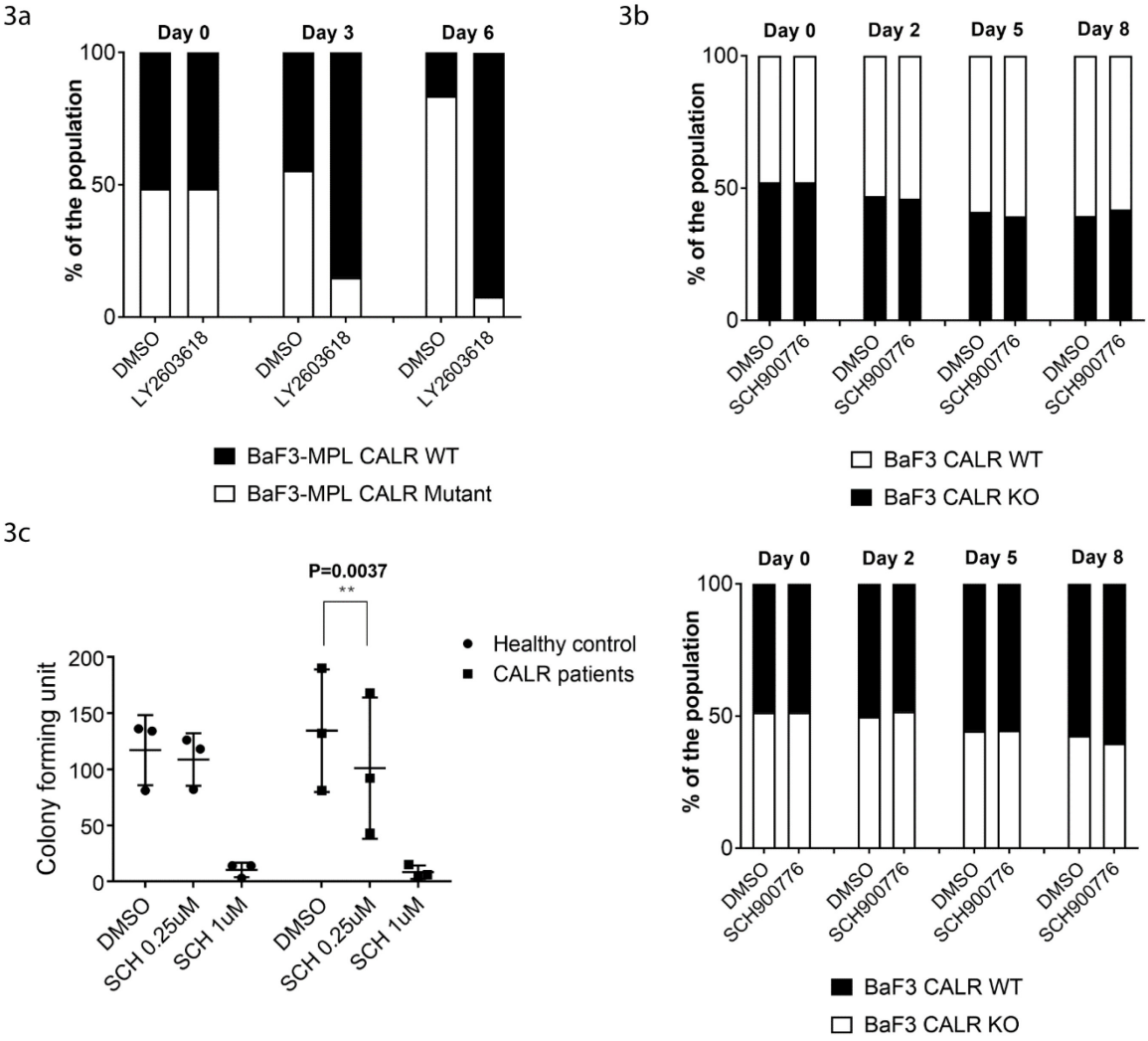

Figure 2.2. 4 CHK1 inhibition induced replication stress in CALR mutated cells

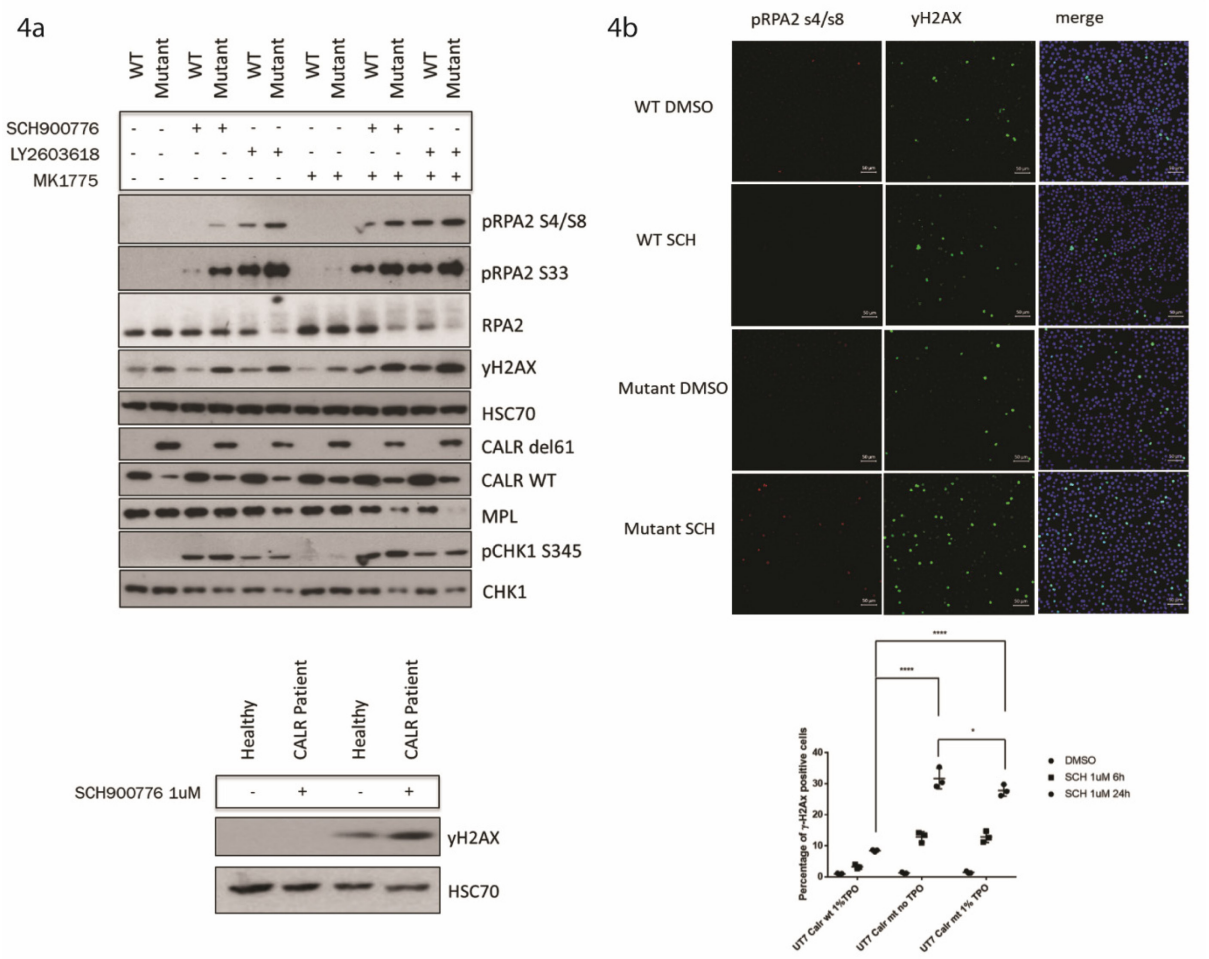

Figure 2.2. 5 Cell cycle analysis of CHK1 inhibitor treated UT7-TPO cells

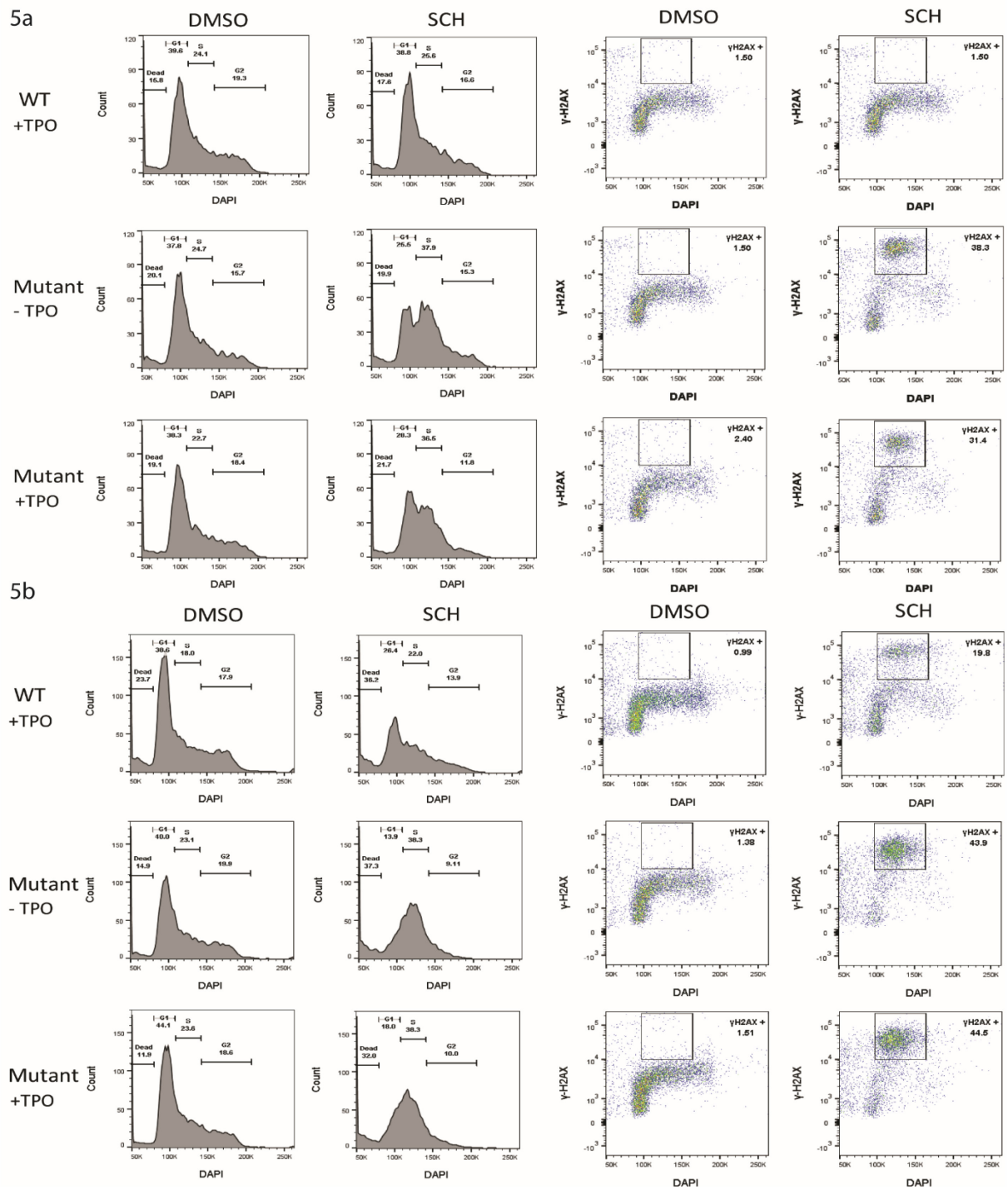

Figure 2.2.1 Drug screen identified ATR-CHK1 pathway as treatment target in mutated CALR cell line

a. Schematic diagram of drug screening workflow. UT7-TPO CALR del61/WT cell line was used for the first round of screen. 10uM or higher dose of each drug was tested in a 3-day CellTiter-Glo Cell Viability Assay. The hits were called based on cytotoxicity and were used for the second round of screen in both UT7-TPO CALR WT and UT7-TPO CALR del61/WT cell line in a 4-dose response. Wild type cell line was growing in 1% TPO.

b. Volcano plot of all single doses of all drugs in the second round screening result. POC (percentage of control) represents cell viability with one individual dose of drug normalized to DMSO control. POC difference= POC of CALR wild type cell line – POC of CALR mutant cell line. Each value is calculated by means of 3 technical replicates. Color of each points indicates the dose of drug in use. P value is calculated by unpaired t-test comparing viability of wild type and mutant cells of each dose of drugs.

c. Hits calling of screen using single-dose comparison between mutant and wild type cells. Hits were called when any dose of an individual drug met these criteria: POC of wild type cell line – POC of mutant cell line >25% AND p-value < 0.05. 2 ATR inhibitors (AZD6738, AZ20) and 1 CHK1 inhibitor (LY2603618) were labeled in the graph.

d. Plot of area under the curve (AUC) of all the drugs tested in the second round of screen. AUC is calculated as a sum of all POC values of each individual drug in a 4-dose response. Each POC value is calculated as mean of 3 technical replicates. Color represents toxic frequency. If the lowest tested concentrations of a given compound give POCs lower than 50, the compound is labeled “Toxic”. Toxic frequency represents the number of cell lines in which a compound was toxic (0= not toxic in any cell lines, 1 = toxic in one cell line, 2 = toxic in both cell lines).

e. Hits calling using AUC comparison in CALR mutant and wild type cell lines. Hits were called when one drug met the following criteria: AUC(CALR WT) – AUC(CALR mutant) > 50 AND AUC(CALR WT) – stdev(CALR WT) > AUC(CALR mutant)) – stdev(CALR mutant). One ATR inhibitor (AZD6738) and one CHK1 inhibitor (LY2803618) were called as hits and labeled in the graph.

Figure 2.2.2 Selective cytotoxicity of CHK1 inhibitors in CALR mutated cell lines

a. Representative FACS plot of the competition assay in UT7-TPO cell lines treated with CHK1 inhibitor. Day 12 time point of CALR WT (mCherry negative) and CALR del58/WT (mCherry positive) cells treated with DMSO or 1uM of SCH900776.

b. Competition assay of UT7-TPO CALR wild type and mutant cell lines incubated with 0.8uM of CHK1 inhibitor LY2603618. Wild type (mCherry negative) and mutant cells (mCherry positive) (left panel) or reverse color set-up (right panel) were mixed at 1:1 ratio and were co-cultured with LY2603618 and supplemented with 1% of TPO conditioned media for 12 days. Cells were collected at each time point and measured by FACS.

c. Competition assay of UT7-TPO CALR wild type and mutant cell lines incubated with 1uM of CHK1 inhibitor SCH900776. Wild type (mCherry negative) and mutant cells (mCherry positive) or reverse color set-up (right panel) were mixed at 1:1 ratio and were co-cultured with SCH900776 and supplemented with 1% of TPO conditioned media for 12 days.

Figure 2.2.3 Selective cytotoxicity of CHK1 inhibitors in Ba/F3 and primary patient cells

a. Competition assay in BaF3-MPL CALR wild type and CALR del79/WT cell line incubated with 0.8uM LY2603618. Wild type (mCherry postive) and mutant cells (mCherry negative) were co-cultured with LY2603618 and supplemented with 1% of TPO conditioned media for 6 days.

b. Competition assay of BaF3-MPL CALR wild type and CALR knockout cell line incubated with 1uM SCH900776. Top panel: CALR WT (mCherry negative) and CALR mutant (mCherry positive). Bottom panel: CALR WT (mCherry positive) and CALR mutant (mCherry negative).

c. Colony formation assay of healthy individuals and CALR patients following SCH900776 treatment. CD34+ cells were isolated from PBMCs of 3 healthy individuals and 3 CALR patients. 2000 cells were plated with 0.25uM, 1uM SCH900776 or DMSO in MethoCult H4434 classic media for 10 days.

Figure 2.2.4 CHK1 inhibition induced replication stress in CALR mutated cells

a. Top panel: western blot analysis of UT7-TPO CALR WT and CALR del58/WT whole cell lysates following treatment of indicated drugs for 24h. 1uM SCH900776, 0.8uM LY2603618, 0.3uM MK1775 were used as single agent treatment. 0.2μM MK1775 combined with 0.17μM SCH900776 and 0.2μM MK1775 combined with 0.13μM LY2603618 were used for combination treatment. Bottom panel: western blot analysis of cell lysates of CD34+ cells from 1 healthy control and 1 CALR ins5 patient. CD34+ cells were treated with 1uM SCH900776 for 24h before collection.

b. Top panel: Immunofluorescence of UT7-TPO CALR WT and CALR del58/WT following 1uM SCH900776 treatment for 6h. Green: γ-H2AX; blue: DAPI. Bottom panel: Quantification of γ-H2AX positive cells in UT7-TPO WT and mutant cells after 6 and 24h treatment of SCH900776. Two-way analysis of variance followed by Tukey's multiple comparisons test was used for statistical analysis. * $p<0.05$; **** $p<0.0001$.

Figure 2.2.5 Cell cycle analysis of CHK1 inhibitor treated UT7-TPO cells

a. Left panel: histogram of DAPI staining at 24h time point in UT7-TPO CALR WT and del58/WT cell lines with the treatment of 1uM SCH900776 or DMSO control. Right panel: co-staining with DAPI and γ-H2AX.

b. Staining of 72h time point collection.

Supplementary figure S2.2. 1 Dose response curves of ATR and CHK1 inhibitors in UT7-TPO cell lines

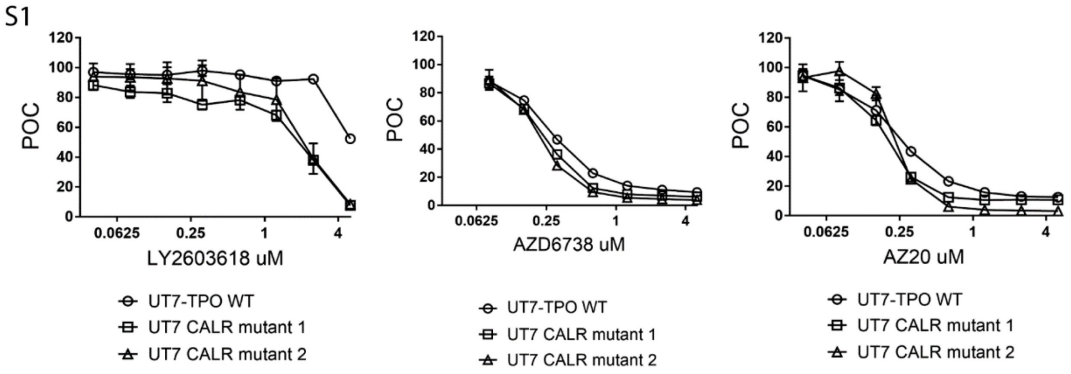

Supplementary figure S2.2. 2 Competition assay using CALR del61/WT cell line with CHK1 inhibitor treatment

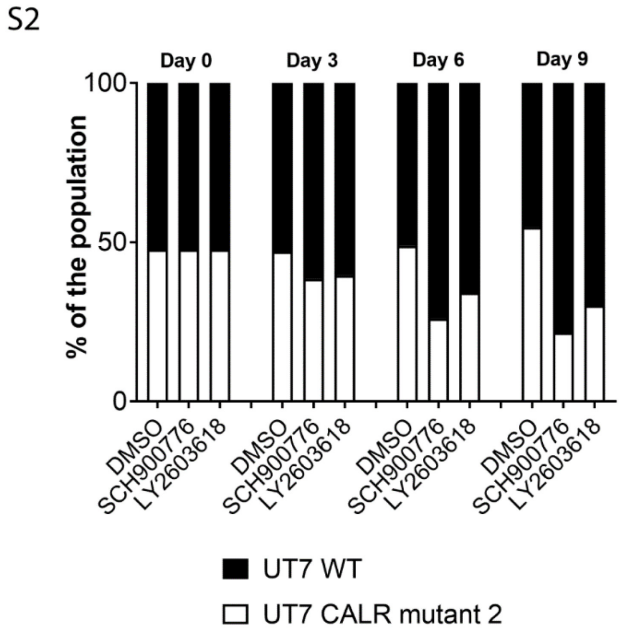

Supplementary figure S2.2. 3 Competition assay in Ba/F3-MPL JAK2 WT and JAK2V617F cells lines with CHK1 inhibitor treatment

S3

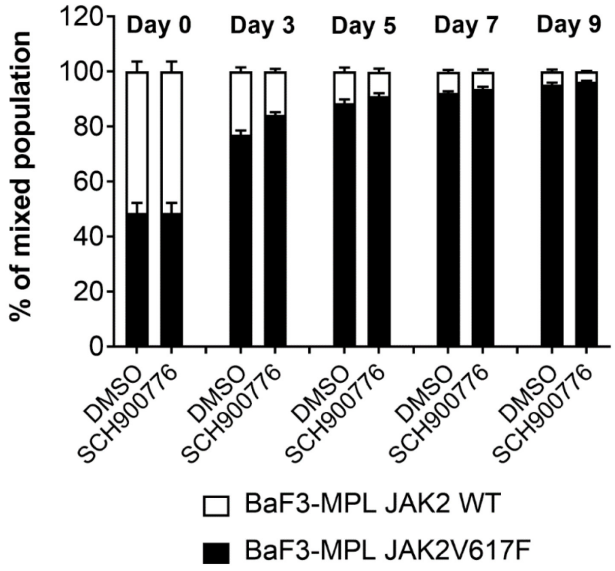

Figure S2.2.1 Dose response curves of ATR and CHK1 inhibitors in UT7-TPO cell lines

72h drug dose response of CHK1 inhibitor LY2603618, ATR inhibitor AZD6738 and AZ20 in UT7-TPO wild type and mutant cell lines. 1%TPO conditioned media was added to UT7-TPO wild type cells. No cytokine was used for mutant cell lines. 2 individual mutant clones were tested.

Figure S2.2.2 Competition assay using CALR del61/WT cell line with CHK1 inhibitor treatment

Wild type (mCherry positive) and mutant cells (mCherry negative) were with 1uM of CHK1 inhibitor SCH900776 or 0.8uM LY2603618.

Figure S2.2.3 Competition assay in Ba/F3-MPL JAK2 WT and JAK2V617F cells lines with CHK1 inhibitor treatment

Ba/F3-MPL cells transduced with pMSCV-JAK2WT (GFP negative) and pMSCV-JAK2V617F type (GFP positive) were with 1uM of CHK1 inhibitor SCH900776 or 0.8uM LY2603618.

3 DISCUSSION

3.1 General discussion of calreticulin biology

In this thesis, Although the focus of the scientific projects was on discovering novel therapeutic approaches of CALR mutated MPN, we were also interested in gain further in depth understanding of mutant CALR biology in the context of MPN disease. In this section, I would like to discuss a few key points of elusive mechanistic questions of mutant CALR and the effect on the scientific projects recorded in the thesis.

The current disease mechanistic model of mutant CALR has been established, supported by experimental evidence from a number of studies(173–182). Mutant calreticulin activate JAK-STAT pathway through thrombopoietin receptor, leading to clonal expansion of HSCs and megakaryocytic lineages. It is worth to mention that, although it seems to be a gain-of-function effect of mutant protein the acts as disease phenotype driver, it is likely that the mutation also partially impairs the wild type protein function. One of the supporting study of this hypothesis was conducted by the group of Mario Cazzola, describing a vulnerability of CALR mutated megakaryocytes to perturbations of intracellular calcium metabolism(172). This phenomenon was more striking in cells carrying type I mutation in which more calcium binding sequences of CALR were lost. However, it is surprising that the effect of CALR mutations on calcium metabolism has been mostly overlooked in the field. Indeed, the gain-of-function effect on thrombopoietin receptor perfectly explains the clinical phenotype that the mutations only occur in ET and PMF with thrombocytosis as main disease feature. Deficiency in calcium metabolism, on the other hand, could potentially uncover vulnerability of CALR mutated cells, which might suggest novel therapeutic approach. Therefore, the author believes this to be a promising venue for MPN research.

The other unanswered question is the mechanism of the occurrence of CALR mutation subtypes. A few studies have tried to explore the difference between type I and type II mutation. From our experience in protein purification and expression in cell lines, CALR ins5 seems to be a more stable protein than CALR del52, which was also observed by a study from Araki and colleagues(178). However, we could not rule out the potential artefact that the Flag-tag at c terminus of the protein affects the protein stability. Marty and colleagues revealed a stronger phenotype of thrombocytosis and myelofibrosis transformation from mice carrying type I CALR mutation over type II mutation(174). In a later study carried out by the same group, no significant phenotypic change was induced by rare type-I and II like mutations compared with the predominant type I and II mutations respectively(229). This is another interesting finding,

suggesting that the predominance of type I and II mutations might be partially due to the genetic occurrence rather than the clonal driving and disease causing ability of the mutations. Despite the mentioned discoveries, the biology behind the biased frequency of different subtypes of CALR mutations is still elusive.

The protein structure of mutant calreticulin is another intriguing point to discuss. As neither mutant nor wild type specific c-terminal peptide has been structurally resolved, it is only based on the biochemical assays to conclude the mutant tail mediates the formation of multimerization of CALR and the interaction with MPL(181). Cryo-electron microscopy technology has emerged to be an alternative powerful tool to solve the structure of proteins that cannot be crystallized. It might be a possible way to acquire mutant protein structure in the future.

3.2 Discussion of result 2.1

MPN remain to be a group of diseases with very high-unmet medical needs. The discovery of *JAK2*, *CALR* and *MPL* mutations have revolutionized the management of MPN patients but the corresponding therapeutic approaches are relatively under-developed. In particularly, few treatment approaches manage to specifically eliminate malignant clones, manifested by the reduction of mutant allele burden. Given the fact that MPN diseases are caused by clonal expansion of those clones, it would always be an ultimate goal of the treatment to remove them, The Interferon-α based treatment remains to be the most promising therapy to trigger patients' molecular remission, as a number of clinical trials have shown sustainable molecular effect in both *JAK2V617F* and *CALR* patients (79–81,230–232). However, a recent study has shown that *CALR* patients are less sensitive to the treatment compared with *JAK2V617F* patients(110). Apart from interferon-based treatment, ruxolitinib and hydroxyurea also reduced *JAK2V617F* allele burden in some patients, but the molecular responders are minority(233).

Among the clinically approved first-line therapies for MPN, ruxolitinib is the only targeted therapy. As the most important disease driver other than *JAK2V617F*, CALR mutations contribute to a large cohort of *JAK2* negative ET and PMF patients who could potentially benefit from a CALR-based targeted therapy. Thus, to search for pharmaceuticals that inhibit the oncogenic function of mutant CALR has great clinical significance. However, different from JAK2, a kinase that belongs to the second most targeted group of proteins, calreticulin is a novel target for small molecule inhibitors and requires an exploration of an effective targeting domain. In this study, we propose a group of docking compounds targeting glycan binding domain of calreticulin. We chose this domain as target for two reasons. Firstly, genetic evidence supporting the importance of glycan binding domain of mutant calreticulin in its oncogenic function has been obtained by a few studies(173,179,180). Mutagenesis

experiments pinpoint specific amino acids such as W319, D135 and Y109 to be indispensable for JAK-STAT pathway activation. Our own study suggested other amino acids in the pocket such as K111 and D317 to be essential too (Figure 2.1.1c). Secondly, co-crystallization of calreticulin and the synthetic tetrasaccharide has provided high-resolution structural information for computational docking study. Since disease-causing mutations of calreticulin are exclusively located at its c-terminus, we have speculated that the structure information of globular domain from wild type calreticulin should apply also to the mutant protein.

Through an exploration of a large set of chemical structures by computational analysis as well as cell-based cytotoxicity screen validation, we selected hematoxylin as our top hit. In our Ba/F3-MPL cell line models, we compared the selectivity of hematoxylin with HU and ruxolitinib which are standard-use treatments in MPN clinics and a superior selectivity effect of our compound was observed (Figure 2.1.6, S2.1.5). The on-target effect of the drug could also be confirmed by testing the drug in cells carrying CALR with a truncation of c-terminus as well as in CALR KO cells. In both cases the hypersensitivity to the drug was abolished (Figure 2.1.3b,c). To show this selective cytotoxicity as an effect in more than just one cell line model, we performed the drug cytotoxicity study in UT7-TPO cell line model as well as in patients' CD34+ cells, where the selectivity was retained (Figure 2.1.2d, 2.1.7a, S2.1.2). The result from patient primary samples was indeed encouraging to us, so we carried on exploring the mechanism of the drug efficacy.

It is worth to mention that we as well bear certain risks of targeting this domain. As it is located in the common part of wild type and mutated calreticulin, the compound would potentially affect the chaperone function of the wild type protein. Our CETSA result also suggested the compound binding to both mutant and wild type proteins as expected (Figure 2.1.4b). For this reason, we initiated our validation through a cell-based cytotoxicity assay, aiming to find compounds that show a dose range in which mutant cells are killed but wild type cells from an isogenic background tolerate. Interestingly, we manage to generate viable *CALR* knockout cell lines in Ba/F3 cells and the *CALR* -/- cell lines do not show growth deficiency, suggesting the gene is dispensable to the cells. This is also supported by the evidence that CALR is generally not highly expressed in hematopoietic tissues. Moreover, the essentiality of CALR suggested by mice study is due to its function in maintaining calcium homeostasis especially in the embryonic stage(168). Targeting glycan binding domain should not affect its calcium binding function and therefore could have a compromised toxicity in wild type cells. We also expect a quantitative abundance difference between intracellular wild type and mutant calreticulin proteins, supported by multiple studies and our own results(178,182). This could as well contribute to a therapeutic dosing window of the drug.

We set up the co-culture competition assay that mimicked the *in vivo* clonality of the malignant cells. The selective depletion of mutant clones by hematoxylin treatment suggested the potential use of the drug to reduce allele burden (Figure 2.1.2f, S2.1.2). Furthermore, since the mixed wild type and mutant clones were cultured and treated in the presence of TPO, this is a proof that cytokine is unable to rescue the mutant cells from hematoxylin-induced cell death, which is also confirmed by our apoptosis assay result (Figure 2.1.3a). This phenomenon could be at least partially explained by our western blot result showing the MPL is also downregulated together with mutant CALR following the drug treatment (Figure 2.1.5bc). The mechanism of how the drug reduces MPL is still elusive to us. The other hypothesis is that MPL is not properly glycosylated in the presence of mutant CALR and this could affect the receptor trigger downstream signaling upon TPO. The aberrant glycosylation of MPL in CALR mutated cells is supported by two studies(173,180). Thirdly, upon the drug treatment, both the inhibition of JAK-STAT5 signaling along with induction of apoptotic pathway contribute to the selective killing, which cannot be rescued by the rescue of cytokine signaling only.

The interaction of mutant calreticulin with MPL is an important marker for the on-target effect of our drug. Through the NanoBRET assay, it was the first time that a small molecule inhibitor was shown to reduce this interaction (Figure 2.1.4a). This result further confirmed that glycan binding domain is crucial to this interaction, supported by the previously published mutagenesis studies(179,180). To elucidate the binding mechanism, a structural study of co-crystallized drug-protein interacting complex is demanded, which is also important for a search of high-affinity binding compound.

An interesting observation upon the drug treatment was that mutant CALR protein was reduced by hematoxylin treatment. In contrast, wild type CALR was not reduced concurrently in the heterozygous mutant cells, which suggested that the effect was unlikely to be at transcriptional level (Figure 2.1.5bc). Indeed, mRNA level of both wild type and mutant CALR was slightly upregulated rather than downregulated (Figure 2.1.5a). After showing that blocking proteasomal or lysosomal degradation could not rescue the reduced mutant protein, we inhibited the secretary pathway by using brefeldin A and managed to achieve a rescue effect (Figure 2.1.5d). We hypothesize that after losing KDEL ER retention signal, the mutant protein relies on its interaction with MPL to retain its presence intracellularly. The disruptive interaction upon the compound treatment makes the protein lose its anchor at the cellular membrane and therefore increases its secretion (Figure 2.1.7 bottom panel).

The medical use of hematoxylin and its derivatives also requires further investigation. As a natural chemical compound that has been primarily used for histology staining, whether hematoxylin can be used as a pharmaceutical is still a question mark. It worth to point out that hematein, the oxidized form of hematoxylin, rather than hematoxylin itself is the actual dye

used in histology H&E staining. Hematein also needs metal ions as mordant to act as basic dye for nuclear staining. We believe the selective cytotoxicity of hematoxylin in mutant cells was not due to its DNA binding property, supported by the fact that hematein was less effective than hematoxylin in our assay(Figure 2.1.6, S2.1.5). However, it still requires experimental investigation that if oxidization or other chemical reactions of hematoxylin occurs when it is delivered to the cells. Interestingly, hematein was identified as a casein kinase II inhibitor in a study and was injected into mice without severe toxicity(234,235), which provides evidence of usage safety of the compound *in vivo*.

Also, hematoxylin's effective dose in our cell-based assays is in micromolar to milimolar range. The relatively high usage dose might imply low affinity of the target engagement of the compound. We endeavor to search for more potent analogues or derivatives but only brazilin achieves lower IC50 in the cytotoxicity assay whereas compromised selectivity is observed. The production of hematoxylin is also limited to the extraction from its original wood source. *De novo* synthesis of the chemical has not been achieved so far, which also restricts the production of other derivatives. Despite the issues of the chemical, we hope to propose hematoxylin as a pioneer lead compound and glycan binding domain of calreticulin as a valid drug target. Further understanding of the chemical space would be required to develop more potent drugs.

3.3 Discussion of result 2.2

Apart from the strategy of directly targeting our protein of interest, we have also tried to search for a synthetic lethal pathway of CALR-mutated cells. Through an unbiased large library chemical screen, we identified ATR-CHK1 pathway as the potential target (Figure 2.2.1a-e). This is supported by the screening result that although our drug library includes the majority of clinical tested drugs with annotated targets, no pathway other than ATR-CHK1 has more than two inhibitors showed up as top hits. We further validated our result by the competition assay (Figure 2.2.2). Different from hematoxylin which induces apoptotic effect in less than 24 hours after adding to the cells, CHK1 and ATR inhibitors require longer treatment time that allows cells to replicate in order to show the selectivity. This is also the case shown by previous studies involving DNA repair targeting agents. For instance, the effect of PARP inhibitors on BRCA1/2 deficient cells were assessed by colony formation assays over 10 days culture(236). In our assay, CHK1 inhibitors showed better effect than ATR inhibitors, which could be explained by the fact that the development of CHK1 inhibitors are at a more advanced stage than ATR inhibitors due to the technical difficulty in ATR protein purification and lack of structure information(220). In the treatment of primary human samples, CHK1 inhibitor showed a preferential inhibition in CALR patient samples at nanomolar concentration range (Figure 2.2.3c).

There has been a few studies linking MPN pathogenesis to DNA damage and repair pathways. An in vivo study of transgenic mice model showed that elevation of ROS and DNA double strand breaks was caused by *JAK2V617F* mutation(237). Impairment of replication fork progression as well as defective cell cycle checkpoint was found in *JAK2V617F* patient samples in another study(238). A more recent study showed that MPN driver mutations upregulate components of homologous recombination and non-homologous end joining pathways to cope with increased DNA double-strand breaks. Although the variability of sensitivity to PARP inhibitor is present in patient samples, combination treatment with ruxolitinib and HU showed efficacy in xenograft mice models(239). Even though the association of aberrant DNA damage and repair with MPN diseases has been shown, it seems that increased DNA damage is a general phenomenon in MPN regardless of the mutation types. However, in our study, we showed that cells carrying *CALR* mutation but not *JAK2V617F* mutation were vulnerable to CHK1 inhibitors (Figure S2.2.3). We also did not observe activation of ROS in CALR-mutated cell line regardless of the inhibitor treatment, which rules out the ROS involvement in the drug vulnerability (Data not shown).

Upon the inhibition of ATR and CHK1, we observed induction of pan-nuclear staining of γ-H2AX, phosphorylation of RPA and S-phase cell cycle arrest, leading to an RS phenotype (Figure 2.2.4a,b, Figure 2.2.5). We first hypothesized that this might be due to a loss-of-function of wild type calreticulin in mutant cells. As two independent studies have found enrichment of CALR at stalled replication fork, this suggests a possible involvement of wild type calreticulin in DNA replication(240,241). However, we exclude this hypothesis because the lack of selectivity of CHK1 inhibitors in CALR knockout cell lines, indicating that gain-of-function of mutant CALR is the cause of drug selectivity (Figure 2.2.3b). A recent publication has shown nuclear localization of mutant CALR and the interaction with transcription factors(242). However, the proteomics or biochemical fractionation study often involves nuclear protein contamination, particularly when the interactome of a chaperone protein is studied. Whether mutant CALR could translocate into nucleus and participate in DNA replication is still elusive.

As CHK1 inhibitors have been tested in clinical trials for a few types of cancer, the safety and toxicity of the drug has been well studied. In the majority of cases, CHK1 or ATR inhibitors are tested in combination with another DNA replication targeted chemotherapy such as alkylating agents and antimetabolites drugs. This could suggest a potential enhanced efficacy if the drugs are combined with hydroxyurea which is used as a first-line therapy in MPN. A preclinical study has suggested efficacy of combination treatment of CHK1 inhibitor and HU in melanoma and lung cancer models(214). In our study, we could also show a significant enhancement of DNA replication stress when the two agents combined, suggest a promise in applying this treatment

in MPN. Another study has shown global RPA exhaustion as the mechanism of cell death caused by ATR inhibition upon induction of RS by HU(201). All these studies support the use of ATR-CHK1 inhibition in MPN therapy.

3.4 Conclusion & future prospects

We conclude from our results that glycan binding domain of calreticulin is a promising drug target and hematoxylin is our top drug hit to achieve this goal. Selective killing of CALR mutated clones can be achieved by our drug based on *in vitro* and *ex vivo* studies.

We also conclude that ATR-CHK1 as another promising target in CALR mutated cells. The mutant cells might possess vulnerability in response to DNA damage inhibitors due to elevated replication stress.

Limited by the time and resources, our research has limitations and further experiments are needed for the development of calreticulin targeted therapy in MPN. To evaluate the suitability of calreticulin as a drug target, we propose animal studies to clarify the potential harm by the loss of wild type calreticulin. Although the embryonic lethal effect of *CALR* germline knockout has been addressed, no *in vivo* study clarifies *CALR* function in adult stage. *CALR* expression is comparably low in hematopoietic tissue and *CALR* deletion does not impair cell growth in our Ba/F3 cell line, indicating that the gene might not be essential in the hematopoietic system. However, delivering small molecule inhibitors will not be restricted to the hematopoietic system, so it is still an important task to evaluate the toxicity of targeting calreticulin. An inducible CALR KO transgenic mice model should be generated to assess the essentiality of calreticulin in adult mice. Furthermore, a glycan binding deficient CALR knock-in transgenic model will be of great value to genetically validate this domain as drug target. As a further step of *in vitro* mutagenesis study, to assess whether or not a glycan binding deficient mutant CALR can induce an ET-like phenotype *in vivo* would be a crucial proof-of-principle experiment. With the same purpose, the experiment could also be done using a transduction-transplantation model instead to shorten the experiment length.

We would also like to develop a high-throughput screening assay using purified recombinant mutant CALR. Although we have shown the promise of targeting glycan binding domain by docking compounds, searching for more potent compounds as well as allosteric inhibitors would be necessary for further drug development. It would also be interesting to investigate if any chemicals show superior affinity binding to the mutant protein. To achieve this, we need to purify both mutant and wild type calreticulin protein as native form and develop an assay to detect compound binding. The potential assays to be used for this purpose include thermal shift assay (TSA), surface plasmon resonance (SPR) based assay and DNA-Encoded Library Technology (ELT). Considering the requirement of high sensitivity for many assays to detect small molecule binding, we could also use CALR-MPL interaction as readout for screening.

We also would like to test our drugs in a mutant CALR transgenic mice model for *in vivo* efficacy evaluation. Many CHK1 inhibitors have been tested *in vivo* or even in clinical trials. These data

can provide us references regarding concentration of the drug to be tested. In the case of hematoxylin, a dose-escalation toxicity study will be required prior to the efficacy study because the chemical is not regularly used for *in vivo* injection. Using CD45.1/2 system, we could distinguish donors from transgenic CALR mutated and wild type mice. Bone marrow transplantation of a mixture of mutated and wild type cells into lethally radiated recipient mice is planned to be conducted. After the engraftment, the drug will be injected and both hematological and molecular response will be recorded.

4 Materials and Methods

4.1 Materials and Methods for result 2.1

Molecular docking

A complete 3D structural model of human calreticulin was built through homology modeling, using several experimental structures from Protein Data Bank as templates (Table 2)(146,147,157,243).

Table 2 Experimental structures used as templates to build the complete structural model of human calreticulin

PDB	Organism	Length	Resolution Å	Year	Ligand
3POW	*Homo sapiens*	265	1.65	2011	Ca2+
3RG0	*Mus musculus*	332	2.57	2011	Ca2+
3O0W	*Mus musculus*	273	1.95	2010	α-d-glucose, α-d-mannose, Ca2+
1HHN	*Rattus norvegicus*	101	NMR	2001	NA

The structure of human calnexin and human ER mannosidase I was built using their published X-ray structure PDB 1JHN(223) and PDB 1FMI(224).

The sequences of target and template proteins were aligned initially using Multalin and resulting alignment was further refined based on secondary structure propensity and disorder profiles. Templates secondary structure elements were assigned using DSSP (244).

Ligands structure files were downloaded from ChemSpider Database (http://www.chemspider.com).

Before the docking procedure, all structures of proteins and ligands were prepared using Autodock Tools(245) in the following steps:

1) Gasteiger partial charges were added

2) Rotatable bonds were set. For ligands, default rotatable bonds (identified by Autodock Tools) were maintained, while protein structures were maintained rigid.

3) In a first step of coarse docking, gridbox size was set to cover the whole protein structure (Table 3), to identify all putative interaction sites in each protein-ligand system. Grid spacing was set at 1Å.

Table 3 Grid dimensions and position of grid center for all protein systems

	x points	y points	z points	Grid center coordinates (x, y, z)
calreticulin	110	110	110	7.216; 0; 0
calnexin	88	100	106	0.15; -14.058; 30.61
ERManI	70	70	70	0.113; -1.693; 3.429

Number of modes was set at 100; exhaustiveness search value was set at 50.

Autodock Vina was used for compounds docking(246). Each compound was subjected to 5 independent runs of blind docking, each round generating 20 conformations (in total 100 conformations for each protein-ligand complex).

For all protein-ligand complexes, each set of 100 was visually analysed in PyMol 2.0 (247) (https://pymol.org) and involved several steps:

1) identification of binding regions on protein surface and detailed description of favorable interactions between protein residues and ligand atoms

2) identification of protein secondary structure elements in each complex

3) analysis of sequence conservation level for each residue involved in interaction with ligands

Cell culture

Ba/F3, UT-TPO and HEK293T cells were cultured in RPMI, IMDM and DMEM media (Sigma-Aldrich, Austria) respectively, supplemented with 10% fetal bovine serum (Sigma-Aldrich) and 1% Penicillin Streptomycin (Sigma-Aldrich). Ba/F3 cells were maintained with 5% WEHI-3B conditioned media as murine IL-3 supplement. UT7-TPO cells were maintained with 5% TPO conditioned media produced by murine 3T3 fibroblasts overexpressing vector encoding human TPO. Ba/F3-MPL cell lines were generated as previously described(176).

Compound

All the compounds were dissolved in DMSO or Milli-Q H2O. Hematoxylin, hematein and hydroxyurea/Hydroxycarbamide, brefeldin A, chloroquine diphosphate salt, MG132 were purchased from Sigma-Aldrich.

Brazilin, NSC7241 and NSC681607 were provided by the NCI Developmental Therapeutic Program's Open Compound Repository.

Protosappanin B was purchased from Cambridge Chemicals USA.

Ruxolitinib (CAS 1092939-17-7) was purchased from Selleckchem USA.

L-HEM1, L-HEM2 and L-HEM3 were synthesized by Lesyk group from Danylo Halytsky Lviv National Medical University.

Transduction

Human CALR wild-type (WT) and CALR del52 sequences were cloned into the pMSCV-IRES-puromycin retroviral vector. The plasmids were then used to transfect the Platinum-E (Plat-E) Retroviral Packaging Cell Line (CELL BIOLABS, INC, USA) using the Calcium Phosphate Transfection Kit (Thermo Fisher Scientific, USA) for retroviral production. Viral supernatant was then collected, and spin-infection of Ba/F3-MPL cells at 1200g, 37°C, for 45min, was performed for viral transduction. The transduced cell lines were selected with 1ug/ml puromycin until they were stably proliferating.

Generation of CALR mutant and knockout cell line models by CRISPR/Cas9 technology

The following single guide RNAs were used to target murine and human endogenous CALR gene locus:

Table 4 List of sgRNA sequences to generate mutations in CALR

Aim	sgRNA sequence	Species
CALR exon9 mutations in Ba/F3 cells	GAGGCTTAAGGAAGAAGAAG	Mouse
CALR exon9 mutations in UT7-TPO cells	GGACGAGGAGCAGAGGCTTA	Human
CALR knockout in Ba/F3 cells	GTGAGCAGAATATCGACTGTG	Mouse

The gRNA oligos were cloned into pSpCas9(BB)-2A-Puro (PX459) V2.0 vector which is a gift from Feng Zhang lab (Addgene plasmid # 62988)(248). The recipient cell lines were transfected using the Amaxa® Cell Line Nucleofector® Kit V (Lonza, Switzerland) and selected by 1ug/ml puromycin for 48h. Puromycin was then withdrawn and cells were singularized into 384-well plates. Cytokines were refreshed every 3 days during the process with the exception that disease frameshift CALR mutant clones were selected with cytokine-free media for 7 days

after singularization. The genotype of the outgrown colonies was analyzed by Fragment Length Analysis and Sanger Sequencing (Microsynth, Austria).

Cell viability assay

Ba/F3 and UT7-TPO were plated 5000 cells/well and 16000 cells/well into 96-well plates with the desirable concentrations of drugs or cytokines added in a total volume of 100ul. 72 hours later, the CellTiter-Glo luminescent Cell Viability Assay (Promega, Austria) was used to determine the cell viability. The luminescent signal was detected by a VICTOR Multilabel Plate Reader (PerkinElmer, USA). Dose response data was analyzed by Graphpad Prism 7.0.

Competition assay

To determine long-term viability, a two-color competition assay was used. Cell lines were transduced with pMSCV-IRES-GFP/mCherry constructs and the fluorescence positive cells were sorted by SH800Z Cell Sorter (Sony, Austria). GFP/mCherry positive cell lines were 1:1 ratio mixed with their non-fluorescent control cells and went through drug treatment for 3-12 days. Drugs and cytokines were refreshed every 3 days. Cell samples at each time point were analyzed by BD LSRFortessa™ cell analyzer (BD Biosciences, USA).

Alternatively, QIAamp DNA Mini Kit (Qiagen, Germany) was used to extract DNA samples from the mixed population and polymerase chain reaction (PCR) was performed with the following primer pairs to amplify the human CALR mutated sequence:

5'-[FAM]GGCAAGGCCCTGAGGTGT-3'

3'-GGCCTCAGTCCAGCCCTG-5'

The PCR products were diluted 1:50 and analyzed by Fragment Length Analysis (Microsynth) and the mutant CALR allelic burder was calculated as follows:

Mutant CALR allelic burden = Mutant peak height / (Mutant peak height + WT peak height)

Apoptosis assay by Annexin V/PI staining

Ba/F3-MPL CALR WT and mutant cell lines were treated with hematoxylin at 20uM or equivalent DMSO control for 24h before collection. eBioscience™ Annexin V Apoptosis Detection Kit (Invitrogen) was used based on manufactorer's instruction. 5ul of eBioscience™ Propidium Iodide Staining Solution (Invitrogen) was added to each sample for 10min before analyzed by BD LSRFortessa™ cell analyzer without washing.

Western blot

2 million Ba/F3-MPL CALR wild type or mutant cells were treated with hematoxylin or the equivalent volume of DMSO in total volume of 15ml of RPMI media in T75 flasks (Thermal Fisher Scientific). Cells were collected and lysed in NP-40 buffer supplemented with cOmplete™, Mini, EDTA-free Protease Inhibitor Cocktail (Sigma-Aldrich) and PhosSTOP™ (Sigma-Aldrich). The following antibodies were used for western blot: Calregulin Antibody (F-4) (Santa Cruz Biotechnology), Anti-HSC70(B-6) (Santa Cruz Biotechnology), Anti-Stat5 (N20)(Santa Cruz Biotechnology), anti-pYSTAT5 (Tyr694)(Thermo Fisher Scientific, USA), anti-TPOR/cMpl (Merck Millipore), Cleaved PARP (Asp214) (Cell Signaling Technology). HRP-linked anti-mouse and anti-rabbit antibodies (GE Healthcare Life Sciences) were used as secondary antibodies. Clarity™ Western ECL Blotting Substrates (Bio-Rad) were used for the chemiluminescence detection method.

NanoBRET assay

cDNAs coding for MPL and erythropoietin receptor (EpoR) were cloned into a modified pNL-N vector (Promega, Neitherland) to generate an N-terminal fusion of the Nano-luciferase to the receptors. cDNAs coding for wild type and the del52 mutant CALRs were cloned into the pHT-C vector to generate C-terminal HaloTag fused constructs (Promega). EBNA cells were transiently transfected using the Transit-LT1 reagent (Mirus Biotech, Belgium) with both one NanoLuciferase-receptor construct and one CALR-HaloTag construct per condition. 24 hours post transfection, cells were re-plated into 96-well luciferase plate following manufacter instructions (Promega) in OptiMeM – 4 % FBS – 100nM 618-ligand (NanoBRET Kit, Promega) with specific concentrations of hematoxylin (from 2mM to 20nM), vehicle (water) or no additional substrate. Cells were then kept for another 24 hours in an incubator at 37°C – 8%

CO2. The next day, each well was washed with DMEM/F12 (50:50) – no FBS – no Phenol red medium before adding pre-warmed (37°C) DMEM/F12 (50:50) – 1X NanoGlo substrate (NanoBRET kit, Promega) to each well. The plate was then analyzed for bioluminescence resonance energy transfer (BRET) according to the manufacturer's protocol on a GloMax Discover multiplate reader (Promega) at 37°C using the 450BP (donor) and 600LP (acceptor) built-in filters. Each condition was repeated as three biological replicates in each independent experiment (n experiments = 2). Statistical test was calculated by non-parametric multiple comparison with control Steel's method.

Cellular thermal shift assay

Human CALR WT, ins5 and MPL sequences were cloned into pcDNA3.1 vector. HEK293T cells were transfected with pcDNA3.1 CALR WT, pcDNA3.1 CALR ins5 and pcDNA3.1 CALR MPL constructs respectively using Calcium Phosphate Transfection Kit (Thermo Fisher Scientific) according to manufacture instructions. Cells were lysed in NP40 Cell Lysis Buffer containing cOmplete™, Mini, EDTA-free Protease Inhibitor Cocktail (Sigma-Aldrich). Cell lysates were diluted to 0.8-1.2mg/ml. Hematoxylin or DMSO were added into cell lysate followed by 30min incubation on ice. Each sample was then aliquoted into Eppendorf tubes and heated at different temperatures on a heating block for 6min before cooling down at room temperature for 3min. All the samples were then centrifuged at 14000 x g for 40 min at 4C. The soluble fractions were then transferred to new tubes and analyzed by western blot. The assay was adapted from published protocols(225,226).

Real-time PCR

1 million cells from each sample were collected and washed by PBS twice. RNA samples were extracted by RNeasy Mini Kit (Qiagen). Taqman(R) Gene Expression Assays (Mm01545399_m1) was used to quantify the expression of CALR and the real-time PCR reaction was performed using a 7500 Fast Real-Time PCR machine (Thermo Fisher Scientific). Statistical test was calculated using the two-tailed Student's t test.

CD34 positive cell isolation and expansion

The collection and study of the patients' samples was approved by the ethics committee in the Medical University of Vienna and conducted in accordance with the Declaration of Helsinki. The patients was given written informed consent in advance. Whole blood or buffy coat was collected in EDTA tubes. Peripheral blood mononuclear cells (PBMCs) were isolated by SepMate™-50 (STEMCELL Technologies, Germany) according to manufactorer's instructions.

After isolation of PBMCs, EasySep™ Human CD34 Positive Selection Kit (STEMCELL Technologies) was used to isolate CD34 positive cells according to the manufacturer's instructions. The isolated cells were then expanded in StemSpan™ SFEM II (STEMCELL Technologies) with addition of StemSpan™ CD34+ Expansion Supplement (STEMCELL Technologies) for no more than 8 days before assays or storage.

Colony formation assay

2000 human CD34 positive cells were plated in 1ml of Methocult H4434 classic medium (STEMCELL Technologies, Germany) with 40uM hematoxylin or DMSO control. Cells were incubated for 14 days before colony counting. Statistical test was calculated using two-way ANOVA with Sidak's multiple comparisons test.

4.2 Materials and Methods for result 2.2

High-throughput drug screen

The screen was performed in Platform Austria for Chemical Biology (PLACEBO) using a customized library of 89172 compounds. UT7-TPO cells were seeded at a density of 16000 cells/well in 384-well plates. UT7-TPO CALR del61/WT cell line was used for first-round cytotoxicity screen. Both UT7-TPO parental and UT7-TPO CALR del61/WT cell lines were used for the second-round selectivity screen. Each condition had 3 technical replicates. The CellTiter-Glo assay was used to measure cell viability after 72 hours incubation. Proteosomal inhibitor Bortezomib was used as the positive control at an assay concentration of 13.5 uM. Equivalent amount of DMSO (0.135%) was used as negative control. Z-factor was calculated for each plate(249). Only the plates with Z-factor > 0 passed quality control and were taken into analysis.

To compare compounds across plates with different signal, a percentage of control (POC) was calculated by linear regression, setting the mean signal of the DMSO wells to 100% and the mean signal of the PosCon wells to 0% for each plate individually.

Chemicals

All drugs used for initial screen and dose-response validation were provided by PLACEBO. Follow up validation used for other assays were performed with drugs from the following suppliers:

LY2603618 (CAS No.: 911222-45-2, Cayman Chemical Company)

SCH900776/MK8776 (CAS No.: 891494-63-6, MedChemExpress)

MK1775 (CAS No.: 955365-80-7, MedChemExpress)

Dose response assay

UT7-TPO and BaF3-MPL cell lines were seeded at a density of 16000/well and 5000/well respectively in 96-well plates. ½ serial dilution of the drug was used and equivalent amount of DMSO was added to each well. Cell viability was measured by the CellTiter-Glo® Luminescent Assay (Promega) according to the manufacture instruction at 72h after the treatment.

Competition assay

All mCherry positive cell lines were generated by transducing recipient cells with retrovirus carrying pMSCV-mCherry constructs produced by HEK293T cells and sorted by Sony SH800 sorter. mCherry positive and negative cells were mixed at 1:1 ratio in the presence of cytokine and drug at day 0. 2.5 million were seeded for UT7-TPO cells and 0.5 million were seeded for BaF3-MPL cells both in 10ml of media. Cells were counted and re-plated at the initial density after each time point collection. Media, cytokine and drugs were also refreshed. Samples were analyzed by BD LSRFortessa™ (BD Biosciences).

Western blot

Western blot was conducted as described in Materials and Methods 4.1. The following antibodies was used (Table 5).

Table 5 List of antibodies used in western blot

Antibody	Species	Manufacturer	Catalog number	Dilution
pRPA (S4/S8)	Rabbit	Bethyl Laboratories	A300-245A	1:1000
pRPA (S33)	Rabbit	Bethyl Laboratories	A300-246A	1:1000
RPA	Mouse	Abcam	ab2175	1:1000
HSC70	Mouse	Santa Cruz Biotechnology	sc-7298	1:30000
yH2AX-S139	Rabbit	Cell Signalling Technology	9718	1:1000
pChk1-S345	Rabbit	Cell Signalling Technology	2348	1:1000
Chk1	Mouse	Santa Cruz Biotechnology	sc-56291	1:1000
SAT601 (mutant calreticulin)	Rabbit	Myelopro		1:5000
Calregulin (calreticulin)	Mouse	Santa Cruz Biotechnology	sc-373863	1:2000
c-MPL	Rabbit	Merck/Millipore	06-944	1:3000
GAPDH	Mouse	Santa Cruz Biotechnology	sc-32233	1:30000

Immunofluorescence

After treatment, cells were plated on 10% (v/v) poly L-lysine (Sigma) coated slides 1h at 37C for immobilization. Cells were then washed twice with PBS and fixed in 4% Paraformaldehyde solution (PFA) (Santa Cruz) at room temperature for 15 minutes. For γ-H2AX staining, a pre-extraction step was done by adding 0.2% (v/v) Triton-X (Sigma) in PBS on slides for 1 minute on ice. Permeablization was done by 0.5% Triton-X in PBS for 5min at room temperature. Cells were then washed in PBS with 0.1% (v/v) Tween20 (Sigma) for 5min three times. 5% (m/v) BSA in PBS with 0.1% Tween was used for blocking 1h at room temperature. Primary antibodies were then diluted in blocking buffer for overnight staining at 4°C. Cells were then washed in PBS Tween solution for 3 times before secondary antibody staining for 1h at room temperature. Cells were again washed for 3 times before nuclei staining by 0.1% (m/v) DAPI for 10min at room temperature. Cells were then washed twice and ProLong™ Gold Antifade Mountant medium (ThermoFisher Scientific) was applied. The slides were covered by a cover slip and dried for 48h at room temperature before analyzed or stored at 4°C.

Zeiss LSM700 confocal microscope was used for image scanning. 405nm laser was used for DAPI signal detection and 639nm laser was used to detect Alexa-fluor 647 signal. 20X (0.8NA) Plan-Apochromat objective lens and a pinhole size of 1 airy unit was used for image capture. Image was analyzed by ZEN black 2010 software. Quantification of positive stained cells was analyzed by CellProfiler.

Table 6 List of antibodies used in immunofluorescence

Primary Antibody	**Species**	**Manufacturer**	**Catalog number**	**Dilution**
pRPA (S4/S8)	Rabbit	Sigma	PLA0071	1:100
yH2AX-S139	Mouse	Merck Millipore	JBW301	1:1000
Rabbit IgG Isotype Control	Rabbit	Invitrogen	02-6102	
Mouse IgG1 kappa Isotype control	Mouse	eBioscience	14-4714-82	
Secondary Antibody				
Anti-rabbit IgG (H+L) Alexa Fluor 488	Goat	Invitrogen	A-11034	1:1000
Anti-mouse IgG (H+L) Alexa Fluor 647	Goat	Invitrogen	A-21235	1:1000

Cell cycle analysis by FACs

1 million cells were collected and fixed in 70% ice-cold ethanol (Bartelt) for minimum 2 hours. Cells were then washed with PBS and blocked in 5% BSA solution for 1h. yH2AX antibody (1:1000, Merck) was used as primary antibody for 1h staining at room temperature. Cells were washed by PBS and stained with anti-mouse IgG (H+L) Alexa Fluor 647 (1:1000, Invitrogen) for 1h at room temperature in the dark. 1mg/ml DAPI solution was then used to stain DNA for 20min at RT in dark. Samples were analyzed by BD LSRFortessa™ (BD Biosciences).

Reference

1. Golub R, Cumano A. Embryonic hematopoiesis. Blood Cells, Mol Dis. 2013;
2. Orkin SH, Zon LI. Hematopoiesis: An Evolving Paradigm for Stem Cell Biology. Cell. 2008 Feb;132(4):631–44.
3. Scadden DT. The stem-cell niche as an entity of action. Nature. 2006.
4. Fuchs E, Tumbar T, Guasch G. Socializing with the neighbors: stem cells and their niche. Cell. 2004;
5. Jan M, Ebert BL, Jaiswal S. Clonal hematopoiesis. Semin Hematol. 2017;54(1):43–50.
6. Hoggatt J, Pelus LM. Hematopoiesis. In: Brenner's Encyclopedia of Genetics: Second Edition. 2013.
7. Doulatov S, Notta F, Laurenti E, Dick JE. Hematopoiesis: A human perspective. Cell Stem Cell. 2012;10(2):120–36.
8. Robb L. Cytokine receptors and hematopoietic differentiation. Oncogene. 2007;26(47):6715–23.
9. Metcalf D. ASH 50th anniversary review Hematopoietic cytokines. Blood. 2009;111(2):485–91.
10. Nervi B, Link DC, DiPersio JF. Cytokines and hematopoietic stem cell mobilization. J Cell Biochem. 2006;
11. Ogawa M. Differentiation and proliferation of hematopoietic stem cells. Blood. 1993;
12. Rieger MA, Hoppe PS, Smejkal BM, Eitelhuber AC, Schroeder T. Hematopoietic cytokines can instruct lineage choice. Science (80-). 2009;
13. Fujio K, Nosaka T, Kojima T, Kawashima T, Yahata T, Copeland NG, et al. Molecular cloning of a novel type 1 cytokine receptor similar to the common gamma chain. Blood. 2000;
14. Ferrao R, Wallweber HJA, Ho H, Tam C, Franke Y, Quinn J, et al. The Structural Basis for Class II Cytokine Receptor Recognition by JAK1. Structure. 2016;
15. Baker SJ, Rane SG, Reddy EP. Hematopoietic cytokine receptor signaling. Oncogene.

2007.

16. Baum CM, Weissman IL, Tsukamoto AS, Buckle AM, Peault B. Isolation of a candidate human hematopoietic stem-cell population. Proc Natl Acad Sci U S A. 1992;

17. Okada S, Nakauchi H, Nagayoshi K, Nishikawa S, Miura Y, Suda T. In vivo and in vitro stem cell function of c-kit- and Sca-1-positive murine hematopoietic cells. Blood. 1992;

18. Macaulay IC, Svensson V, Labalette C, Ferreira L, Hamey F, Voet T, et al. Single-Cell RNA-Sequencing Reveals a Continuous Spectrum of Differentiation in Hematopoietic Cells. Cell Rep. 2016;

19. Buenrostro JD, Corces MR, Lareau CA, Wu B, Schep AN, Aryee MJ, et al. Integrated Single-Cell Analysis Maps the Continuous Regulatory Landscape of Human Hematopoietic Differentiation. Cell. 2018;

20. Attar A. Changes in the Cell Surface Markers During Normal Hematopoiesis: A Guide to Cell Isolation. Glob J Hematol Blood Transfus. 2014;

21. Challen GA, Boles N, Lin KKY, Goodell MA. Mouse hematopoietic stem cell identification and analysis. Cytometry Part A. 2009.

22. Wadleigh M, Tefferi A. Classification and diagnosis of myeloproliferative neoplasms according to the 2008 World Health Organization criteria. Int J Hematol. 2010;91(2):174–9.

23. Arber DA, Orazi A, Hasserjian R, Thiele J, Borowitz MJ, Le Beau MM, et al. The 2016 revision to the World Health Organization classification of myeloid neoplasms and acute leukemia. Blood. 2016/04/14. 2016;127(20):2391–405.

24. Sattler M, Griffin JD. Mechanisms of transformation by the BCR/ABL oncogene. Int J Hematol. 2001;

25. Lugo TG, Pendergast AM, Muller AJ, Witte ON. Tyrosine kinase activity and transformation potency of bcr-abl oncogene products. Science (80-). 1990;

26. Druker BJ, Tamura S, Buchdunger E, Ohno S, Segal GM, Fanning S, et al. Effects of a selective inhibitor of the Ab1 tyrosine kinase on the growth of Bcr-Ab1 positive cells. Nat Med. 1996;

27. Levine RL, Wadleigh M, Cools J, Ebert BL, Wernig G, Huntly BJ, et al. Activating mutation in the tyrosine kinase JAK2 in polycythemia vera, essential thrombocythemia, and myeloid metaplasia with myelofibrosis. Cancer Cell. 2005/04/20. 2005;7(4):387–97.

28. Kralovics R, Passamonti F, Buser AS, Teo S, Tiedt R, Passweg JR, et al. A Gain-of-

Function Mutation of JAK2 in Myeloproliferative Disorders. N Engl J Med. 2005 Apr 28;352(17):1779–90.

29. Baxter EJ, Scott LM, Campbell PJ, East C, Fourouclas N, Swanton S, et al. Acquired mutation of the tyrosine kinase JAK2 in human myeloproliferative disorders. Lancet. 2005/03/23. 2005;365(9464):1054–61.

30. James C, Ugo V, Le Couedic JP, Staerk J, Delhommeau F, Lacout C, et al. A unique clonal JAK2 mutation leading to constitutive signalling causes polycythaemia vera. Nature. 2005/03/29. 2005;434(7037):1144–8.

31. Klampfl T, Gisslinger H, Harutyunyan AS, Nivarthi H, Rumi E, Milosevic JD, et al. Somatic mutations of calreticulin in myeloproliferative neoplasms. N Engl J Med. 2013/12/12. 2013;369(25):2379–90.

32. Nangalia J, Massie CE, Baxter EJ, Nice FL, Gundem G, Wedge DC, et al. Somatic CALR mutations in myeloproliferative neoplasms with nonmutated JAK2. N Engl J Med. 2013/12/12. 2013;369(25):2391–405.

33. Pikman Y, Lee BH, Mercher T, McDowell E, Ebert BL, Gozo M, et al. MPLW515L is a novel somatic activating mutation in myelofibrosis with myeloid metaplasia. PLoS Med. 2006/07/13. 2006;3(7):e270.

34. Pardanani AD, Levine RL, Lasho T, Pikman Y, Mesa RA, Wadleigh M, et al. MPL515 mutations in myeloproliferative and other myeloid disorders: A study of 1182 patients. Blood. 2006;

35. Boddu P, Chihara D, Masarova L, Pemmaraju N, Patel KP, Verstovsek S. The co-occurrence of driver mutations in chronic myeloproliferative neoplasms. Ann Hematol. 2018;

36. Xing CY, Li HY, Wu JB, Gao SM. Co-occurrence of JAK2 V617F and an uncommon CALR del (p.K368fs*51) mutation facilitates JAK2/STAT signaling in polycythemia vera. Leukemia and Lymphoma. 2016.

37. Zamora L, Xicoy B, Cabezón M, Fernandez C, Marcé S, Velez P, et al. Co-existence of JAK2 V617F and CALR mutations in primary myelofibrosis. Leukemia and Lymphoma. 2015.

38. Ahmed RZ, Rashid M, Ahmed N, Nadeem M, Shamsi TS. Coexisting JAK2V617F and CALR exon 9 mutations in myeloproliferative neoplasms - do they designate a new subtype? Asian Pacific Journal of Cancer Prevention. 2016.

39. Milosevic Feenstra JD, Nivarthi H, Gisslinger H, Leroy E, Rumi E, Chachoua I, et al.

Whole-exome sequencing identifies novel MPL and JAK2 mutations in triple-negative myeloproliferative neoplasms. Blood. 2016;

40. Schischlik F, Kralovics R. Mutations in myeloproliferative neoplasms–their significance and clinical use. Expert Review of Hematology. 2017.

41. Vainchenker W, Kralovics R. Genetic basis and molecular pathophysiology of classical myeloproliferative neoplasms. Blood. 2016/12/29. 2016;

42. Kralovics R. Genetic complexity of myeloproliferative neoplasms. Leukemia. 2008;22(10):1841–8.

43. Grinfeld J, Nangalia J, Baxter EJ, Wedge DC, Angelopoulos N, Cantrill R, et al. Classification and Personalized Prognosis in Myeloproliferative Neoplasms. N Engl J Med. 2018;379(15):1416–30.

44. Steensma DP. Clinical consequences of clonal hematopoiesis of indeterminate potential. Blood advances. 2018.

45. Steensma DP, Bejar R, Jaiswal S, Lindsley RC, Sekeres MA, Hasserjian RP, et al. Clonal hematopoiesis of indeterminate potential and its distinction from myelodysplastic syndromes. Blood. 2015.

46. Boettcher S, Ebert BL. Clonal hematopoiesis of indeterminate potential. J Clin Oncol. 2019;

47. Yang Y, Akada H, Nath D, Hutchison RE, Mohi G. Loss of Ezh2 cooperates with Jak2V617F in the development of myelofibrosis in a mouse model of myeloproliferative neoplasm. Blood. 2016;

48. Jacquelin S, Straube J, Cooper L, Vu T, Song A, Bywater M, et al. Jak2V617F and Dnmt3a loss cooperate to induce myelofibrosis through activated enhancer-driven inflammation. Blood. 2018;

49. Sashida G, Wang C, Tomioka T, Oshima M, Aoyama K, Kanai A, et al. The loss of Ezh2 drives the pathogenesis of myelofibrosis and sensitizes tumor-initiating cells to bromodomain inhibition. J Exp Med. 2016;

50. Rampal R, Ahn J, Abdel-Wahab O, Nahas M, Wang K, Lipson D, et al. Genomic and functional analysis of leukemic transformation of myeloproliferative neoplasms. Proc Natl Acad Sci. 2014;

51. Harutyunyan A, Klampfl T, Cazzola M, Kralovics R. p53 Lesions in Leukemic Transformation. N Engl J Med. 2011;

52. Malcovati L, Papaemmanuil E, Bowen DT, Boultwood J, Della Porta MG, Pascutto C, et al. Clinical significance of SF3B1 mutations in myelodysplastic syndromes and myelodysplastic/myeloproliferative neoplasms. Blood. 2011;

53. Geyer HL, Mesa RA. Review Article Therapy for myeloproliferative neoplasms : when , which agent , and how ? 2015;124(24):277–86.

54. Rumi E, Cazzola M. How I treat essential thrombocythemia. 2016;128(20):2403–15.

55. Vannucchi AM, Harrison CN. Emerging treatments for classical myeloproliferative neoplasms. 2018;129(6):693–704.

56. Kiladjian J, Harrison C. Myeloproliferative neoplasms and personalized medicine : the perfect match ? 2015;1493–4.

57. Björkholm M, Hultcrantz M, Derolf ÅR. Leukemic transformation in myeloproliferative neoplasms: Therapy-related or unrelated? Best Practice and Research: Clinical Haematology. 2014.

58. Kennedy JA, Atenafu EG, Messner HA, Craddock KJ, Brandwein JM, Lipton JH, et al. Treatment outcomes following leukemic transformation in Philadelphia-negative myeloproliferative neoplasms. Blood. 2013;

59. Yogarajah M, Tefferi A. Leukemic Transformation in Myeloproliferative Neoplasms: A Literature Review on Risk, Characteristics, and Outcome. Mayo Clinic Proceedings. 2017.

60. Lim SN, Lee JH, Lee JH, Kim DY, Kim SD, Kang YA, et al. Allogeneic hematopoietic cell transplantation in adult patients with myelodysplastic/myeloproliferative neoplasms. Blood Res. 2013;

61. Verstovsek S, Mesa RA, Gotlib J, Levy RS, Gupta V, DiPersio JF, et al. A Double-Blind, Placebo-Controlled Trial of Ruxolitinib for Myelofibrosis. N Engl J Med. 2012;

62. Harrison C, Kiladjian J-J, Al-Ali HK, Gisslinger H, Waltzman R, Stalbovskaya V, et al. JAK Inhibition with Ruxolitinib versus Best Available Therapy for Myelofibrosis. N Engl J Med. 2012;

63. Vannucchi AM, Kiladjian JJ, Griesshammer M, Masszi T, Durrant S, Passamonti F, et al. Ruxolitinib versus standard therapy for the treatment of polycythemia vera. N Engl J Med. 2015;

64. Harrison CN, Vannucchi AM, Kiladjian J-J, Al-Ali HK, Gisslinger H, Knoops L, et al. Long-term findings from COMFORT-II, a phase 3 study of ruxolitinib vs best available

therapy for myelofibrosis. Leukemia. 2016;

65. Cervantes F, Vannucchi AM, Kiladjian JJ, Al-Ali HK, Sirulnik A, Stalbovskaya V, et al. Three-year efficacy, safety, and survival findings from COMFORT-II, a phase 3 study comparing ruxolitinib with best available therapy for myelofibrosis. Blood. 2013;

66. Verstovsek S, Mesa RA, Gotlib J, Gupta V, DiPersio JF, Catalano J V., et al. Long-term treatment with ruxolitinib for patients with myelofibrosis: 5-year update from the randomized, double-blind, placebo-controlled, phase 3 COMFORT-I trial. J Hematol Oncol. 2017;

67. Cervantes F., A. M. Vannucchi J-JK. Long-term safety, efficacy, and survival findings from comfort-ii, a phase 3 study comparing ruxolitinib with best available therapy (bat) for the treatment of myelofibrosis (mf). Blood. 2012;

68. Verstovsek S, Gotlib J, Mesa RA, Vannucchi AM, Kiladjian JJ, Cervantes F, et al. Long-Term survival in patients treated with ruxolitinib for myelofibrosis: COMFORT-I and-II pooled analyses. J Hematol Oncol. 2017;

69. Verstovsek S, Vannucchi AM, Griesshammer M, Masszi T, Durrant S, Passamonti F, et al. Ruxolitinib versus best available therapy in patients with polycythemia vera: 80-week follow-up from the RESPONSE trial. Haematologica. 2016;

70. Verstovsek S, Passamonti F, Rambaldi A, Barosi G, Rosen PJ, Rumi E, et al. A phase 2 study of ruxolitinib, an oral JAK1 and JAK2 inhibitor, in patients with advanced polycythemia vera who are refractory or intolerant to hydroxyurea. Cancer. 2014;

71. Passamonti F, Griesshammer M, Palandri F, Egyed M, Benevolo G, Devos T, et al. Ruxolitinib for the treatment of inadequately controlled polycythaemia vera without splenomegaly (RESPONSE-2): a randomised, open-label, phase 3b study. Lancet Oncol. 2017;

72. J.-J. K, S. C, C. D, C. C, J.-D. R. Treatment of polycythemia vera with hydroxyurea and pipobroman: Final results of a randomized trial initiated in 1980. J Clin Oncol. 2011;

73. Verstovsek S, Kantarjian H, Mesa RA, Pardanani AD, Cortes-Franco J, Thomas DA, et al. Safety and Efficacy of INCB018424, a JAK1 and JAK2 Inhibitor, in Myelofibrosis. N Engl J Med. 2010;

74. Quintás-Cardama A, Vaddi K, Liu P, Manshouri T, Li J, Scherle PA, et al. Preclinical characterization of the selective JAK1/2 inhibitor INCB018424: Therapeutic implications for the treatment of myeloproliferative neoplasms. Blood. 2010;

75. Pardanani A, Tefferi A, Jamieson C, Gabrail N, Lebedinsky C, Gao G, et al. A phase 2

randomized dose-ranging study of the JAK2-selective inhibitor fedratinib (SAR302503) in patients with myelofibrosis. Blood Cancer J. 2015;

76. Harrison CN, Schaap N, Vannucchi AM, Kiladjian JJ, Tiu R V., Zachee P, et al. Janus kinase-2 inhibitor fedratinib in patients with myelofibrosis previously treated with ruxolitinib (JAKARTA-2): a single-arm, open-label, non-randomised, phase 2, multicentre study. Lancet Haematol. 2017;

77. Mesa RA, Vannucchi AM, Mead A, Egyed M, Szoke A, Suvorov A, et al. Pacritinib versus best available therapy for the treatment of myelofibrosis irrespective of baseline cytopenias (PERSIST-1): an international, randomised, phase 3 trial. Lancet Haematol. 2017;

78. Mascarenhas J, Hoffman R, Talpaz M, Gerds AT, Stein B, Gupta V, et al. Pacritinib vs best available therapy, including ruxolitinib, in patients with myelofibrosis: A randomized clinical trial. JAMA Oncol. 2018;

79. Kiladjian JJ, Giraudier S, Cassinat B. Interferon-alpha for the therapy of myeloproliferative neoplasms: targeting the malignant clone. Leukemia. 2015/11/26. 2016;30(4):776–81.

80. Quintas-Cardama A, Kantarjian H, Manshouri T, Luthra R, Estrov Z, Pierce S, et al. Pegylated interferon alfa-2a yields high rates of hematologic and molecular response in patients with advanced essential thrombocythemia and polycythemia vera. J Clin Oncol. 2009/10/15. 2009;27(32):5418–24.

81. Quintas-Cardama A, Abdel-Wahab O, Manshouri T, Kilpivaara O, Cortes J, Roupie AL, et al. Molecular analysis of patients with polycythemia vera or essential thrombocythemia receiving pegylated interferon alpha-2a. Blood. 2013/06/21. 2013;122(6):893–901.

82. Jatiani SS, Baker SJ, Silverman LR, Premkumar Reddy E. JAK/STAT pathways in cytokine signaling and myeloproliferative disorders: Approaches for targeted therapies. Genes and Cancer. 2010.

83. Staerk J, Constantinescu SN. The JAK-STAT pathway and hematopoietic stem cells from the JAK2 V617F perspective. JAK-STAT. 2012;

84. Rodig SJ, Meraz MA, White JM, Lampe PA, Riley JK, Arthur CD, et al. Disruption of the Jak1 gene demonstrates obligatory and nonredundant roles of the Jaks in cytokine-induced biologic responses. Cell. 1998;

85. Parganas E, Wang D, Stravopodis D, Topham DJ, Marine JC, Teglund S, et al. Jak2 is

essential for signaling through a variety of cytokine receptors. Cell. 1998;

86. Neubauer H, Cumano A, Müller M, Wu H, Huffstadt U, Pfeffer K. Jak2 deficiency defines an essential developmental checkpoint in definitive hematopoiesis. Cell. 1998;

87. Park SO, Wamsley HL, Bae K, Hu Z, Li X, Choe S woon, et al. Conditional Deletion of Jak2 Reveals an Essential Role in Hematopoiesis throughout Mouse Ontogeny: Implications for Jak2 Inhibition in Humans. PLoS One. 2013;

88. Nosaka T, Van Deursen JMA, Tripp RA, Thierfelder WE, Witthuhn BA, McMickle AP, et al. Defective lymphoid development in mice lacking Jak3. Science (80-). 1995;

89. Park SY, Saijo K, Takahashi T, Osawa M, Areas H, Hirayama N, et al. Developmental defects of lymphoid cells in Jak3 kinase-deficient mice. Immunity. 1995;

90. Russell SM, Tayebi N, Nakajima H, Riedy MC, Roberts JL, Aman MJ, et al. Mutation of Jak3 in a patient with SCID: Essential role of Jak3 in lymphoid development. Science (80-). 1995;

91. O'Shea JJ, Husa M, Li D, Hofmann SR, Watford W, Roberts JL, et al. Jak3 and the pathogenesis of severe combined immunodeficiency. Mol Immunol. 2004;

92. Karaghiosoff M, Neubauer H, Lassnig C, Kovarik P, Schindler H, Pircher H, et al. Partial impairment of cytokine responses in Tyk2-deficient mice. Immunity. 2000;

93. Shimoda K, Tsutsui H, Aoki K, Kato K, Matsuda T, Numata A, et al. Partial impairment of interleukin-12 (IL-12) and IL-18 signaling in Tyk2-deficient mice. Blood. 2002;

94. Quintás-Cardama A, Verstovsek S. Molecular pathways: JAK/STAT pathway: Mutations, inhibitors, and resistance. Clin Cancer Res. 2013;19(8):1933–40.

95. Rawlings JS, Rosler KM, Harrison DA. The JAK/STAT signaling pathway. J Cell Sci. 2004;

96. Levy DE, Darnell JE. STATs: Transcriptional control and biological impact. Nat Rev Mol Cell Biol. 2002;3(9):651–62.

97. Toms A V., Deshpande A, McNally R, Jeong Y, Rogers JM, Kim CU, et al. Structure of a pseudokinase-domain switch that controls oncogenic activation of Jak kinases. Nat Struct Mol Biol. 2013;

98. McNally R, Toms A V., Eck MJ. Crystal structure of the FERM-SH2 module of human Jak2. PLoS One. 2016;

99. Thomas SJ, Snowden JA, Zeidler MP, Danson SJ. The role of JAK/STAT signalling in

the pathogenesis, prognosis and treatment of solid tumours. Br J Cancer. 2015;

100. Stark GR, Darnell JE. The JAK-STAT Pathway at Twenty. Immunity. 2012.

101. Yamaoka K, Saharinen P, Pesu M, Holt VET, Silvennoinen O, O'Shea JJ. The Janus kinases (Jaks). Genome Biology. 2004.

102. Bateman A, Martin MJ, O'Donovan C, Magrane M, Alpi E, Antunes R, et al. UniProt: The universal protein knowledgebase. Nucleic Acids Res. 2017;

103. Bateman A, Martin MJ, O'Donovan C, Magrane M, Apweiler R, Alpi E, et al. UniProt: A hub for protein information. Nucleic Acids Res. 2015;

104. Lim CP, Cao X. Structure, function, and regulation of STAT proteins. Molecular BioSystems. 2006.

105. Durbin JE, Hackenmiller R, Simon MC, Levy DE. Targeted disruption of the mouse Stat1 gene results in compromised innate immunity to viral disease. Cell. 1996;

106. Meraz MA, White JM, Sheehan KCF, Bach EA, Rodig SJ, Dighe AS, et al. Targeted disruption of the Stat1 gene in mice reveals unexpected physiologic specificity in the JAK-STAT signaling pathway. Cell. 1996;

107. Leung S, Qureshi SA, Kerr IM, Darnell JE, Stark GR. Role of STAT2 in the alpha interferon signaling pathway. Mol Cell Biol. 2015;

108. Li X, Leung S, Qureshi S, Darnell JE, Stark GR. Formation of STAT1-STAT2 heterodimers and their role in the activation of IRF-1 gene transcription by interferon-α. J Biol Chem. 1996;

109. Schubert C, Allhoff M, Tillmann S, Maié T, Costa IG, Lipka DB, et al. Differential roles of STAT1 and STAT2 in the sensitivity of JAK2V617F- vs. BCR-ABL-positive cells to interferon alpha. J Hematol Oncol. 2019;

110. Czech J, Cordua S, Weinbergerova B, Baumeister J, Crepcia A, Han L, et al. JAK2V617F but not CALR mutations confer increased molecular responses to interferon-α via JAK1/STAT1 activation. Leukemia. 2019;

111. Mullally A, Bruedigam C, Poveromo L, Heidel FH, Purdon A, Vu T, et al. Depletion of Jak2V617F myeloproliferative neoplasm-propagating stem cells by interferon-α in a murine model of polycythemia vera. Blood. 2013;

112. Shimoda H, Van Deursen J, Sangster MY, Sarawar SR, Carson RT, Tripp RA, et al. Lack of IL-4-induced Th2 response and IgE class switching in mice with disrupted Stat6 gene. Nature. 1996;

113. Kaplan MH, Schindler U, Smiley ST, Grusby MJ. Stat6 is required for mediating responses to IL-4 and for the development of Th2 cells. Immunity. 1996;

114. Thierfelder WE, Van Deursen JM, Yamamoto K, Tripp RA, Sarawar SR, Carson RT, et al. Requirement for Stat4 in interleukin-12-mediated responses of natural killer and T cells. Nature. 1996;

115. Takeda H, Tanaka T, Shi W, Matsumoto M, Minami M, Kashiwamura SI, et al. Essential role of Stat6 in IL-4 signalling. Nature. 1996;

116. Kaplan MH, Sun YL, Hoey T, Grusby MJ. Impaired IL-12 responses and enhanced development of Th2 cells in Stat4- deficient mice. Nature. 1996;

117. Liu X, Robinson GW, Wagner KU, Garrett L, Wynshaw-Boris A, Hennighausen L. Stat5a is mandatory for adult mammary gland development and lactogenesis. Genes Dev. 1997;

118. Dong J, Tong T, Reynado AM, Rosen JM, Huang S, Li Y. Genetic manipulation of individual somatic mammary cells in vivo reveals a master role of STAT5a in inducing alveolar fate commitment and lactogenesis even in the absence of ovarian hormones. Dev Biol. 2010;

119. Udy GB, Towers RP, Snell RG, Wilkins RJ, Park S-H, Ram PA, et al. Requirement of STAT5b for sexual dimorphism of body growth rates and liver gene expression. Proc Natl Acad Sci. 2002;

120. Takeda K, Noguchi K, Shi W, Tanaka T, Matsumoto M, Yoshida N, et al. Targeted disruption of the mouse Stat3 gene leads to early embryonic lethality. Proc Natl Acad Sci U S A. 1997;

121. Walz C, Ahmed W, Lazarides K, Betancur M, Patel N, Hennighausen L, et al. Essential role for Stat5a/b in myeloproliferative neoplasms induced by BCR-ABL1 and JAK2 V617F in mice. Blood. 2012;

122. Grisouard J, Shimizu T, Duek A, Kubovcakova L, Hao-Shen H, Dirnhofer S, et al. Deletion of Stat3 in hematopoietic cells enhances thrombocytosis and shortens survival in a JAK2-V617F mouse model of MPN. Blood. 2015;

123. Yan D, Hutchison RE, Mohi G. Critical requirement for Stat5 in a mouse model of polycythemia vera. Blood. 2012;

124. Walz C, Lazarides K, Patel N, Hennighausen L, Zaleskas VM, Van Etten RA. Essential Role for Stat5a/b in Myeloproliferative Neoplasms Induced by BCR-ABL1 and Jak2 V617F. Blood. 2009;

125. Kralovics R, Guan Y, Prchal JT. Acquired uniparental disomy of chromosome 9p is a frequent stem cell defect in polycythemia vera. Exp Hematol. 2002;

126. Scott LM, Tong W, Levine RL, Scott MA, Beer PA, Stratton MR, et al. JAK2 exon 12 mutations in polycythemia vera and idiopathic erythrocytosis. N Engl J Med. 2007/02/03. 2007;356(5):459–68.

127. Passamonti F, Elena C, Schnittger S, Skoda RC, Green AR, Girodon F, et al. Molecular and clinical features of the myeloproliferative neoplasm associated with JAK2 exon 12 mutations. Blood. 2011;

128. Vannucchi AM, Antonioli E, Guglielmelli P, Pardanani A, Tefferi A. Clinical correlates of JAK2V617F presence or allele burden in myeloproliferative neoplasms: A critical reappraisal. Leukemia. 2008.

129. Passamonti F, Rumi E. Clinical relevance of JAK2 (V617F) mutant allele burden. Haematologica. 2009.

130. Larsen TS, Pallisgaard N, M??ller MB, Hasselbalch HC. The JAK2 V617F allele burden in essential thrombocythemia, polycythemia vera and primary myelofibrosis - Impact on disease phenotype. Eur J Haematol. 2007;

131. Manuscript A, Aberg K a., McClay JL, Nerella S, Clark S, Kumar G, et al. NIH Public Access. Mol Psychiatry. 2013;

132. Li J, Kent DG, Chen E, Green AR. Mouse models of myeloproliferative neoplasms: JAK of all grades. Dis Model Mech. 2011;4(3):311–7.

133. Gurney AL, Carver-Moore K, De Sauvage FJ, Moore MW. Thrombocytopenia in c-mpl-deficient mice. Science (80-). 1994;

134. Varghese LN, Defour JP, Pecquet C, Constantinescu SN. The thrombopoietin receptor: Structural basis of traffic and activation by ligand, mutations, agonists, and mutated calreticulin. Front Endocrinol (Lausanne). 2017;8(MAR):1–13.

135. Albu RI, Constantinescu SN. Extracellular domain N-glycosylation controls human thrombopoietin receptor cell surface levels. Front Endocrinol (Lausanne). 2011;

136. Staerk J, Lacout C, Sato T, Smith SO, Vainchenker W, Constantinescu SN. An amphipathic motif at the transmembrane-cytoplasmic junction prevents autonomous activation of the thrombopoietin receptor. Blood. 2006;

137. Constantinescu SN, Huang LJ shen, Nam H song, Lodish HF. The erythropoietin receptor cytosolic juxtamembrane domain contains an essential, precisely oriented,

hydrophobic motif. Mol Cell. 2001;

138. Bénit L, Courtois G, Charon M, Varlet P, Dusanter-Fourt I, Gisselbrecht S. Characterization of mpl cytoplasmic domain sequences required for myeloproliferative leukemia virus pathogenicity. J Virol. 1994;

139. Alexander WS, Metcalf D, Dunn AR. Point mutations within a dimer interface homology domain of c-Mpl induce constitutive receptor activity and tumorigenicity. EMBO J. 1995;

140. Pikman Y, Lee BH, Mercher T, McDowell E, Ebert BL, Gozo M, et al. MPLW515L is a novel somatic activating mutation in myelofibrosis with myeloid metaplasia. PLoS Med. 2006;

141. Ding J, Komatsu H, Wakita A, Kato-Uranishi M, Ito M, Satoh A, et al. Familial essential thrombocythemia associated with a dominant-positive activating mutation of the c-MPL gene, which encodes for the receptor for thrombopoietin. Blood. 2004;

142. Michalak M, Corbett EF, Mesaeli N, Nakamura K, Opas M. Calreticulin: one protein, one gene, many functions. Biochem J. 1999;

143. Michalak M, Groenendyk J, Szabo E, Gold LI, Opas M. Calreticulin, a multi-process calcium-buffering chaperone of the endoplasmic reticulum. Biochem J. 2009/01/13. 2009;417(3):651–66.

144. Gelebart P, Opas M, Michalak M. Calreticulin , a Ca 2 + -binding chaperone of the endoplasmic reticulum. 2005;37:260–6.

145. Gardai SJ, Mcphillips KA, Frasch SC, Janssen WJ, Starefeldt A, Murphy-ullrich JE, et al. Cell-Surface Calreticulin Initiates Clearance of Viable or Apoptotic Cells through trans -Activation of LRP on the Phagocyte. 2005;123:321–34.

146. Chouquet A, Païdassi H, Ling WL, Frachet P, Houen G, Arlaud GJ, et al. X-ray structure of the human calreticulin globular domain reveals a peptide-binding area and suggests a multi-molecular mechanism. PLoS One. 2011;6(3):1–9.

147. Ellgaard L, Riek R, Herrmann T, Guntert P, Braun D, Helenius A, et al. NMR structure of the calreticulin P-domain. Proc Natl Acad Sci U S A. 2001/03/15. 2001;98(6):3133–8.

148. Kozlov G, Pocanschi CL, Rosenauer A, Bastos-Aristizabal S, Gorelik A, Williams DB, et al. Structural basis of carbohydrate recognition by calreticulin. J Biol Chem. 2010;285(49):38612–20.

149. Baksh S, Michalak M. Expression of calreticulin in Escherichia coli and identification of

its Ca2+ binding domains. J Biol Chem. 1991;

150. Nakamura K, Zuppini A, Arnaudeau S, Lynch J, Ahsan I, Krause R, et al. Functional specialization of calreticulin domains. J Cell Biol. 2001;

151. Mesaeli N, Nakamura K, Zvaritch E, Dickie P, Dziak E, Krause K, et al. Calreticulin Is Essential for Cardiac Development. 1999;144(5):857–68.

152. Mery L, Mesaeli N, Michalak M, Opas M, Lew DP, Krause KH. Overexpression of calreticulin increases intracellular Ca2+storage and decreases store-operated Ca2+influx. J Biol Chem. 1996;

153. Rauch F, Prud'Homme J, Arabian A, Dedhar S, St-Arnaud R. Heart, brain, and body wall defects in mice lacking calreticulin. Exp Cell Res. 2000;

154. Periasamy M, Kalyanasundaram A. SERCA pump isoforms: Their role in calcium transport and disease. Muscle and Nerve. 2007.

155. Bezprozvanny I. The inositol 1,4,5-trisphosphate receptors. Cell Calcium. 2005;

156. Wijeyesakere SJ, Rizvi SM, Raghavan M. Glycan-dependent and -independent interactions contribute to cellular substrate recruitment by calreticulin. J Biol Chem. 2013;288(49):35104–16.

157. Kozlov G, Pocanschi CL, Rosenauer A, Bastos-Aristizabal S, Gorelik A, Williams DB, et al. Structural basis of carbohydrate recognition by calreticulin. J Biol Chem. 2010/10/01. 2010;285(49):38612–20.

158. Lamriben L, Graham JB, Adams BM, Hebert DN. N-Glycan-based ER Molecular Chaperone and Protein Quality Control System: The Calnexin Binding Cycle. Traffic. 2016.

159. Tannous A, Pisoni GB, Hebert DN, Molinari M. N-linked sugar-regulated protein folding and quality control in the ER. Seminars in Cell and Developmental Biology. 2015.

160. Trombetta ES. The contribution of N-glycans and their processing in the endoplasmic reticulum to glycoprotein biosynthesis. 2003;13(9):77–91.

161. Aebi M. N-linked protein glycosylation in the ER. Biochimica et Biophysica Acta - Molecular Cell Research. 2013.

162. Bieberich E. Synthesis, Processing, and Function of N-glycans in N-glycoproteins. In 2014.

163. Wearsch PA, Cresswell P. The quality control of MHC class I peptide loading. Current

Opinion in Cell Biology. 2008.

164. Sadasivan B, Lehner PJ, Ortmann B, Spies T, Cresswell P. Roles for calreticulin and a novel glycoprotein, tapasin, in the interaction of MHC class I molecules with TAP. Immunity. 1996;

165. Gao B, Adhikari R, Howarth M, Nakamura K, Gold MC, Hill AB, et al. Assembly and antigen-presenting function of MHC class I molecules in cells lacking the ER chaperone calreticulin. Immunity. 2002;

166. Parker JMR, Groenendyk J, Müller-Esterl W, Opas M, Guo L, Michalak M, et al. Identification by Mutational Analysis of Amino Acid Residues Essential in the Chaperone Function of Calreticulin. J Biol Chem. 2005;281(4):2338–46.

167. Kapoor M, Ellgaard L, Gopalakrishnapai J, Schirra C, Gemma E, Oscarson S, et al. Mutational analysis provides molecular insight into the carbohydrate-binding region of calreticulin: pivotal roles of tyrosine-109 and aspartate-135 in carbohydrate recognition. Biochemistry. 2004/01/07. 2004;43(1):97–106.

168. Guo L, Nakamura K, Lynch J, Opas M, Olson EN, Agellon LB, et al. Cardiac-specific Expression of Calcineurin Reverses Embryonic Lethality in Calreticulin-deficient Mouse *. 2002;277(52):50776–9.

169. Kim SY, Im K, Park SN, Kwon J, Kim JA, Lee DS. CALR, JAK2, and MPL mutation profiles in patients with four different subtypes of myeloproliferative neoplasms: Primary myelofibrosis, essential thrombocythemia, polycythemia vera, and myeloproliferative neoplasm, unclassifiable. Am J Clin Pathol. 2015;

170. Guglielmelli P, Lasho TL, Rotunno G, Score J, Mannarelli C, Pancrazzi A, et al. The number of prognostically detrimental mutations and prognosis in primary myelofibrosis: An international study of 797 patients. Leukemia. 2014;

171. Tefferi A, Nicolosi M, Mudireddy M, Szuber N, Finke CM, Lasho TL, et al. Driver mutations and prognosis in primary myelofibrosis: Mayo-Careggi MPN alliance study of 1,095 patients. Am J Hematol. 2018;

172. Pietra D, Rumi E, Ferretti V V., Di Buduo CA, Milanesi C, Cavalloni C, et al. Differential clinical effects of different mutation subtypes in CALR-mutant myeloproliferative neoplasms. Leukemia. 2016;30(2):431–8.

173. Chachoua I, Pecquet C, El-Khoury M, Nivarthi H, Albu RI, Marty C, et al. Thrombopoietin receptor activation by myeloproliferative neoplasm associated calreticulin mutants. Blood. 2016;127(10):1325–35.

174. Marty C, Pecquet C, Nivarthi H, El-Khoury M, Chachoua I, Tulliez M, et al. Calreticulin mutants in mice induce an MPL-dependent thrombocytosis with frequent progression to myelofibrosis. Blood. 2016;127(10):1317–24.

175. Balligand T, Achouri Y, Pecquet C, Chachoua I, Nivarthi H, Marty C, et al. Pathologic activation of thrombopoietin receptor and JAK2-STAT5 pathway by frameshift mutants of mouse calreticulin. Leukemia. 2016.

176. Nivarthi H, Chen D, Cleary C, Kubesova B, Jäger R, Bogner E, et al. Thrombopoietin receptor is required for the oncogenic function of CALR mutants. Leukemia. 2016.

177. Elf S, Abdelfattah NS, Chen E, Perales-Patón J, Rosen EA, Ko A, et al. Mutant calreticulin requires both its mutant C-terminus and the thrombopoietin receptor for oncogenic transformation. Cancer Discov. 2016;6(4):368–81.

178. Araki M, Yang Y, Masubuchi N, Hironaka Y, Takei H, Morishita S, et al. Activation of the thrombopoietin receptor by mutant calreticulin in CALR-mutant myeloproliferative neoplasms. Blood. 2016;127(10):1307–16.

179. Elf S, Abdelfattah NS, Baral AJ, Beeson D, Rivera JF, Ko A, et al. Defining the requirements for the pathogenic interaction between mutant calreticulin and MPL in MPN. Blood. 2017/12/31. 2018;131(7):782–6.

180. Pecquet C, Chachoua I, Roy A, Balligand T, Vertenoeil G, Leroy E, et al. Calreticulin mutants as oncogenic rogue chaperones for TpoR and traffic-defective pathogenic TpoR mutants. Blood. 2019;blood-2018-09-874578.

181. Araki M, Yang Y, Imai M, Mizukami Y, Kihara Y, Sunami Y, et al. Homomultimerization of mutant calreticulin is a prerequisite for MPL binding and activation. Leukemia. 2018/06/28. 2018;

182. Han L, Schubert C, Köhler J, Schemionek M, Isfort S, Brümmendorf TH, et al. Calreticulin-mutant proteins induce megakaryocytic signaling to transform hematopoietic cells and undergo accelerated degradation and Golgi-mediated secretion. J Hematol Oncol. 2016;9(1):1–14.

183. Shide K, Kameda T, Yamaji T, Sekine M, Inada N, Kamiunten A, et al. Calreticulin mutant mice develop essential thrombocythemia that is ameliorated by the JAK inhibitor ruxolitinib. Leukemia. 2016/11/04. 2016;

184. Li J, Prins D, Park HJ, Grinfeld J, Gonzalez-Arias C, Loughran S, et al. Mutant calreticulin knockin mice develop thrombocytosis and myelofibrosis without a stem cell self-renewal advantage. Blood. 2017/12/29. 2018;131(6):649–61.

185. Erdile LF, Wold MS, Kelly TJ. The primary structure of the 32-kDa subunit of human replication protein A. J Biol Chem. 1990;

186. Umbricht CB, Erdile LF, Jabs EW, Kelly TJ. Cloning, overexpression, and genomic mapping of the 14-kDa subunit of human replication protein A. J Biol Chem. 1993;

187. Erdile LF, Heyer WD, Kolodner R, Kelly TJ. Characterization of a cDNA encoding the 70-kDa single-stranded DNA-binding subunit of human replication protein A and the role of the protein in DNA replication. J Biol Chem. 1991;

188. Bochkarev A, Bochkareva E, Frappier L, Edwards AM. The crystal structure of the complex of replication protein A subunits RPA32 and RPA14 reveals a mechanism for single-stranded DNA binding. EMBO J. 1999;

189. Vassin VM, Anantha RW, Sokolova E, Kanner S, Borowiec JA. Human RPA phosphorylation by ATR stimulates DNA synthesis and prevents ssDNA accumulation during DNA-replication stress. J Cell Sci. 2009;

190. Nuss JE, Patrick SM, Oakley GG, Alter GM, Robison JG, Dixon K, et al. DNA Damage Induced Hyperphosphorylation of Replication Protein A. 1. Identification of Novel Sites of Phosphorylation in Response to DNA Damage †. Biochemistry. 2005 Jun;44(23):8428–37.

191. Binz SK, Sheehan AM, Wold MS. Replication Protein A phosphorylation and the cellular response to DNA damage. DNA Repair (Amst). 2004 Aug;3(8–9):1015–24.

192. Wang H, Guan J, Wang H, Perrault AR, Wang Y, Iliakis G. Replication protein A2 phosphorylation after DNA damage by the coordinated action of ataxia telangiectasia-mutated and DNA-dependent protein kinase. Cancer Res. 2001;

193. Zuazua-Villar P, Ganesh A, Phear G, Gagou ME, Meuth M. Extensive RPA2 hyperphosphorylation promotes apoptosis in response to DNA replication stress in CHK1 inhibited cells. Nucleic Acids Res. 2015 Aug 13;43(20):9776–87.

194. Zou L, Elledge SJ. Sensing DNA damage through ATRIP recognition of RPA-ssDNA complexes. Science (80-). 2003;

195. Liu S, Shiotani B, Lahiri M, Maréchal A, Tse A, Leung CCY, et al. ATR Autophosphorylation as a Molecular Switch for Checkpoint Activation. Mol Cell. 2011;

196. Ward IM, Chen J. Histone H2AX Is Phosphorylated in an ATR-dependent Manner in Response to Replicational Stress. J Biol Chem. 2001;

197. Paull TT, Rogakou EP, Yamazaki V, Kirchgessner CU, Gellert M, Bonner WM. A critical

role for histone H2AX in recruitment of repair factors to nuclear foci after DNA damage. Curr Biol. 2000;

198. Liu Q, Guntuku S, Cui XS, Matsuoka S, Cortez D, Tamai K, et al. Chk1 is an essential kinase that is regulated by Atr and required for the G2/M DNA damage checkpoint. Genes Dev. 2000;

199. Zhao H, Piwnica-Worms H. ATR-Mediated Checkpoint Pathways Regulate Phosphorylation and Activation of Human Chk1. Mol Cell Biol. 2002;

200. Sanchez Y, Wong C, Thoma RS, Richman R, Wu Z, Piwnica-Worms H, et al. Conservation of the Chk1 checkpoint pathway in mammals: Linkage of DNA damage to Cdk regulation through Cdc25. Science (80-). 1997;

201. Toledo LI, Altmeyer M, Rask MB, Lukas C, Larsen DH, Povlsen LK, et al. ATR prohibits replication catastrophe by preventing global exhaustion of RPA. Cell. 2014;156(1–2):374.

202. Wang X, Kennedy RD, Ray K, Stuckert P, Ellenberger T, D'Andrea AD. Chk1-Mediated Phosphorylation of FANCE Is Required for the Fanconi Anemia/BRCA Pathway. Mol Cell Biol. 2007;

203. Sørensen CS, Hansen LT, Dziegielewski J, Syljuåsen RG, Lundin C, Bartek J, et al. The cell-cycle checkpoint kinase Chk1 is required for mammalian homologous recombination repair. Nat Cell Biol. 2005;

204. Greenberg et al. N. Causes and Consequences of Stress. Integr Comp Biol. 2014;42(3):508–16.

205. Kotsantis P, Petermann E, Boulton SJ. Mechanisms of Oncogene-Induced Replication Stress: Jigsaw Falling into Place. Cancer Discov. 2018 May;8(5):537–55.

206. Dominguez-Sola D, Ying CY, Grandori C, Ruggiero L, Chen B, Li M, et al. Non-transcriptional control of DNA replication by c-Myc. Nature. 2007;

207. Kotsantis P, Silva LM, Irmscher S, Jones RM, Folkes L, Gromak N, et al. Increased global transcription activity as a mechanism of replication stress in cancer. Nat Commun. 2016;7:1–13.

208. Neelsen KJ, Zanini IMY, Herrador R, Lopes M. Oncogenes induce genotoxic stress by mitotic processing of unusual replication intermediates. J Cell Biol. 2013;

209. Nogueira V, Park Y, Chen CC, Xu PZ, Chen ML, Tonic I, et al. Akt Determines Replicative Senescence and Oxidative or Oncogenic Premature Senescence and

Sensitizes Cells to Oxidative Apoptosis. Cancer Cell. 2008;14(6):458–70.

210. Karp JE, Thomas BM, Greer JM, Sorge C, Gore SD, Pratz KW, et al. Phase I and pharmacologic trial of cytosine arabinoside with the selective checkpoint 1 inhibitor Sch 900776 in refractory acute leukemias. Clin Cancer Res. 2012;18(24):6723–31.

211. Montano R, Chung I, Garner KM, Parry D, Eastman A. Preclinical Development of the Novel Chk1 Inhibitor SCH900776 in Combination with DNA-Damaging Agents and Antimetabolites. Mol Cancer Ther. 2012;11(2):427–38.

212. Doi T, Yoshino T, Shitara K, Matsubara N, Fuse N, Naito Y, et al. Phase I study of LY2603618, a CHK1 inhibitor, in combination with gemcitabine in Japanese patients with solid tumors. Anticancer Drugs. 2015;26:1043–53.

213. Herůdková J, Paruch K, Khirsariya P, Souček K, Krkoška M, Vondálová Blanářová O, et al. Chk1 Inhibitor SCH900776 Effectively Potentiates the Cytotoxic Effects of Platinum-Based Chemotherapeutic Drugs in Human Colon Cancer Cells. Neoplasia. 2017 Oct;19(10):830–41.

214. Oo ZY, Proctor M, Stevenson AJ, Nazareth D, Daignault SM, Lanagan C, et al. Combined use of subclinical hydroxyurea and CHK1 inhibitor effectively controls melanoma and lung cancer progression, with reduced normal tissue toxicity compared to gemcitabine. 2019;

215. Montano R, Thompson R, Chung I, Hou H, Khan N, Eastman A. Sensitization of human cancer cells to gemcitabine by the Chk1 inhibitor MK-8776: Cell cycle perturbation and impact of administration schedule in vitro and in vivo. BMC Cancer. 2013;13.

216. Hauge S, Naucke C, Hasvold G, Joel M, Elise Rødland G, Juzenas P, et al. Combined inhibition of Wee1 and Chk1 gives synergistic DNA damage in S-phase due to distinct regulation of CDK activity and CDC45 loading. Oncotarget. 2017;8(7):10966–79.

217. Chaudhuri L, Vincelette ND, Koh BD, Naylor RM, Flatten KS, Peterson KL, et al. CHK1 and WEE1 inhibition combine synergistically to enhance therapeutic efficacy in acute myeloid leukemia ex vivo. Haematologica. 2014;99(4):688–96.

218. Kwok M, Davies N, Agathanggelou A, Smith E, Oldreive C, Petermann E, et al. ATR inhibition induces synthetic lethality and overcomes chemoresistance in TP53-or ATM-defective chronic lymphocytic leukemia cells. Blood. 2016;127(5):582–95.

219. Ronco C, Martin AR, Demange L, Benhida R. ATM, ATR, CHK1, CHK2 and WEE1 inhibitors in cancer and cancer stem cells. Medchemcomm. 2017;8:295–319.

220. Qiu Z, Oleinick NL, Zhang J. ATR/CHK1 inhibitors and cancer therapy. Radiother Oncol.

2018;126(3):450–64.

221. Gopalakrishnapai J, Gupta G, Karthikeyan T, Sinha S, Kandiah E, Gemma E, et al. Isothermal titration calorimetric study defines the substrate binding residues of calreticulin. Biochem Biophys Res Commun. 2006;

222. Thomson SP, Williams DB. Delineation of the lectin site of the molecular chaperone calreticulin. Cell Stress Chaperones. 2005;

223. Schrag JD, Bergeron JJM, Li Y, Borisova S, Hahn M, Thomas DY, et al. The structure of calnexin, an ER chaperone involved in quality control of protein folding. Mol Cell. 2001;

224. Vallée F, Karaveg K, Herscovics A, Moremen KW, Howell PL. Structural basis for catalysis and inhibition of N-glycan processing class I α1,2-mannosidases. J Biol Chem. 2000;

225. Molina DM, Jafari R, Ignatushchenko M, Seki T, Larsson EA, Dan C, et al. Monitoring Drug Target Engagement in Cells and Tissues Using the Cellular Thermal Shift Assay. Science (80-). 2013;

226. Jafari R, Almqvist H, Axelsson H, Ignatushchenko M, Lundbäck T, Nordlund P, et al. The cellular thermal shift assay for evaluating drug target interactions in cells. Nat Protoc. 2014;

227. Guzi TJ, Paruch K, Dwyer MP, Labroli M, Shanahan F, Davis N, et al. Targeting the Replication Checkpoint Using SCH 900776, a Potent and Functionally Selective CHK1 Inhibitor Identified via High Content Screening. Mol Cancer Ther. 2011;

228. King C, Diaz H, Barnard D, Barda D, Clawson D, Blosser W, et al. Characterization and preclinical development of LY2603618: a selective and potent Chk1 inhibitor. Invest New Drugs. 2014 Apr 10;32(2):213–26.

229. Toppaldoddi KR, da Costa Cacemiro M, Bluteau O, Panneau-Schmaltz B, Pioch A, Muller D, et al. Rare type 1-like and type 2-like calreticulin mutants induce similar myeloproliferative neoplasms as prevalent type 1 and 2 mutants in mice. Oncogene. 2019;

230. Kiladjian JJ, Cassinat B, Chevret S, Turlure P, Cambier N, Roussel M, et al. Pegylated interferon-alfa-2a induces complete hematologic and molecular responses with low toxicity in polycythemia vera. Blood. 2008;

231. Verger E, Cassinat B, Chauveau A, Dosquet C, Giraudier S, Schlageter MH, et al. Clinical and molecular response to interferon-alpha therapy in essential

thrombocythemia patients with CALR mutations. Blood. 2015/10/22. 2015;126(24):2585–91.

232. Cassinat B, Verger E, Kiladjian JJ. Interferon alfa therapy in CALR-mutated essential thrombocythemia. N Engl J Med. 2014/07/10. 2014;371(2):188–9.

233. Deininger M, Radich J, Burn TC, Huber R, Paranagama D, Verstovsek S. The effect of long-term ruxolitinib treatment on JAK2p.V617F allele burden in patients with myelofibrosis. Blood. 2015;

234. Hung MS, Xu Z, Lin YC, Mao JH, Yang CT, Chang PJ, et al. Identification of hematein as a novel inhibitor of protein kinase CK2 from a natural product library. BMC Cancer. 2009;

235. Hung MS, Xu Z, Chen Y, Smith E, Mao JH, Hsieh D, et al. Hematein, a casein kinase II inhibitor, inhibits lung cancer tumor growth in a murine xenograft model. Int J Oncol. 2013;

236. Farmer H, McCabe H, Lord CJ, Tutt AHJ, Johnson DA, Richardson TB, et al. Targeting the DNA repair defect in BRCA mutant cells as a therapeutic strategy. Nature. 2005;

237. Marty C, Lacout C, Droin N, Le Couédic JP, Ribrag V, Solary E, et al. A role for reactive oxygen species in JAK2 V617F myeloproliferative neoplasm progression. Leukemia. 2013;

238. Chen E, Ahn JS, Massie CE, Clynes D, Godfrey AL, Li J, et al. JAK2V617F promotes replication fork stalling with disease-restricted impairment of the intra-S checkpoint response. Proc Natl Acad Sci. 2014;

239. Nieborowska-Skorska M, Maifrede S, Dasgupta Y, Sullivan K, Flis S, Le BV, et al. Ruxolitinib-induced defects in DNA repair cause sensitivity to PARP inhibitors in myeloproliferative neoplasms. Blood. 2017;130(26):2848–59.

240. Alabert C, Bukowski-Wills JC, Lee SB, Kustatscher G, Nakamura K, De Lima Alves F, et al. Nascent chromatin capture proteomics determines chromatin dynamics during DNA replication and identifies unknown fork components. Nat Cell Biol. 2014;16(3):281–91.

241. Sirbu BM, McDonald WH, Dungrawala H, Badu-Nkansah A, Kavanaugh GM, Chen Y, et al. Identification of proteins at active, stalled, and collapsed replication forks using isolation of proteins on nascent DNA (iPOND) coupled with mass spectrometry. J Biol Chem. 2013;288(44):31458–67.

242. Pronier E, Cifani P, Merlinsky TR, Berman KB, Somasundara AVH, Rampal RK, et al.

Targeting the CALR interactome in myeloproliferative neoplasms. JCI Insight. 2018;

243. Pocanschi CL, Kozlov G, Brockmeier U, Brockmeier A, Williams DB, Gehring K. Structural and functional relationships between the lectin and arm domains of calreticulin. J Biol Chem. 2011/06/10. 2011;286(31):27266–77.

244. Corpet F. Multiple sequence alignment with hierarchical clustering. Nucleic Acids Res. 1988;

245. Morris GM, Huey R, Lindstrom W, Sanner MF, Belew RK, Goodsell DS, et al. AutoDock4 and AutoDockTools4: Automated Docking with Selective Receptor Flexibility. J Comp Chem. 2009;

246. Oleg Trott, Olson AJ. AutoDock Vina: Improving the Speed and Accuracy of Docking with a New Scoring Function, Efficient Optimization, and Multithreading. J Comput Chem. 2009;

247. DeLano W. . Pymol: An open-source molecular graphics tool. CCP4 Newsl Protein Crystallogr. 2002;

248. Ran FA, Hsu PD, Wright J, Agarwala V, Scott DA, Zhang F. Genome engineering using the CRISPR-Cas9 system. Nat Protoc. 2013/10/26. 2013;8(11):2281–308.

249. Zhang JH, Chung TDY, Oldenburg KR. A simple statistical parameter for use in evaluation and validation of high throughput screening assays. J Biomol Screen. 1999;

Appendix

The following document was the inventor notification from the European Patent Office (EPO).

Europäisches Patentamt
European Patent Office
Office européen des brevets

European Patent Office
80298 MUNICH
GERMANY

Questions about this communication ?
Contact Customer Services at www.epo.org/contact

JIA, Ruochen
c/o Myelopro Diagnostics and Research GmbH
Lazarettgasse 14, BT25.3
1090 Vienna
AUTRICHE

Date
14.12.18

Reference	Application No./Patent No.
	18202112.1 - 1110
Applicant/Proprietor	
Myelopro Diagnostics and Research GmbH	

Designation as inventor - communication under Rule 19(3) EPC

You have been designated as inventor in the above-mentioned European patent application. Below you will find the data contained in the designation of inventor and further data mentioned in Rule 143(1) EPC:

DATE OF FILING	: 23.10.18
PRIORITY	: / /
TITLE	: COMPOUNDS TARGETING MUTANT CALRETICULIN
DESIGNATED STATES	: AL AT BE BG CH CY CZ DE DK EE ES FI FR GB GR HR HU IE IS IT LI LT LU LV MC MK MT NL NO PL PT RO RS SE SI SK SM TR

INVENTOR (PUBLISHED = 1, NOT PUBLISHED = 0):

1/ZAGRIJTSCHUK, Oleh/Zieglergasse 55/2/4/1070 Vienna/AT
1/JIA, Ruochen/c/o Myelopro Diagnostics and Research GmbH Lazarettgasse 14, BT25.3/1090 Vienna/AT

DECLARATION UNDER ARTICLE 81 EPC:
The applicant(s) has (have) acquired the right to the European patent as employer(s).

Receiving Section

Europäisches Patentamt • European Patent Office • Office européen des brevets

EPO Form 1048 10.09

page 1 of 1

CV

Ruochen Jia

PERSONAL INFORMATION

Date of birth: 13.09.1988

Nationality: Chinese

Email: regmjia@gmail.com

Tel: 06607892175

Address: 54/12 Albertgasse, 1080, Vienna

PROFESSIONAL EXPERIENCE

09.2015 - : PhD student in biomedicine

Dr. Robert Kralovics group, CeMM, Vienna

Molecular docking study of mutant calreticulin and small molecule drug development in myeloproliferative neoplasms

High-throughput drug screening to identify compounds which are synthetic lethal to mutant calreticulin

CRISPR-Cas9 genome-wide screen in mutant CALR cell line

05.2013 – 09.2015: Research assistant

Prof. Dr. Daniel Hochhauser group, University College London, UK

Project collaboration with MERCK Serono

Investigating interaction of MEK inhibition with a novel anticancer drug in pancreatic cancer

Role of reactive oxygen species in combination therapy of oxaliplatin and cetuximab

Training of bachelor/summer school students

10.2012 – 03.2013: Research Intern

Prof. Dr. Daniel Hochhauser group, University College London, UK

Technical development and optimization of cell-based cytotoxicity assay and biochemical assays

General technical support to the research group

09.2011 – 09.2012: Master degree of cancer research, Merit

Theoretical training of biology and therapy of cancer research

Completion of a research project investigating the interaction of EGFR with Cyclin D1 in the role of modulating homologous recombination repair (Distinction)

09.2007 – 06.2015: Bachelor degree of biological science,

Shandong university, China. GPA 88.65%

Courses: molecular biology, biochemistry, analytical chemistry, genetics, animal biology, microbiology

Practical course in biology and chemistry laboratory

PROFESSIONAL TECHNIQUES

Biochemical assays: western blot, co-immunoprecipitation, thermal shift assay, protein production and purification

Cell biology assays: cell cytotoxicity assays, DNA transfection, viral transduction, immunofluorescence, FACs

Molecular biology assays: molecular cloning, CRISPR-cas9 library preparation and amplification, RNA extraction and purification, NGS and RNA seq sample preparation, site-directed mutagenesis

Computer skills: Microsoft office, R programming, Pymol, Autodock, Adobe illustrator, Fiji, GraphPad Prism, Cellprofiler

PROFESSIONAL ACHIEVEMENTS

Publications:

Vena F#, Jia R#, Esfandiari A, Garcia-Gomez JJ, Rodriguez-Justo M, Ma J, Syed S, Crowley L, Elenbaas B, Goodstal S, Hartley JA, Hochhauser D. MEK inhibition leads to BRCA2

downregulation and sensitization to DNA damaging agents in pancreas and ovarian cancer models. Oncotarget. 2018 Jan 22;9(14):11592-11603.

Santoro V, Jia R, Thompson H, Nijhuis A, Jeffery R, Kiakos K, Silver AR, Hartley JA, Hochhauser D. Role of Reactive Oxygen Species in the Abrogation of Oxaliplatin Activity by Cetuximab in Colorectal Cancer. J Natl Cancer Inst. 2015 Dec 30;108(6):djv394.

Patent:

Compounds targeting mutant calreticulin --- European patent office (EPO)

CONFERENCE/SYMPOSIUM ATTENDENCE

7th INTERNATIONAL CONFERENCE ON MYELOPROLIFERATIVE NEOPLASMS 2016

23rd Congress of the European Hematology Association (EHA) 2018

24th Congress of the European Hematology Association (EHA) 2019